Gene Profiling of Identified Neurons to Dissect Molecular Mechanisms Involved in Spinal Reflex Assembly

Inauguraldissertation

zur
Erlangung der Wuerde eines Doktors der Philosophie
vorgelegt der
Philosophisch – Naturwissenschaftlichen Fakultaet
der Universitaet Basel

von

Andreas Friese
aus Luedenscheid, Deutschland

Karlsruhe, 2010

Genehmigt von der Philosophisch – Naturwissenschaftlichen Fakultaet
der Universitaet Basel

auf Antrag von:

Professor Dr. Silvia Arber
(Dissertationsleitung)

Professor Dr. Pico Caroni
(Korreferat)

Basel, 11.11.2008

Prof. Dr. Eberhard Parlow
(Dekan)

TABLE OF CONTENT

Acknowledgements

First of all, I would like to express my immense gratitude to Prof. Dr. Silvia Arber for supervising my PhD dissertation at the Biozentrum and at the FMI in Basel. During the course of my studies, she was always supportive of my research projects and offered helpful and critical advice. I am thankful to Silvia for leaving me the freedom to develop my personal and scientific skills to pursue a future career in industry.

Also, I would like to thank Prof. Dr. Pico Caroni, Dr. Botond Roska and Dr. Edward Oakeley for their support of my studies as members of my thesis committee.

I wish to thank all the current and former members of the Arber lab for such a nice collaboration and inspiring atmosphere. In particular I would like to thank Ina Kramer, Vera Niederkofler, Eline Pecho Vrieseling and David Ladle for teaching me many experiments and keeping me motivated throughout 5 years in Silvia's lab. Many thanks also to all members of the FMI facilities for their continuous support being it at the cryostat, microscope or any other state of the art instrument at FMI.

I am particularly indebted to Monika Mielich. It was a great pleasure working side by side with her and receiving her support in most of my projects, in the lab as well as in private life.

Special thanks also to Smita Saxena and Ivan Galimberti from the group of Pico Caroni for becoming good friends and sharing fantastic moments, especially beyond the walls of FMI.

I am grateful to my family for their continuous support and effort, which allowed me to pursue my goals and to accomplish these studies. Thank all of you!

Chapter I - INTRODUCTION

Topic of my PhD Thesis

Over the past decades, the concept has emerged that sophisticated neuronal circuits in the brain are the cellular correlates of this enormous repertoire of functions that the brain is capable of performing. However, very little information is yet available about how neuronal circuits assemble with such precision during development (Jessell, 2000; McConnell, 1995). To begin to address these questions, we investigated the development of the spinal monosynaptic stretch reflex circuit, which represents the basis for all final common pathways to regulate skeletal muscle contraction and relaxation (Chen et al., 2003). Due to its relatively simple anatomy with two main neuronal components and its easy accessibility, the function and thus the precision in connectivity of this neuronal circuit is well understood. In the spinal monosynaptic stretch reflex circuit, a subpopulation of dorsal root ganglia (DRG) sensory neurons (Ia proprioceptive afferents) form direct synaptic contacts with motor neurons in the ventral spinal cord, which in turn control the contraction of muscles in the periphery (Eccles et al., 1957). It therefore represented an ideal system to study molecular pathways specifying neuronal connectivity in a defined neuronal circuit during development. The main aim of this project was to enhance our insight in the genetic cascades controlling the specification and connectivity in developing neuronal circuits, with a particular emphasis on the spinal monosynaptic reflex circuit.

Wiring the Central Nervous System

Correct wiring of the nervous system is required to respond and interact with a large number of different environmental cues. The central nervous system (CNS) consists of two major information processing networks; the brain and the spinal cord. These two complex relay stations are composed of a vast repertoire of cell types defined by distinct morphologies, physiological functions and defined projections into target areas or onto other neurons. The human brain consists of approximately 100 billion neurons, each connected to as many as 10.000 other neurons. The brain acts as control center of the CNS and is responsible for behavior. It is tightly linked to the primary sensory

apparatus of vision, hearing, sense of taste, olfaction etc. The brain controls a variety of functions automatically without awareness, such as body homeostasis, blood pressure and body temperature. It is also the site controlling cognition, perception, attention, memory and emotion. In order to control movement, the brain possesses multiple parallel neuronal tracts connected to diverse neuronal cell types in the spinal cord. Different regulatory areas in the brain control voluntary and involuntary muscle functions. Certain movements, for example reflexes and locomotion, require very fast and automatic actions that can be controlled by the spinal cord alone (Eccles et al., 1957; Sherrington, 1910). All of these functions are carried out in a precisely timed sequence of events that are regulated by multiple inter - connected neuronal subpopulations in the mature CNS.

DRG – Dorsal Root Ganglia

DRG are located adjacent to the spinal cord along the whole rostro- to caudal axis and contain sensory neurons (SNs) projecting peripherally among other regions to muscles, joints and the skin. Centrally, all of these sensory neurons innervate the spinal cord. Afferents project to distinct laminae in the spinal cord (Rexed, 1952; Rexed, 1954). Ia proprioceptive afferents project specifically to the ventral spinal cord and form direct connections with motor neurons to form the monosynaptic stretch reflex circuit, whereas cutaneous afferents mainly terminate in the dorsal to intermediate spinal cord. The peripheral and central branch of DRG sensory neurons are also often named distal and proximal nerve branch conducting action potentials from the periphery to the CNS; the spinal cord. DRG sensory neurons can be subdivided into three main neuronal subpopulations based on their capability to communicate distinct peripheral stimuli to the CNS, such as heat, cold, touch or limb movements.

DRG sensory neurons can be categorized based on their expression of a particular neurotrophin tyrosine receptor kinase. Most SNs are small diameter cutaneous neurons and express the TrkA receptor responsive to nerve growth factor (NGF) (Carroll et al., 1992; Huang and Reichardt, 2003; Molliver et al., 1997; Patel et al., 2000). Mechanical sensation is conveyed through larger mechano-responsive neurons, which express TrkB and can

be activated through BDNF and neurotrophin 4 (NT4) (Ehrhard and Otten, 1994). Information about limb movement and spatial positioning is sensed through a class of large diameter DRG SNs; the TrkC+ proprioceptive afferents dependent on the neurotrophin 3 (NT3) (Ernfors et al., 1994; Klein et al., 1994; Oakley et al., 1997). A different class of DRG neurons positive for the receptor tyrosine kinase Ret, signal through glia cell line derived neurotrophic factor (GDNF) proteins (Baudet et al., 2000; Haase et al., 2002; Molliver et al., 1997; Yamamoto et al., 1996).

From Birth to Molecular Classification of DRG SN Subpopulations

To date, only a broad classification of neuronal subpopulations in DRG has been established mainly based on specific termination zones in the periphery and spinal cord as well as by unique molecular characteristics (Anderson, 1999; Rexed, 1952; Rexed, 1954). The following paragraphs will describe the segregation of these DRG subpopulations and key factors involved in this process during development. All subpopulations are derived from neural crest cells (NCC) originating from the neural tube and expressing a common transcription factor called islet1 (Isl1) (Anderson, 1999). DRG neuron differentiation requires precisely timed events of NCC migration from the neural tube, neurogenesis, subpopulation specification and axonal outgrowth to target areas. Subpopulation specification takes place already as early as NCC start migrating ventrally to form the DRG. Early migrating cells will be the future mechanoreceptive and proprioceptive large diameter SNs positive for TrkB and TrkC. The larger late migrating cell population will give rise to small diameter TrkA+ DRG SNs. A group of basic helix loop helix factors called neurogenins (ngn1 and ngn2) is required for the determination of DRG SN fate (Ma et al., 1999; Sommer et al., 1996; Zirlinger et al., 2002). Migrating NCCs express first the bHLH differentiation factor *ngn2* that is extinguished by embryonic day E10.5. In contrast, *Ngn1* expression starts later only after NCCs have reached their end position where DRG are formed. Mutant analysis showed that *ngn1* mutant animals do not show any apparent phenotype in the CNS where *ngns* are co-expressed in overlapping regions. This suggests a functional redundancy of *ngn* genes at least in some regions of the CNS. In the DRG

however, Ma *et al* showed in mutant models that *ngn1* and *ngn2* are required for two phases of DRG SN differentiation. Loss of *ngn2* expression can be compensated with a delay by *ngn1* expression resulting in a loss of early born *ngn2* dependent larger diameter SNs. *Ngn1* mutant animals show a severe decrease in DRG size caused by almost a complete loss of later born TrkA+ nociceptive DRG SNs. In contrast, the ngn2 dependent TrkB+ and TrkC+ large diameter population seems to develop normally. Nevertheless, quantifications showed approximately a 30% reduction in TrkC+ and TrkB+ cells during embryonic development in *ngn1* mutant animals, suggesting that a small population of TrkC+ and TrkB+ DRG neurons requires ngn1 (Ma et al., 1999). However, to date there is no evidence that ngn1 or ngn2 specify DRG SN subpopulations.

Cell Lineage Commitment – "Runx-ing" the DRG

In the immune system, Runx proteins have been shown to be responsible for lineage specification. Runx transcription factors are characterized by a Runt DNA - binding domain and heterodimerize with a common cofactor CBFβ (Ito, 2004). In mammals there are three members of the Runt family, namely Runx1, Runx2 and Runx3. The Runt transcription factors *Runx1* and *Runx3* have been shown to be selectively expressed in defined subsets of DRG neurons. At embryonic stages, Runx3 expression has been reported to be exclusively expressed by TrkC+ proprioceptive afferents. In contrast, the TrkA+ nociceptive and thermoceptive DRG SN subpopulation is positive for *Runx1*. *Runx3* deficient mice exhibit severe impairments in monosynaptic stretch reflex formation and therefore behavioral defects (Levanon et al., 2002). Gene expression studies showed that Runx expression occurs soon after DRG neurons are born. However, its expression with respect to Trk receptor expression was not addressed. Recent studies indicate that Runx activity could be directly linked to DRG diversification of cutaneous and proprioceptive subpopulations. Mutant animal studies showed that Runx3 activity is required for the switch off TrkB in TrkB/TrkC hybrid cells at early embryonic stages to obtain a pure TrkC proprioceptive population (Kramer et al., 2006). The larger nociceptive TrkA+ population (~80% of all DRG SNs) differentiates further into a non-

peptidergic TrkA- population by up-regulation of the glia cell line-derived neurotrophic factor (GDNF) receptor Ret (Patel et al., 2000) in many nociceptive DRG neurons. This non-peptidergic cell population also acquires the ability to bind isolectin B4 (IB4). Recently, it was shown that NGF is required for the maturation of TrkA-/Ret+ DRG sensory neurons, but not for the induction of this subpopulation (Luo et al., 2007). The smaller peptidergic group of nociceptive DRG neurons expresses TrkA, the receptor for nerve growth factor (NGF). This population also expresses the neuropeptide calcitonin gene-related peptide (CGRP) and is therefore called peptidergic neuron population.

Similar to the role of Runx3 in cell lineage determination between TrkC+ and TrkB+ cells, the question arose whether Runx1 plays a role in lineage fragmentation of nociceptive DRG sensory neurons. At postnatal day P30 a complete fragmentation took place and TrkA expression is down-regulated in all Runx1 expressing cells. In contrast, down-regulation of Runx1 leads to the establishment of stable peptidergic phenotypic cells being TrkA+/Ret+ and Runx1-. Conditional Runx1 elimination from premigratory NCCs induces a dramatic change in nociceptive DRG SN proportions. As expected, elimination of Runx1 leads to a significant up-regulation in expression of TrkA in DRG neurons. Along the same line, Ret expression which in *wild-type* animals induced upon down-regulation of TrkA, is elevated in conditional *Runx1* mutant animals (Chen et al., 2006).

In summary, specific waves of ngn1 and ngn2 expression trigger neurogenesis to guide NCCs into distinct sensory lineages. Later during development, Runx transcription factors are key molecules involved in the specification of DRG neuronal cell types.

Cutaneous Afferents	**Mechano-receptive Afferents**	**Proprioceptive Afferents**
70-80 %	**5-10 %**	**10-20 %**
TrkA+	TrkB+	TrkC+
NGF dependent	BDNF & NT 4/5 dependent	NT3 dependent

Table 1: Neurotrophin receptor dependent DRG sensory neuron classification. In adult, cutaneous afferents further subdivide into TrkA-/Runx1+ and TrkA+/Ret+ cell populations.

Formation of the Monosynaptic Stretch Reflex Circuit – What is known?

The interplay between sensory and motor components is key to control precise muscle contraction and relaxation. A muscle stretch results in lengthening of extrafusal muscle fibers, but also in a lengthening of intrafusual muscle fibers. Muscle spindles consist of intrafusal muscle fibers and are arranged in parallel to extrafusual (skeletal) muscle fibers. Muscle spindles are innervated by Ia proprioceptive afferents and gamma motor neurons. Stretching of muscle spindles leads to activation of Ia proprioceptive afferents relaying muscle stretch information from the periphery to the central nervous system (Landmesser, 2001; Mears and Frank, 1997; Sanes and Lichtman, 2001). Action potentials propagating through Ia afferent axons from the action potential initiation site in the muscle spindle, activate motor neurons at the sensory-motor synapse in the ventral spinal cord, which project to the same or related muscle (Luscher et al., 1984). This activation elicits an action potential in α-motor neurons to induce a muscle contraction in the periphery. Alpha motor neurons innervate extrafusual muscle fibers and are quite different from intrafusal musle fibers, which are innervated by gamma motor neurons. Golgi tendon

organs (GTO) located at the insertion point of skeletal muscle fibers are innervated by Ib proprioceptive afferents (Zelena and Soukup, 1977a; Zelena and Soukup, 1977b). Muscle tension causes a conformational change of Ib afferent terminals and results in opening stretch sensitive cation channels. This causes a depolarization and an action potential is propagated into the spinal cord where Ib afferents make connections to interneurons.

To better understand the process of neuronal circuit formation and in particular formation of the monosynaptic stretch reflex, and its genetic cascades involved, it is important to first determine the sequential mechanisms of how neuronal subpopulations in the spinal cord emerge and how sensory - motor connectivity is established during development. This paragraph will focus on genes known to be involved in the formation of the monosynaptic stretch reflex circuit. Figure 1 shows an outline of the basic neuronal components of the monosynaptic stretch reflex circuit.

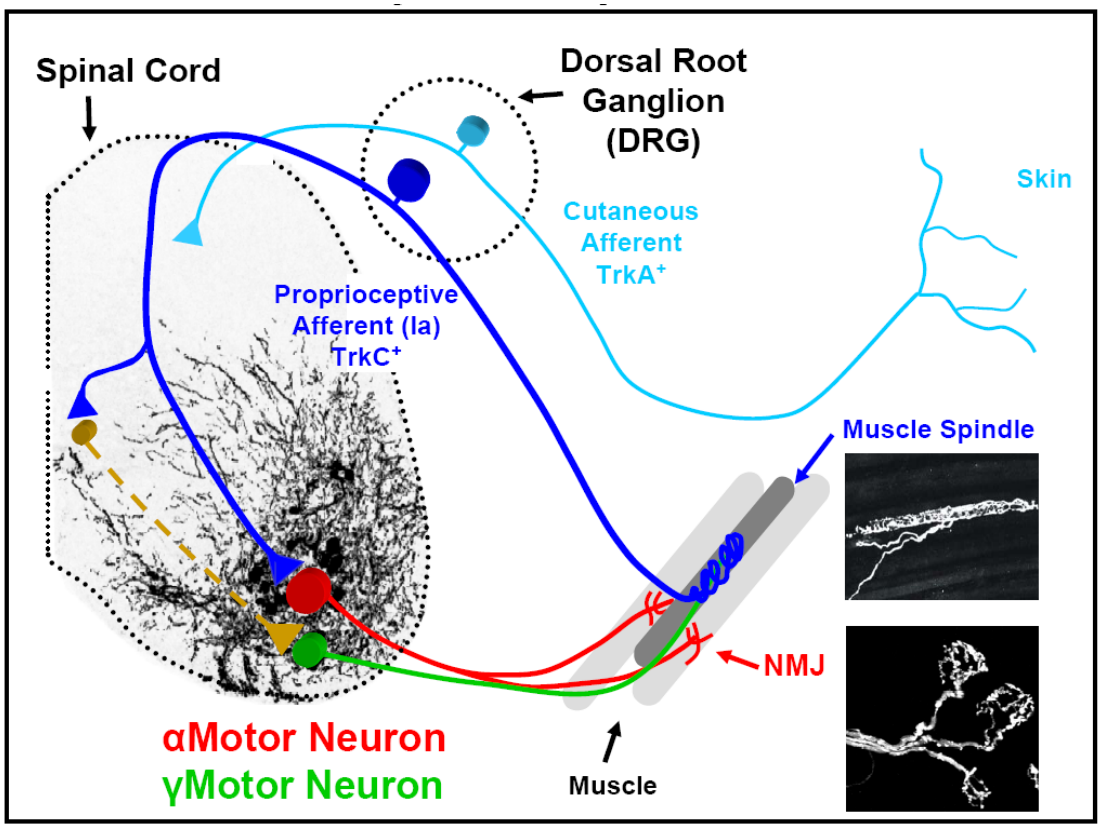

Figure 1: Assembly of the monosynaptic stretch reflex circuit. Cutaneous afferents project to the dorsal spinal cord and peripherally to the skin are outlined in light-blue. Ia

proprioceptive afferents encompass only a small fraction of DRG SNs and form direct connections to motor neurons; Ia proprioceptive afferents are outlined in dark-blue. Adapted from (Arber et al., 2000).

In the spinal cord an early *sonic-hedgehog* signaling pathway initiates the expression of specific *homeodomain* transcription factors in neuronal progenitor domains (Jessell, 2000).

As early as embryonic time point E11.5, before motor neuron axons reach their target area in the periphery, motor neuron groups projecting to individual muscles are coupled electrically to each other by gap junctions, which is necessary for burst generation activity (Chang et al., 1999; Kiehn, 2006; Milner and Landmesser, 1999). Two main phases of motor circuit formation can be distinguished. The first phase begins shortly after motor neuron generation at approximately embryonic time point E12.5 in mouse. The main motor neuron neurotransmitter is acetylcholine, which acts excitatory. Acetylcholine serves as the basis for motor neuron activation through connections to other motor and inhibitory neurons. Glycine and GABA provided by interneurons still have an excitatory mode of action during this first phase and contribute positively to pattern generation. Burst alternation however, is not in place at this early time point. One reason could be the later establishment of postnatal inhibitory transmission, which is involved in burst alternation patterns (Milner and Landmesser, 1999; Myers et al., 2005).

The second phase of motor neuron activation is controlled through up-regulation of the excitatory neurotransmitter glutamate. A shift from excitatory neurotransmission by Glycine and GABA to inhibition takes place in interneurons. After the second phase of circuit assembly motor neurons are matured and processes have been formed to the periphery (~E17.5) (Mentis et al., 2005; Myers et al., 2005; Nishimaru et al., 2005).

To date it is unclear how the switch and initiation from excitatory to inhibitory neurotransmission is controlled and what factors are involved in this process.

Interestingly, this shift is initiated at around the developmental stage when motor axons reach their target region in the muscles. MN columns can be

specified based on the distinct expression of a combinatorial code of LIM gene expression. However, to date, the sartorius and femorotibialis motor neuron pools can not be differentiated based on their transcriptional code, but already exhibit different burst durations at E4 in the developing chick. This observation suggests already the existence of selective cell surface molecules for maintaining these bursting differences (Milner and Landmesser, 1999) regulated through unknown transcription factors. *Ets* genes have been shown to be expressed in subpopulations and more specifically even in pool restricted manners. The expression onset of these *Ets* transcription factors matches well with the time point when axons reach their targets in the periphery suggesting that target - derived signals are required for the expression of these genes. In fact, it was shown that limb ablation in chick prevents the expression of two Ets gene family members, *Er81* and *Pea3*, in the DRG and MNs (Lin et al., 1998). After induction, these Ets transcription factors may be required for the regulation of genetic cascades providing pool specific cell identities initiating the expression of distinct sets of cell surface markers. Recent work has shown using transgenic mice that *Er81* and *Pea3* are both required for correct circuit assembly of proprioceptive afferents and motor neurons in the developing spinal cord (Arber et al., 2000; Lin et al., 1998; Vrieseling and Arber, 2006). *Er81*$^{-/-}$ mutant animals show severe motor behavior abnormalities. In this mutant mouse, Ia proprioceptive afferents fail to form functional synapses with motor neurons in the ventral part of the spinal cord leading to severe ataxia. In contrast, Pea3 is required for proper elaboration of dendritic trees of subsets of motor neurons in the spinal cord. Motor neurons of *Pea3*$^{-/-}$ mutant animals exhibit alterations in cutaneous maximus dendrite patterning and receive functionally inappropriate sensory inputs. Moreover, these motor neurons show altered cell body positioning and defects in target invasion (Livet et al., 2002; Vrieseling and Arber, 2006). Expression of Er81 and Pea3 is controlled through neurotrophic factors, GDNF and NT3 respectively, in the periphery (Haase et al., 2002; Patel et al., 2003). This principle not only provides evidence that neurotrophic factors are required for cell survival, but also plays crucial roles in establishing specificity and connectivity of neuronal subpopulations. Immediately the

following questions arise: what are the target genes of these transcription factors and which genetic programs do they control? Are there other, maybe parallel genetic programs requiring NT3 and GDNF? Is there a pool specific genetic code controlled by Er81 and Pea3?

Similar to *Er81*$^{-/-}$ mutant animals, complete deletion of NT3 leads to severe defects in sensory – motor connectivity in the ventral spinal cord. *NT3*$^{-/-}$ deficient mice exhibit a significant loss of proprioceptive afferents and peripheral sense organs (Ernfors et al., 1994). No muscle spindles are formed in *NT3*$^{-/-}$ deficient animals, whereas *NT3*$^{+/-}$ heterozygous animals complement only half of the muscle spindles. Motor neurons are not affected by the loss of NT3 in the periphery, although they express *NT3* at embryonic age (Ernfors et al., 1994; Kucera et al., 1995). Prenatal muscle specific ectopic expression of NT3 has recently been shown to disrupt specificity in sensory - motor connections in the spinal cord (Wang et al., 2007).

Again, the exact downstream signaling mechanisms leading to these phenotypic observations are currently only poorly understood. Gene expression profiling experiments of proprioceptive afferents in *NT3*$^{-/-}$ mutant and over - expression animals might discover underlying downstream mechanisms involved in these processes. It was shown that NT3 levels in intrafusal muscle fibers are dependent on the zinc-finger transcription factor *Egr3*. *Egr3*$^{-/-}$ mutant animals exhibit postnatal muscle spindle degeneration and most muscle spindles degenerate by adulthood. Intramuscular injections of NT3 have been shown to restore sensory - motor connections (Chen et al., 2002; Tourtellotte and Milbrandt, 1998). To date, only little literature was published to show the status of cell bodies of gamma efferents in the spinal cord (Gould et al., 2008), yet no molecular markers were identified to trace gamma motor neurons centrally in mice exhibiting muscle spindle defects. Recent studies described the neurotrophic effects of GDNF/Ret signaling for muscle spindle innervating gamma motor neuron survival during developmental programmed cell death (Gould et al., 2008). Mice mutant for *GDNF* or its receptors *GDNF family receptor alpha1* (*GFRα1*) and *Ret* exhibit a significant loss of lumbar motor neurons, which

could be visualized to affect specifically gamma motor neurons by insertion of a reporter allele.
In chapter III of this thesis, we identified a molecular marker to specifically label gamma motor neurons in the lumbar spinal cord. Further analysis suggests that differentiated muscle spindles are required for gamma motor neuron survival.

Much progress has been made during the past years to understand the sequential steps and the required molecules in the formation of the monosynaptic stretch reflex circuit. In fact, various transcription factors have been shown to specify distinct aspects of neuronal circuit assembly in the periphery as well as in the central nervous system. Still, only very little is known about the underlying downstream cascades of these factors. Furthermore, there is only limited understanding of how individual sensory – motor units are formed, innervating distinct muscles or muscle groups.

Abstract of my PhD Project

The central question during my PhD studies was to understand the molecular mechanisms and genetic cascades controlling the sequential specification of distinct classes of dorsal root ganglia (DRG) sensory neurons, with a particular focus on genes involved in controlling connectivity between Ia proprioceptive afferents and motor neurons in the spinal cord. The underlying genetic mechanisms controlling the formation of specific synaptic connections between Ia proprioceptive afferents and motor neurons in the lumbar spinal cord are currently only poorly understood. The main reason for the difficulty of isolating genes responsible for controlling aspects of connectivity was due to the fact that an enormous number of distinct subpopulations exist in the nervous system. In the spinal monosynaptic reflex circuit, proprioceptive afferents in the dorsal root ganglion (DRG) represent only 10-20% of all neurons. Moreover, cell bodies of given sensory neuron subpopulations in the DRG are highly dispersed. Therefore, initial technical difficulties were faced when performing gene expression analysis experiments of individual neuronal subtypes. In our study, we have used mouse genetics to selectively label distinct neuronal subpopulations. These tools allowed purifying defined populations of DRG sensory neurons (Klein et al., 1994) by Fluorescent Activated Cell Sorting (FACS) and subsequent gene expression profiling analysis using Affymetrix GeneChip technology. The aim of the first part of my PhD was the identification of genes involved in the specification and differentiation of DRG SN subtypes. The second major part of this project was the verification of candidate genes isolated from the Affymetrix chip screen experiments and to perform functional experiments to address their role in controlling connectivity between Ia proprioceptive afferents and motor neurons in the spinal cord. First, selected putative regulators were analyzed for their expression profile using *in situ* hybridization experiments on *wild-type* embryos and *TrkC*$^{-/-}$ and *Er81*$^{-/-}$ mutant backgrounds. We focused in particular on genes that were expressed in subpopulations of DRG neurons in *wild-type* embryos, but are not expressed in either *TrkC*$^{-/-}$ or *Er81*$^{-/-}$ mutant mice. Such genes are selectively expressed in proprioceptive DRG neurons or regulated by the transcription factor Er81 and they therefore represented the most

interesting population of genes to assay for function (Arber et al., 2000; Klein et al., 1994).

Our initial gene expression profiling analysis was extended to also isolate novel proprioceptive afferent markers, the expression of which is potentially restricted to distinct sensory neuron pools. We pushed the technical limitations further and used methods to profile proprioceptive afferents from different spinal levels.

Some of the genes identified in our screen were also analyzed functionally. One of these genes is the orphan nuclear receptor *estrogen-related receptor gamma* (*Err3*). We analyzed its function in proprioceptive afferent neuron specification and connectivity in greater detail in the third part of my PhD thesis. Analysis of Err3 expression revealed expression specifically in gamma motor neurons, a motor neuron subpopulation to which no marker gene has been correlated to date. We used various mutant animals to show that muscle spindles are required for gamma motor neuron survival.

Moreover, chapter IV of this thesis addresses a potential role of Err3 in a neurodegenerative disease model for amyotrophic lateral sclerosis (ALS).

Chapter II –INTRODUCTION

Identification of Neuronal Subtype Specific Genes in the DRG and the beginning of a never ending story

To understand complex neuronal network assembly, we study the formation of the monosynaptic stretch reflex circuit. We expect that understanding the underlying mechanisms within this circuit may show case principle applying also to more complex neuronal network assembly. The monosynaptic stretch reflex circuit is easily accessible and consists of two main neuronal components, the dorsal root ganglia (DRG) sensory neurons (SNs) and the motor neurons (MNs) in the ventral spinal cord. Only a few neuronal markers were identified in proprioceptive afferents, whereas no specific molecular marker is known for subpopulations of proprioceptive afferents, namely Ia, Ib or II afferents. Identification of markers could facilitate studies of subpopulation differences of functionally similar classes of neurons such as proprioceptive afferents. In addition, for example GFP driven tracing experiments of these markers, might allow differentiating innervation patterns, axonal morphology or synaptic morphology of these very similar neuronal groups.

Cell body positioning of DRG SN subpopulations is highly dispersed and methods to label individual subpopulations are lacking. Profiling of gene expression of sensory neuron subpopulations has been limited by technical difficulties to obtain samples of functionally pure populations. During my thesis, we established techniques to be able to overcome these problems.

Transgenic mouse strains in which specific subpopulations of neurons are labeled with green fluorescent protein (GFP) allowed us the separation of pure neuronal subpopulations of DRG neurons. Subsequent RNA isolation and gene expression profiling studies revealed a number of genes expressed in distinct patterns in the DRG, but also in the spinal cord. Previous studies also showed that pure neuronal subpopulations facilitate generation of precise genetic fingerprints (Arlotta et al., 2005; Loconto et al., 2003; Nelson et al., 2006; Sugino et al., 2006; Tietjen et al., 2005). Identification of molecular markers at different developmental time points or of different subpopulations

can help to discover transcriptional networks specifying neuronal subpopulations.

Our experiments were focused on three major approaches: First, we isolated genes with enriched expression in the lumbar proprioceptive afferent population, but not cutaneous afferents. A whole outline of our screening approach is shown in Figure 2.

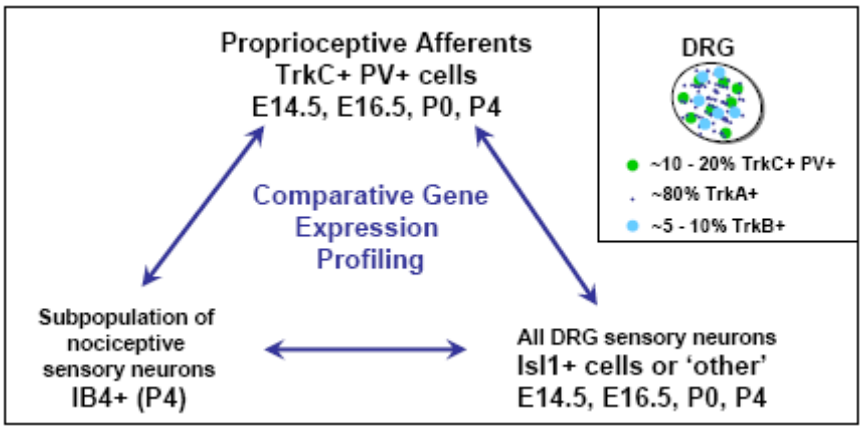

Figure 2: A temporal approach to identify genes specifically expressed by proprioceptive afferents and not cutaneous afferents (IB4+ or TrkC- SNs)

Second, gene expression profiling experiments from very low cell numbers (50-100 cells) allowed the isolation of genes expressed within the coarse classification of Trk receptor subpopulations in all lumbar DRG, but even at specific spinal levels.

A third approach was performed to isolate genes that are differentially regulated in wild-type versus *Er81* mutant proprioceptive afferents (Arber et al., 2000). The ETS transcription factor Er81 is known to play an important role in connectivity between Ia proprioceptive afferents and motor neurons in the developing spinal cord.

Chapter II - RESULTS & DISCUSSION

Using transgenic mouse lines that express GFP in a number of cell types, we isolated three main DRG SN subpopulations at different developmental stages. This enabled us to perform a detailed gene expression profiling analysis with focus on genes highly expressed by proprioceptive afferents around the developmental time point when synapses form between sensory and motor neurons.

GFP Expressing Mouse Lines – the Basis for the Identification and Isolation of Neuronal Subpopulations

Previous work has generated several transgenic mouse lines to genetically label neuronal subpopulations in the DRG. For most of the analysis, we have used a binary Cre-based genetic system to express GFP selectively in proprioceptive afferents, but not in other DRG sensory neurons (Figure 3, (Hippenmeyer et al., 2005)).

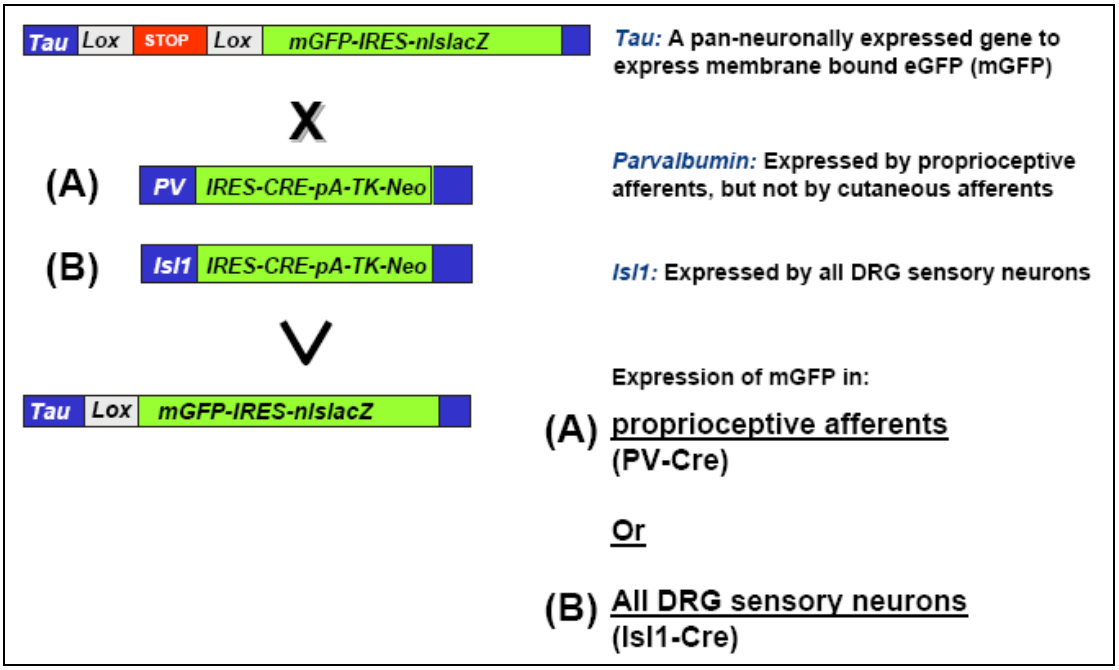

Figure 3: Selective labeling of neuronal subpopulations using a binary Cre-based genetic system. Membrane-linked GFP is activated under the control of the *Tau* promoter in a conditional manner by insertion of a floxed - stop - cassette. Two different Cre lines were used to induce GFP expression. The *PV-Cre* line activates expression in proprioceptive afferents and *Isl1-Cre* mice induce GFP expression in all DRG sensory neurons.

These mouse lines express high levels of membrane-linked GFP under the control of the *Tau* locus allowing to visualize GFP+ proprioceptive afferents and their projections. After cell dissociation procedures of DRG sensory neurons, GFP positive neurons were isolated to purity using Fluorescent Activated Cell Sorting (FACS) as shown in Figure 4.

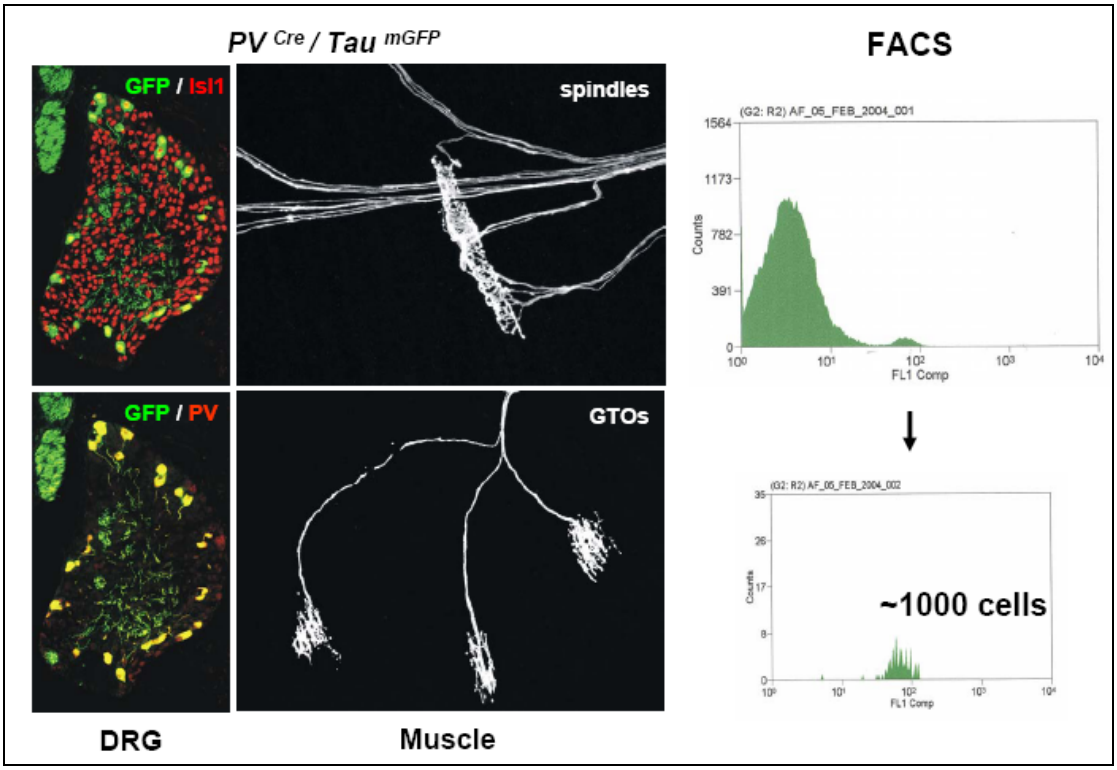

Figure 4: Expression of GFP and PV overlap in the DRG. GFP marks projections into the periphery innervating muscle spindles and Golgi Tendon Organs (GTOs). Isolation of GFP+ neurons of DRG subpopulations using fluorescent activated cell sorting (FACS).

Due to very low cell numbers acquired after cell sorting, methods were established allowing the usage of small RNA quantities in gene profiling experiments. When we started our gene profiling studies on selective neuronal subpopulations, unfortunately not many studies were published describing reproducible whole genome gene expression profiling experiments using Affymetrix GeneChip technology (Klur et al., 2004; Tsujino et al., 2000). The general protocols required a minimum of at least

5µg RNA, better 15µg, as starting material for Affymetrix based hybridization experiments.
Single – cell RNA amplification methods resulted in low “present calls”, meaning the total number of probe sets predicting a present signal was lower than known from whole tissue samples. Moreover, in this study less than 20% of amplified cDNA samples could be used for further gene array hybridizations due to failing expression of house - keeping genes, which were used as positive control and quality measure (Tsujino et al., 2000).

Knowing the difficulties with these state of the art experiments, it was crucial to perform a set of control experiments to address additionally to previous studies the following issues:

A) The effect of amplified RNA versus non amplified RNA in gene expression profiling experiments

B) The effect of different RNA quantities as starting material in RNA amplification reactions for gene expression profiling experiments

C) The effect of fluorescent activated cell sorting (FACS) on gene expression profiles

Comparative Analysis of Amplified RNA versus non-Amplified RNA in Gene Expression Profiling Experiments

Dealing with very low cell numbers, limited the RNA quantities for gene expression analysis. Consequently, we established RNA amplification techniques to overcome these limitations to make use of the limited RNA isolated from DRG subpopulations. Previous studies had shown undesirable side effects, such as irreproducibility of RNA amplification techniques (Klur et al., 2004; Tietjen et al., 2003). Therefore, it was crucial to control the effect of RNA amplification in our experiments. At the beginning of our studies, RNA amplification protocols had been used in a few labs as mentioned above, but it was a highly debated topic, because no study focused in detail on the effect of

RNA amplification and on differences between amplified and non amplified RNA expression profiles.

We isolated RNA from lumbar DRG L1 – L6 of 25 embryos at developmental stage E16.5. This RNA was isolated using the Qiagen RNA isolation kit. Subsequently, the RNA was diluted into different aliquots with the concentration of 10, 100, 1000 and 10,000ng/µl. The 10 and 100ng samples were amplified prior to cRNA synthesis and compared in gene chip expression profiling experiments to the non-amplified RNA samples of 1000 and 10000ng/µl RNA as starting material (Figure 5).

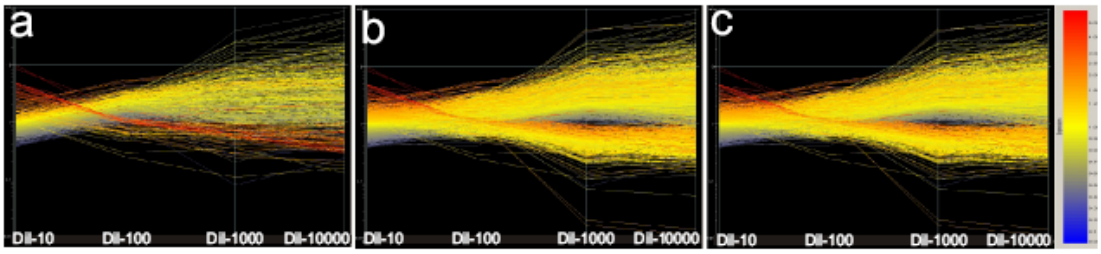

Figure 5: Evaluation of a RNA amplification technique. On the y-axis the signal intensity is shown for given RNA quantities in a log scale. The x-axis represents different RNA concentrations of starting material. a) 513 genes differentially regulated between the amplified samples (10 and 100ng/µl). b) 2558 genes differentially regulated between amplified and non-amplified RNA samples (10 and 1000ng/µl RNA). c) 3062 genes differentially regulated between lowest amplified and highest non-amplified sample (10 and 10000ng/µl).

We found not only as previously described that genes expressed at a low level under-amplify and very high expressed genes over-amplify (Klur et al., 2004). We are able to show that low expressed genes may either over- or under - amplify and vice versa. The same is true for very high expressed genes. The effect of differential amplification efficiency may be based on different GC contents and their secondary structures. Another possibility for the amplification bias might be the binding strength of the polymerases to certain templates. We conclude that RNA amplification is a non-linear process resulting in biased ratios between transcripts after the amplification reaction.

Due to this amplification bias of different starting quantities, it must be considered that genes, which appear in a gene expression profile to be many fold up-regulated, in reality, might simply have the potential to amplify easier and that there is no underlying biological reason for this up-regulation. Surprisingly, we also observed a bias within the amplified RNA datasets (Figure 5). Comparing the gene expression profile of the amplified 10ng and 100ng RNA samples, we see that 513 genes are significantly different between these two conditions. This means that we not only receive an amplification bias within non - amplified and amplified RNA samples, but also within amplified samples of different RNA starting concentrations.

This prompted us to investigate expression profiles from defined cell numbers isolated from one batch of cells after FACS.
We compared gene expression maps from 300, 1000, 5000 cells. Using the same batch of cells, we observe again, that some genes have a tendency to amplify easier than other genes resulting in different transcript concentrations after the amplification reaction. Interestingly, we are able to show that this effect is more severe when we analyze expression profiles of very low cell numbers. Comparing the gene expression profile of 300 versus 1000 cells, 139 genes were at least 2 fold differentially regulated, although the initial batch of cells was the same. Comparing the expression profile of 300 versus 5000 cells, 439 genes were differentially regulated. Comparing the gene expression profile of 1000 versus 5000 cells resulted in almost one identical gene expression profile. Here, 11 genes were at least 2 fold differentially regulated between these 2 conditions (Figure 6). For all profiling experiments, we received reproducibly present calls of about 50%.
This would be the expected present call value of non – amplified RNA samples from whole tissues such as heart or liver. Furthermore, this number also served as control parameter for all gene array experiments to illustrate the degree of occurred RNA degradation and to monitor the efficiency of the RNA amplification reaction.

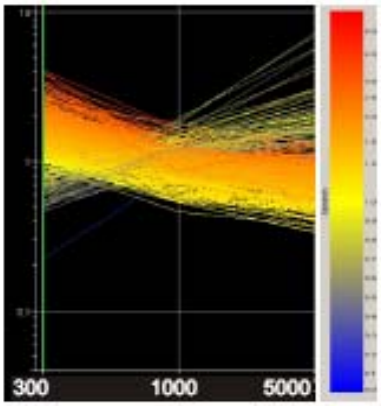

Figure 6: Amplification efficiency using different cell numbers from the same batch of cells. The graph shows certain genes over- or other under-amplifying. Consequently, only RNA samples acquired of the same cell number should be compared to each other.

We decided to sort the cells directly into lysis buffer to prevent any cell loss. To test whether the lysis buffer itself has an effect on the RNA, because the sorting process might take up to a few hours, we sorted GFP+ DRG SNs from one batch of cells at postnatal day P4. Duplicates of samples were sorted at two time points with a break in between of 1.5 hours (t1 and t2). Resulting gene expression analysis revealed only two genes passing a 1-way ANOVA – analysis with at least a two fold change between the two time points t1 and t2 (Figure 7). This result suggests that the RNA in lysis buffer seems to be preserved and stable for a few hours without significant RNA degradation processes. Nevertheless, keeping the cells on ice or a cooled environment prior the sorting procedure may be an additional measure of precaution in order to prevent RNA degradation in intact cells.

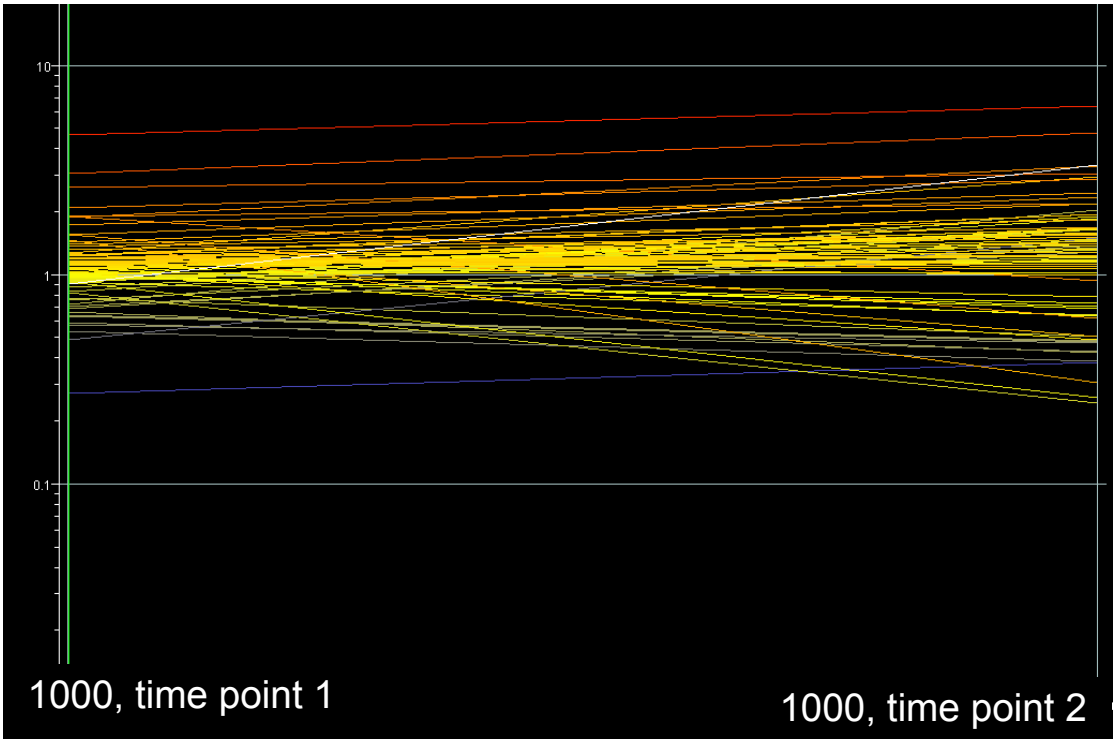

Figure 7: Effect on expression profiles of DRG neurons before and after FACS. Considering only expression data with a cut-off raw value >50 and a fold change of at least 2, only 78 genes are differentially regulated between t1 and t2. By applying a 1-way ANOVA test only two genes were differentially regulated between t1 and t2.

Overall, we considered several issues in our expression profiling experiments to obtain optimum results using RNA amplification techniques. We have shown that amplified samples should not be compared with non-amplified samples. If RNA amplifications are used, same concentrations of RNA samples should be used to minimize the bias due the tendency of over- or under-amplification. Genes expressed at a low level appear to be more affected, as our analysis revealed greater variability. The same holds true when comparing the expression profile of different cell numbers to each other. The same rules might be the basis for other applications to obtain RNA quantities from small cell numbers, such as Laser Capture Microscopy (LCM).

By comparing gene expression profiles from whole tissues with our acquired data on small neuronal subpopulations, we can observe a sensitivity threshold in the data received from these small neuronal subpopulations. As already previously described, whole tissue preparations seem to be more stable and

reliable considering whole genome wide analysis (Tietjen et al., 2003). In contrast to other studies, we describe the limitations of RNA amplification techniques using a few cells only isolated by FACS for gene expression profiling experiments.

Nevertheless, we are able to show that the RNA amplification method combined with Affymetrix GeneChip technology are powerful tools to perform gene expression profiling studies from small cell numbers isolated by FACS under certain conditions, which should be followed throughout all gene profiling experiments.

Pinpointing Novel Proprioceptive Markers for further Analysis

After establishing gene expression analysis from small cell numbers and validating various mouse lines aimed at identifying novel marker genes, a further challenge was to identify the right genes for further analysis. We decided to focus our initial screens on genes expressed at late embryonic and early postnatal stages at a time point when proprioceptive afferents form connections to motor neurons. Genes expressed highly around developmental time point E16.5 by proprioceptive afferents may play important roles in synapse formation, whereas genes highly induced shortly after may regulate synapse strengthening or maintenance (Arber et al., 2000). To get a first impression about the quality of our gene chip results, we asked whether known proprioceptive marker genes are expressed in our gene array experiments in a selective manner as well. We analyzed the expression of 4 genes known to be selectively expressed by proprioceptive afferents; *PV*, *Runx3*, *Er81* and *TrkC*, whereas *Er81* is also expressed by a set of cutaneous neurons from late embryonic stages on (Arber et al., 2000; Kramer et al., 2006). As shown in Figure 8, these four genes show highly enriched expression profiles in the GFP+ population after FACS and gene array analysis.

Gene	Fold Change Raw GFP+ vs GFP- population
Runx3	**67.9**
Er81	**7.7**
PV	**33.9**
TrkC	**47.7**

Figure 8: Known proprioceptive markers are highly enriched in sorted GFP+ cells.

In contrast, pure cutaneous markers are highly enriched in the GFP negative population. *TrkA* is the most enriched gene with a fold change of 100 compared to the GFP positive proprioceptive population. Very similar to *TrkA*, the cutaneous marker *Runx1* is 50fold up-regulated. After validating our approach, we sought to identify new markers genes, specifically expressed

within the TrkC positive population. We performed a candidate based gene approach. Here, we picked genes with high raw values, but also high fold changes between the GFP positive and negative population. Furthermore, we aimed to identify genes that potentially regulate developmental processes such as neuronal diversification, axon guidance and target cell recognition.

To validate the genes identified using an independent method, we focused on *in-situ* hybridization (*ISH*) techniques. Where applicable we also used antibodies to stain for the protein of interest. Furthermore, we made use of a strain of mice in which proprioceptive afferents are lacking. These mice are mutant for the neurotrophin receptor TrkC (Klein et al., 1994). Genes specifically expressed by proprioceptive afferents should be not expressed in mutant DRG of this line.

When we compared expression of some of our top candidates between wild-type and *TrkC*$^{-/-}$ mutant mice on DRG, we indeed found that many of these genes are not expressed in DRG neurons of *TrkC*$^{-/-}$ mutants. On our list, we identified molecules of the axon guidance family. Figure 9 shows expression of Slit2 and Robo1. We also found transcription factors previously not known to be expressed by proprioceptive afferents. As an example, estrogen related receptor 3 is shown in Figure 9. Interestingly, we also found a number of G-protein coupled receptors with highly enriched expression patterns (Figure 9).

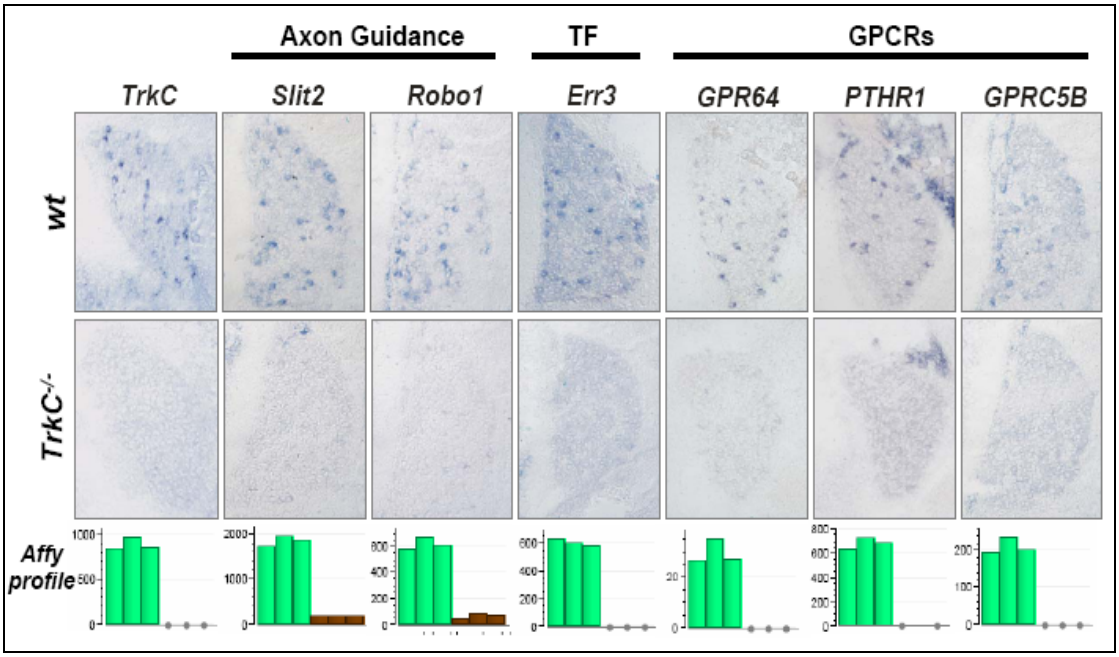

Figure 9: Validation of genes using *in-situ* hybridization experiments on lumbar DRG. The top panel shows genes expressed specifically by proprioceptive afferents confirmed by the absence of expression in the *TrkC*$^{-/-}$ mutant mouse line. The bar graphs on the bottom of the figure represent the raw expression value of the individual gene; in green of PV+ GFP+ cells and in brown of the GFP-, mainly cutaneous DRG population.

A number of other genes (GPR97, Protocadherin 8, Cadherin 13 etc.) have also been verified by *ISH* techniques and are listed in the Appendix. Since the expression of many genes had been confirmed *in vivo*, it is tempting to speculate that genes, which expression had not yet been confirmed by ISH yet, are truly expressed as shown by the expression data.

Of particular interest to us were genes not expressed by all proprioceptive afferents in order to identify programs involved in neuronal subtype specification. So far no marker gene has been identified with an expression pattern restricted to subsets of proprioceptive afferents. These genes could potentially mark Ia proprioceptive afferents forming direct synapses with motor neurons in the spinal cord or Ib afferents that connect to interneurons in the intermediate spinal cord. As discussed already in the introduction, peripherally, these neurons exhibit distinct termination zones in the muscle. Ia afferents terminate on muscle spindles, whereas Ib afferents project to the Golgi Tendon Organs (GTOs) of muscles. Figure 10 shows two such

examples. *Reg2*, a protein previously implicated in MN survival (Nishimune et al., 2000) and the well known growth factor *IGF1* both showed expression profiles with restricted proprioceptive afferent association. *Reg2* is expressed exclusively by very few proprioceptive afferents. In contrast, *IGF1* is expressed by subpopulations of proprioceptive afferents but also some other subpopulations of DRG neurons as became apparent when analyzing its expression pattern in *TrkC* mutant mice.

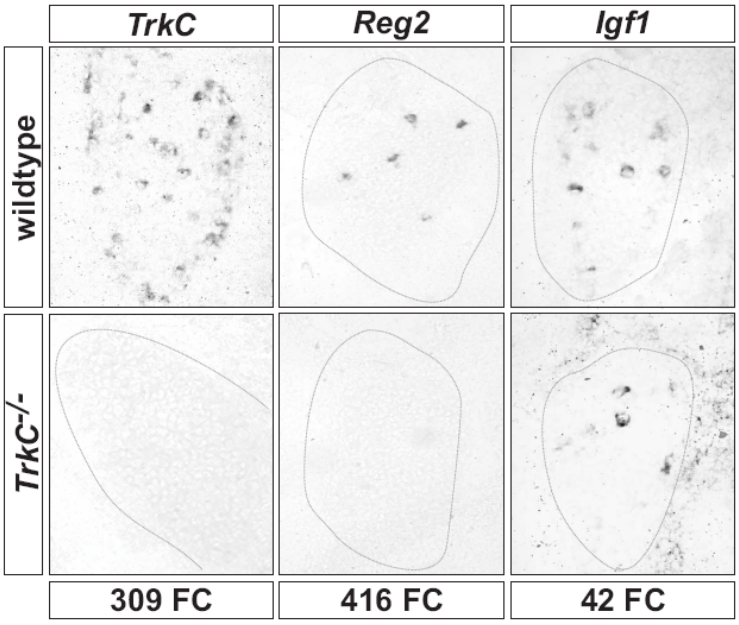

Figure 10: Expression of two genes expressed by subsets of proprioceptive afferents. *Reg2* is expressed exclusively in subsets of proprioceptive afferents, whereas *Igf1* expression is also observed in TrkC negative cells. (FC = Fold Change)

Neuronal development and circuit assembly involves a number of defined mechanisms including cell migration, axon guidance and nerve branching. Therefore, it was not surprising to us to identify molecules involved in these processes. Slit proteins and their Robo receptors are known to have crucial functions in these processes in the brain and spinal cord. Classically, Slit - Robo signaling was described as a repulsive axon guidance mechanism to prevent midline crossing and control cell migration (Bagri et al., 2002; Brose et al., 1999; Kidd et al., 1999; Nguyen-Ba-Charvet et al., 2004; Wang et al., 1999). Slit2 has been shown to also act positively on axon elongation and branching of isolated DRG sensory neurons (Wang et al., 1999). During

development, DRG neurons reach the dorsal root entry zone of the rat spinal cord at developmental time point E12 and bifurcate. Daughter axons run a few segments along the longitudinal axis, before entering the spinal cord (Altman and Bayer, 1984). Slit and Robo proteins are expressed in the spinal cord and DRG neurons. More specifically, expression of Slit proteins in the dorsal spinal cord along the dorsal root entry zone can be observed in rat at E13.5, which is the time point when collaterals start to sprout (Brose et al., 1999; Ma and Tessier-Lavigne, 2007; Wang et al., 1999). Culturing of NGF responsive DRG neurons, which belong to the class of thermo- and nociceptive neurons, respond to the addition of Slit2, brain or spinal cord extracts, by an increase to axon length and branching. The overlapping expression of Slit and Robo proteins in DRG neurons suggest an autocrine/paracrine mode of action to promote proper axonal ingrowth into the spinal cord (Wang et al., 1999). Our data in fact show enriched expression of *Slit2* and *Robo1* at E16.5 specifically in mouse proprioceptive afferents (Figures 9 and 11), suggesting that the Slit2 dependent axonal branching of cutaneous DRG neurons is likely to be dependent on a paracrine and not autocrine mode of action of Slit2 *in vivo*.

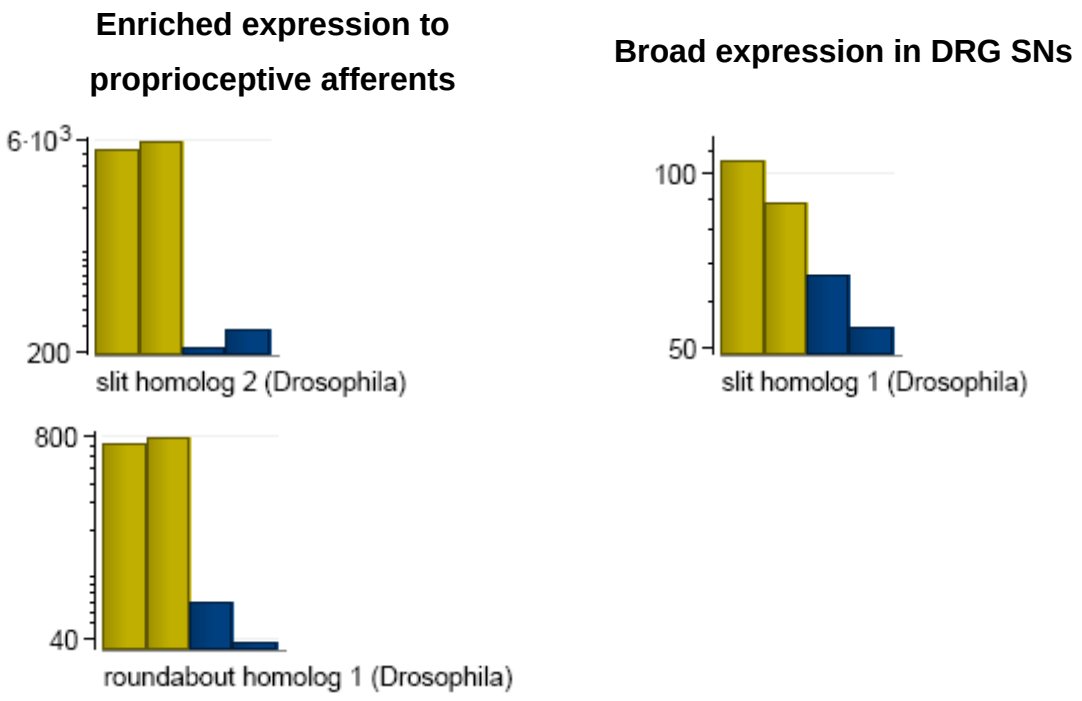

Figure 11: Enriched expression of *Slit2* and *Robo1* in proprioceptive afferents. In contrast, *Slit1* is likely expressed by all DRG sensory neuron subpopulations.

Analysis of *Slit1;Slit2* or *Robo1;Robo2* double deficient mice showed recently that Slit/Robo signaling is not required for the formation of DRG central collaterals (Ma and Tessier-Lavigne, 2007). Instead, longitudinal expression of Slit1 and Slit2 at the dorsal root entry zone has been shown to be crucial for branch repelling actions on DRG neurons. *Slit1;Slit2* or *Robo1;Robo2* double mutant mice exhibit severe misprojections of sensory afferents into the dorsal spinal cord. Thus, Slit/Robo signaling plays a significant role in sensory axon growth and bifurcation (Brose et al., 1999; Ma and Tessier-Lavigne, 2007; Wang et al., 1999).

The complexity of Slit/Robo signaling in axon guidance even further expands as shown recently by the action of two antagonistic isoforms of Robo3. This is a mechanism described so far only for commissural axons in order to inhibit pre- and recrossing of the midline by expressing two different Robo3 isoforms (Chen et al., 2008).

Using our DRG sensory neuron subpopulation specific screening strategy, we were now able to categorize expression of gene families to defined DRG sensory subpopulations. Slit and Robo expression is exemplarily depicted and outlined in Figures 9 and 11.

G protein – coupled receptor Expression in DRG Sensory Neurons

Underlying mechanisms of cell – cell interactions can be revealed by specific secreted molecules such as hormones, neurotransmitters or ions and corresponding groups of cell surface receptors. In our screen, we have identified a number of molecules functioning in cell – cell interaction processes. Cadherins, Protocadherins and various G protein - coupled receptors (GPRs) are only a few of these classes. In the following paragraphs, the differences and expression patterns of a number of GPRs in DRG sensory neurons will be discussed in more detail.

GPRs, also called seven – transmembrane receptors (7TM receptors), have distinct extracellular domains and ligand binding properties. GPRs comprise a panel of over 800 genes encoding different receptor proteins that represent an enormous potential of specific cell signaling players (Robbins et al., 2002;

Robbins et al., 2000; Vassilatis et al., 2003). Based on sequence similarity GPRs can be categorized into three main distinct families: A, B and C:

Group A represents the largest group of a few hundred members, including the rhodopsin-like and olfactory subgroup. Members of this subgroup primarily bind to amines and peptides and have short N termini.

Group B has approximately 25 members, including the secretin-like receptors.

Group C has only few members including the metabotropic-like receptor group containing the metabotropic glutamate receptor family, gamma-aminobutyric acid (GABA) receptors, a Ca^{2+} sensing receptor and taste receptors. This family is characterized by a very large extracellular amino terminal domain.

GPRs are activated upon ligand binding, which triggers the release of a G protein complex activating downstream cascades. To date many of these receptors are considered orphans as their ligands are still unknown (Gilman, 1987; Rodbell et al., 1971). In our screen, we identified three of these orphan GPRs. *ISH* experiments confirmed that *GPRC5B*, *GPR64* and *GPR97* are expressed specifically by proprioceptive afferents at late embryonic stages (Figure 9). GPRC5B belongs to the family of retinoic acid-inducible receptors and was first identified by searching for metabotropic glutamate receptor homologs, which were classified to type C GPRs (Robbins et al., 2002; Robbins et al., 2000). Retinoic acid affects cell growth, differentiation and apoptosis. Downstream retinoid signaling involves activation of at least two known nuclear receptors; namely retinoic acid receptor and retinoid X receptor (Robbins et al., 2002). Recent studies showed that retinoic acid inducible GPRs bind to frizzled receptors, which may lead to activation of the non-canonical Wnt signaling pathway (Harada et al., 2007). Interestingly, it has been shown that the non-canonical Wnt pathway regulates neural crest migration in Xenopus (De Calisto et al., 2005). Possibly one can speculate that this signaling cascade might also be important for neural crest migration of DRG neurons. GPRC5A and GPRC5C are also expressed in the DRG, but

not specifically by proprioceptive afferents. Unlike *GPRC5A* and *GPRC5C*, the *GPRC5B* is predominantly expressed in the spinal cord and brain (Robbins et al., 2002). We obtained the *GPRC5B*$^{-/-}$ mutant mouse line from Delatgen. Initial behavior tests showed an increase in their latency to respond to the hot plate test. It is unlikely that these sensory phenotypic changes are exclusively due to the loss of GPRC5B expression in proprioceptive afferents, since GPRC5B is also highly expressed in other brain regions like the cerebellum and in many neurons of the spinal cord as preliminarily analyzed by Deltagen.

GPR64 (HE6) and *GPR97* belong to the subfamily of the adhesion GPRs (Figures 9 and 12). Both are orphan GPRs, which are characterized by a distinct long N-terminus containing a number of domains also found in proteins, such as cadherin, lectin, laminin. This region might confer functional specificity in cell - cell or cell - extracellular matrix (ECM) interaction (Bjarnadottir et al., 2004), which are essential for cell communication in the central nervous system. Interestingly, as shown in Figure 12, GPR97 and GPR64 can be both categorized into the same phylogenetic cluster within the adhesion-GPR subfamilies.

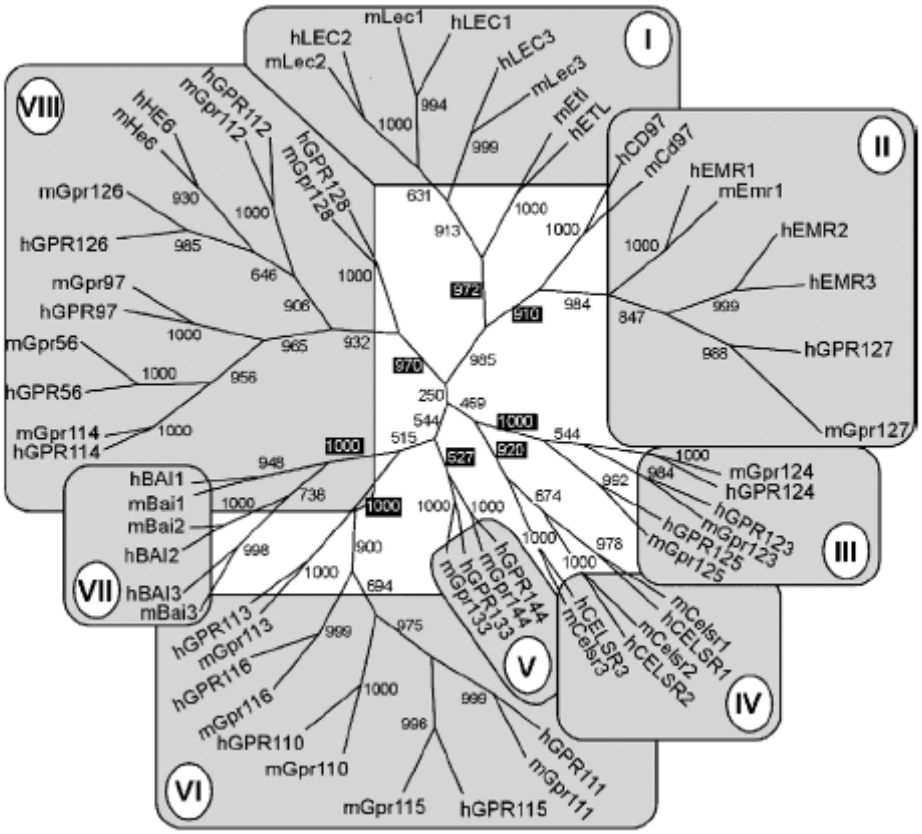

Figure 12: Phylogenetic analysis of eight subclasses of adhesion-GPRs in human and mouse. GPR64 (HE6) and GPR97 both identified in our screens to be specifically expressed by proprioceptive afferents fall into the same cluster of adhesion-GPRs (Bjarnadottir et al., 2004).

This clustering is based on structural amino acid similarity. Nevertheless, the degree of structural similarities within class VIII of the adhesion GPRs might reflect functional correlation.

GPR64 null mutants have been generated. Hemizygous males display a severe decreased fertility caused by a dysregulation of fluid absorption within the efferent ductus leading to a fluid accumulation (Davies B. *et al*, 2004). However, the role of GPR64 in proprioceptive neuronal differentiation has not been analyzed. Broad characterization of mutant animals does not show any defects in spinal reflex circuit assembly (data not shown). One reason might be a compensation effect by another closely related GPR, for example GPR97, which is also exclusively expressed by proprioceptive afferents.

The fourth seven – transmembrane receptor we isolated specifically in proprioceptive afferents, *parathyroid hormone receptor 1* (*PTHR1*), is also a member vaguely related to the adhesion GPR family. The PTHR1 is not a orphan GPR, but binds to parathyroid hormone (Pth) and parathyroid hormone-related peptide (Pthrp) (Guo et al., 2002; Kobayashi et al., 2002). Interestingly, our Affymetrix gene expression profiling data show that the *PTHR2* is enriched in the nociceptive DRG neuron subpopulation (data here not shown). Conditional elimination of *PTHR1*$^{-/-}$ in developing chondrocytes reveals a significant role of PTHR1 signaling in chondrocytes differentiation (Guo et al., 2002; Kobayashi et al., 2002; MacLean and Kronenberg, 2005).
Recently, it has been published that *in vitro* and *in vivo*, Pth/Pthrp signaling through PTHR1 specifically regulates ephrinB2 expression in osteoblasts. Inhibition of ephrinB2/EphB4 signaling resulted in defects of osteoblast differentiation (Allan et al., 2008). Interestingly, both ephrinB2 transcripts on our gene array show extremely elevated signals specific to the proprioceptive afferent population, whereas ephrinB3 and ephrinA1 show elevated expression in nociceptive DRG neurons. Therefore, the PTHR1 – ephrinB2 signaling cascade might also play a role in proprioceptive afferent differentiation.

In contrast to our identified GPRs, several other 7TM receptors had been found to be expressed in subsets of nociceptive DRG sensory neurons. One such class of proteins are Mrg genes (Mas-related GPRs) comprising a family of approximately 50 GPRs (Cox et al., 2008; Dong et al., 2001). Functional studies revealed the involvement of these GPRs detection of painful stimuli. Our and published data indicate that various GPRs are expressed in distinct subsets of DRG sensory neurons and suggest functional specificity in a cell type specific manner to control distinct signaling cascades.

Our data also identified differential expression of another class of proteins involved in cell to cell interaction and recognition. This group of proteins is called cadherins, which comprise a group of more than 100 members. Most of these cadherins are transmembrane proteins, which undergo either homophilic or heterophilic interactions. These molecules are characterized by

a repetition of their extracellular domains called cadherin repeats (Overduin et al., 1995; Shapiro et al., 1995; Wu and Maniatis, 1999). In our screen, we were able to identify a number of cadherins with enriched expression in certain subsets of DRG sensory neurons. Protocadherins reflect the largest subfamily of cadherins. Two such members identified with enriched expression in proprioceptive afferents are *Protocadherin 8* (*Pcdh8*) and *Cadherin 13* (*Cdh13*). Their validation by *ISH* can be found in the Appendix.

In the CNS, cadherins play several roles. On one side newly born neurons have to aggregate to form precise neuronal groups, such as brain nuclei, DRG or motor pools (Arndt et al., 1998; Suzuki et al., 1997; Yoon et al., 2000).

For the sensory – motor system, it has been shown that specific cadherin expression can be correlated to certain motor neuron pools in the developing chick spinal cord (Price et al., 2002). The expression of multiple cadherins in subsets of proprioceptive sensory neurons raises the possibility that these molecules also mark distinct sensory neuron pools and hence play a role in sensory – motor connectivity. Past studies underlined the hypothesis that cadherins have important functions in the development of synaptic connections (Boggon et al., 2002; Carroll et al., 2001; Patel et al., 2006; Redies, 2000; Wu and Maniatis, 1999). This is in particular interesting, because specific cadherin molecules could be localized to synaptic complexes in mouse hindbrain and cerebellum (Inoue et al., 1998) as well as to various other synaptic complexes in chick at the time or soon before synapses are formed (Arndt et al., 1998; Wohrn et al., 1998).

Cdh13 was shown to be expressed in cortico-spinal motor neurons (CSMNs) (Arlotta et al., 2005). A crucial aspect of these neurons is the ability to grow their extremely long axonal projections precisely to the termination zone in order to form connections to specific target cells. Strikingly, *Cdh13* is expressed by CSMNs and proprioceptive afferents, two cell types both forming connections with motor neurons in the ventral spinal cord. Therefore, it is tempting to speculate that expression of molecules such as Cdh13 is involved in such cell-cell interaction processes during the formation of the spinal reflex circuit.

More recently, it has been shown in chicken embryos that *Pcdh1* is expressed in developing chick DRG and plays a crucial role in localizing neural crest cells to DRG (Bononi et al., 2008).
Interestingly, Pcdh8 is among others a Pcdh member for which RNA splicing yields to a neural-specific variant (Makarenkova et al., 2005). Furthermore, a Pcdh8 – like molecule was identified to be induced in brain neurons upon synaptic activity. Blocking of this molecule using antibodies causes a reduction in the excitatory postsynaptic potential amplitude and blockage of long – term potentiation in hippocampal slice cultures (Redies, 2000; Yamagata et al., 1999). Future work with this respect could address the question whether *Pcdh8* expression in subsets of proprioceptive afferents plays a role in synaptic activity of sensory – motor connections of the monosynaptic stretch reflex circuit.
Considering the vast repertoire of Pcdhs and their potential splice variants, it has been postulated that these molecules play a similar role in the vertebrate nervous system like DSCAM molecules in *Drosophila*. Studies over the past years identified that splicing variants of the *Drosophila Dscam* (Down syndrome cell-adhesion molecule) gene give rise to a vast number of cell surface proteins with distinct recognition properties. The variable domains utilize a vast majority of alternative exons encoding in total 19008 different ectodomains (Kohmura et al., 1998; Wojtowicz et al., 2007; Wu and Maniatis, 1999). The divergent expression of cadherins in the DRG might therefore represent a vast repertoire of underlying cell to cell interaction molecules, which possibly plays an important role in the specification of sensory - motor system.

As shown in Figure 10, we identified the *Igf1* gene to be expressed in subpopulations of DRG sensory neurons. Igf1 is known as a potent growth factor and plays important roles in mammalian growth and development. In the CNS, Igf1 was described to function as survival factor, to be involved in sensory map formation, axon guidance and synapse maturation (Chiu et al., 2008; Leinninger et al., 2004; Scolnick et al., 2008). A more precise role of Igf1 will be discussed with respect to the level specific screen.

Reg2 is a further gene identified in our screen with a very interesting expression pattern. In the DRG, a dynamic shift of Reg2 expression is observed after peripheral nerve transection. Only 24 hours after nerve injury Reg2 expression increases rapidly in small DRG SNs, whereas 7 days after nerve crush Reg-2 is expressed selectively in medial and large DRG SNs (Averill et al., 2002). It was shown that Reg-2 expression is expressed in a very dynamic manner in subpopulations of motor neurons during development in rat spinal cord (Nishimune et al., 2000). Furthermore, Reg2 is secreted and acts through an unknown receptor as neurotrophic factor either in an autocrine or paracrine manner to stimulate motor neuron survival through the PI3K/Akt pathway (Nishimune et al., 2000). Possibly in the DRG, Reg2 expression is involved in sensory neuron survival. As it will be discussed in the level - specific screen (next paragraphs), *Reg2* expression is highest in the C7 and L5 DRG, which are the biggest DRG and contain most neurons. Whether there is a role in sensory neuron survival in very low *Reg2* expressing DRG, can only be speculated. In adult, *Reg2* expression is down-regulated to only a very few DRG sensory neurons (Averill et al., 2002). It is possible that Reg2 expression functions in the neuronal survival pathway since it has been shown that it is a signaling intermediate in the CNTF motor neuron survival pathway (Nishimune et al., 2000), which was demonstrated to alleviate vulnerability of motor neurons in vivo of ALS mice.

The orphan nuclear-related receptors and in particular the estrogen-related receptor gamma (Err3) will be outlined in more detail discussing the Er81 downstream cascade and in chapter III.

Our screen was aimed at the identification of novel proprioceptive marker genes. We were able to isolate a number of genes which expression was so far not known to be enriched by proprioceptive afferents. In addition, we have shown that underlying specificity in gene expression of very similar neuronal subpopulations is to a certain extent based on the expression of distinct members of certain gene families. In this thesis, we described so far the expression of two such gene families, namely cadherins (also including the Protocadherin subfamily) and G protein-coupled receptors in further detail.

We next used our knowledge of how to acquire gene expression profiles from small numbers of cells to analyze genetic profiles of even smaller sensory neuron subpopulations. In this approach we profiled DRG sensory neuron populations of defined segmental levels throughout the entire anterior to posterior axis.

Level Specific Gene Expression Profiling of Proprioceptive Afferents

After establishing techniques to find novel proprioceptive markers, we pushed our analysis even further to perform a screen to isolate proprioceptive markers of specific segmental levels along the entire rostro - caudal axis. This strategy allowed us to enrich for genetic fingerprints associated with so called sensory neuron (SN) pools at different spinal levels. SN pools are associated with MN pools and project to defined motor neurons or muscles in the periphery. So far it has been shown by retrograde cell tracing experiments that motor neurons in the spinal cord are stereotypically organized into MN pools (Landmesser, 2001).

In contrast to the well arranged patterns of motor neurons into pools, DRG sensory neurons projecting to defined muscles in the periphery are intermingled, yet are found roughly in DRG at levels adjacent to MN pools in the spinal cord.

We reasoned that genes isolated through this level specific approach might be involved in specifying intrinsic cues programming proprioceptive afferents to innervate distinct muscles or muscle groups. As outlined in Figure 13, much progress has been made over the past years in the identification of molecular pathways specifying motor neuron subpopulations. Transcriptional programs such as the Hox, Ets and Pou class transcription factors are linked to specific MN pools (Dasen et al., 2008; Dasen et al., 2005; Vrieseling and Arber, 2006; Wu et al., 2008). It is known that there is a high degree of selectivity in sensory - motor connectivity centrally with preferential connections between sensory- and MNs projecting to the same muscle peripherally.

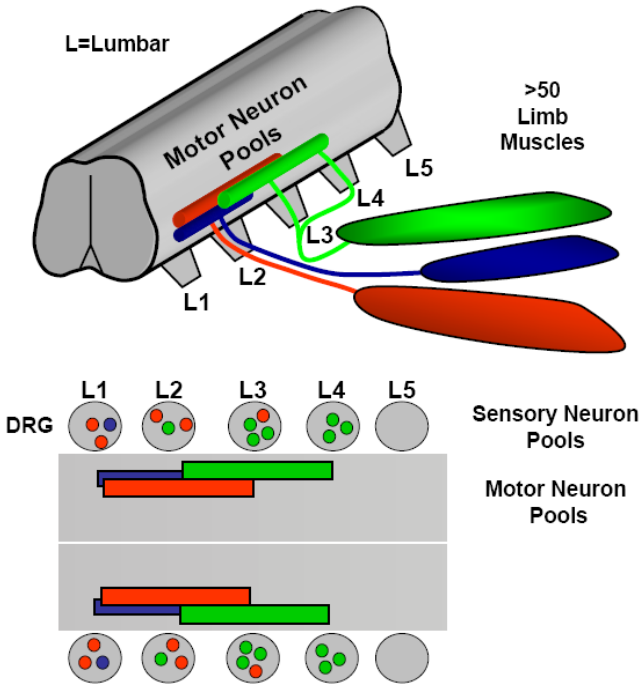

Figure 13: MNs in the ventral spinal cord are organized into so called MN pools and project to defined muscles in the periphery (upper panel). These MN pools express distinct transcription programs such as Hox, POU and Ets transcription factors.
In DRG, DRG sensory neurons projecting to one muscle are not clustered.

The following paragraph will outline the organization of MN pools in the spinal cord and the underlying transcriptional programs involved in their development.

Hox'ing Motor- and DRG Neuron Identity

According to their nomenclature, Hox genes encode a number of homeodomain transcription factors. In *Drosophila*, these factors were shown to control transcriptional programs along the anterior to posterior body axis of animals in order to specify functionally distinct body regions on different segmental levels (Gehring, 1993; Schier and Gehring, 1992). These proteins can either function as activators by enhancing expression of genes to specify a particular body part and they repress transcription of undesired genes, which are relevant to form other body parts.
In the mammalian nervous system it has been shown that a Hox regulatory network specifies postmitotic MN pool identities, such as specific target innervation patterns, expression of distinct molecular profiles and stereotypic cell body positioning in the spinal cord. Hox genes are expressed in distinct motor neuron columns and pools. The lateral motor column (LMC) is specified by Hox6 and Hox10 expression in the brachial and thoracic region, respectively. Preganglionic motor neurons (PGC) in the thoracic level are

specified by Hox9 expression. More specifically, a hox combinatorial code also defines MN subpopulations. As described for the brachial MN pools, further Hox specific clusters specify MN pool identity (Dasen et al., 2008; Dasen et al., 2005).

Manipulating Hox expression in specific MN pools, consequently changes patterns of connectivity and muscle innervation (Dasen et al., 2005). For example, mouse mutants for Hoxc10 and Hoxd10 show severe hindlimb locomotor defects due to failures in MN pool organization, specifically in the lumbar spinal cord (Wu et al., 2008). Recent studies showed that the transcription factor FoxP1 is a key regulator in establishing motor columnar identity during development. *FoxP1*$^{-/-}$ deletion results in non-diversifying MNs, which lack multiple characteristic molecular markers. On the other hand blockade of Hox activity eliminates FoxP1 expression (Dasen et al., 2008; Rousso et al., 2008).

These data show the necessity for a precisely controlled Hox regulatory network to establish MN pool identities, which form selective connections to their target muscles.

Within the DRG, such transcriptional networks to set up SN pools have not been described, yet. We will address the question, whether we can identify similar genetic programs in DRG subpopulations, which potentially might be involved in sensory neuron diversification as it has been found for motor neurons. To isolate level – specific sensory neurons, we purified proprioceptive afferents from defined segmental levels, in order to perform subsequent Affymetrix gene expression analysis. We decided to profile proprioceptive afferents from six segmental levels in the spinal cord as outlined in Figure 14.

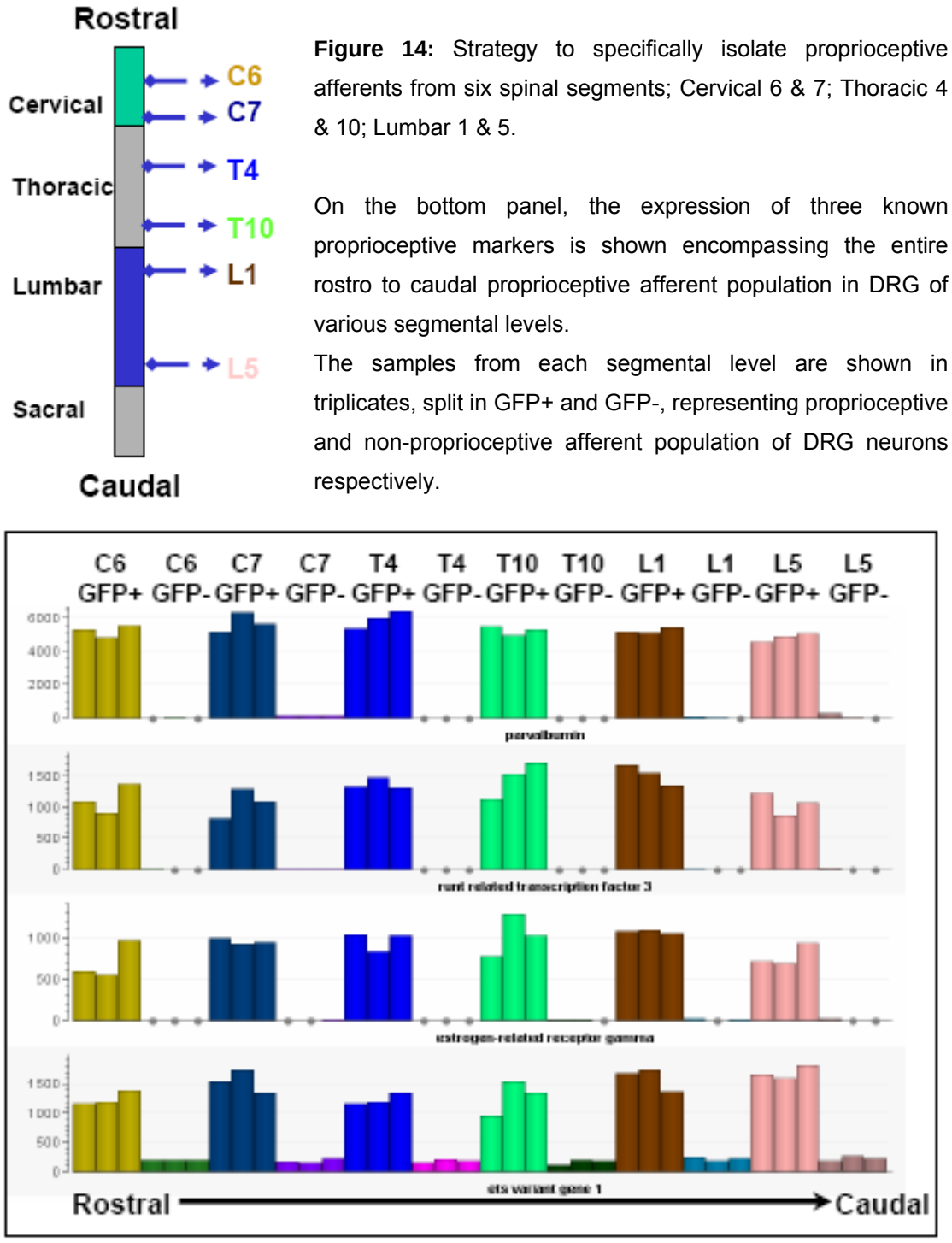

Figure 14: Strategy to specifically isolate proprioceptive afferents from six spinal segments; Cervical 6 & 7; Thoracic 4 & 10; Lumbar 1 & 5.

On the bottom panel, the expression of three known proprioceptive markers is shown encompassing the entire rostro to caudal proprioceptive afferent population in DRG of various segmental levels.

The samples from each segmental level are shown in triplicates, split in GFP+ and GFP-, representing proprioceptive and non-proprioceptive afferent population of DRG neurons respectively.

To profile the segmental levels indicated in Figure 14, we used 8 DRG from four animals dissected bilaterally in triplicates. Due to the fact that the number of isolated proprioceptive afferents from non – limb - level DRG was very low, we decided to use not more than 100 cells isolated from any segmental level. This strategy is based on our initial findings (Chapter II) that approximately the same cell number should be used in comparative gene expression profiling

experiments. Since we had no experience with gene expression analysis of such low cell numbers, we first analyzed genes, the expression of which we knew encompasses the entire rostro to caudal proprioceptive afferent population in the mouse. We focused our analysis on the expression of *Parvalbumin*, *Runx3*, *Er81* (*etv1*) and the newly identified transcription factor *Err3*. As illustrated in Figure 14, we obtained stable expression of all three triplicates for each gene in the GFP+ and GFP- population for all DRG sensory neuron subpopulations analyzed. It is important to note that the level of contamination by proprioceptive afferents into the GFP- cell population is negligible. No signal for *Parvalbumin*, *Runx3* and *Err3* was detected over threshold in the GFP- cell population. In contrast, a low Er81 signal was observed within the GFP- cell population, which can be explained by expression of *Er81* in the cutaneous cell population at late embryonic stages. These data are the basis for a further much more sensitive analysis to isolate genes with varying expression in proprioceptive afferents in rostro to caudal DRGs. As mentioned above, one set of candidates, which we analyzed in more detail were the genes of the Hox family. Previous studies described the expression of Hox genes in defined MN pools organized in a longitudinal manner in the spinal cord. Figure 15 outlines the expression of some selected *Hox* genes in DRG sensory neurons.

The first view illustrates quite diverse expression patterns of different *Hox* genes. Further Hox expression patterns are outlined in the Appendix. Intriguingly, we observe highest expression of *HoxA10* in lumbar DRG. This correlates very well with the observations of Dasen et al, 2005 described already for lumbar motor neuron pools. In contrast to *Hox9* paralog expression in PGC motor neurons (thoracic levels), in DRG sensory neurons *HoxD9* and *HoxA9* expression is highest in lumbar DRG (Figure 15 and Appendix). *Hox9* and *Hox10* paralogs are expressed independently of the cell type in the DRG (cutaneous or proprioceptive), but show rather increasing expression towards distinct segmental levels. In contrast, subpopulations of brachial motor neurons express pool spanning Hox6, Hox3, Hox4 and Hox7 paralogs, which can be clustered into bigger MN pools based on expression of HoxC8 and HoxA5 (Dasen et al., 2008; Dasen et al., 2005).

HoxC8 expression causes a cell - autonomous repression of HoxA5 and therefore forming sharp borders between two very similar neuronal subpopulations to form distinct rostro to caudal motor neuron pool identities. Very similar to the pool specific expression of HoxC8 and HoxC5 in motor neurons (Dasen et al., 2005), we also observe a very sharp border in expression of *HoxC8* and *HoxC5* among proprioceptive afferents in brachial and thoracic levels.

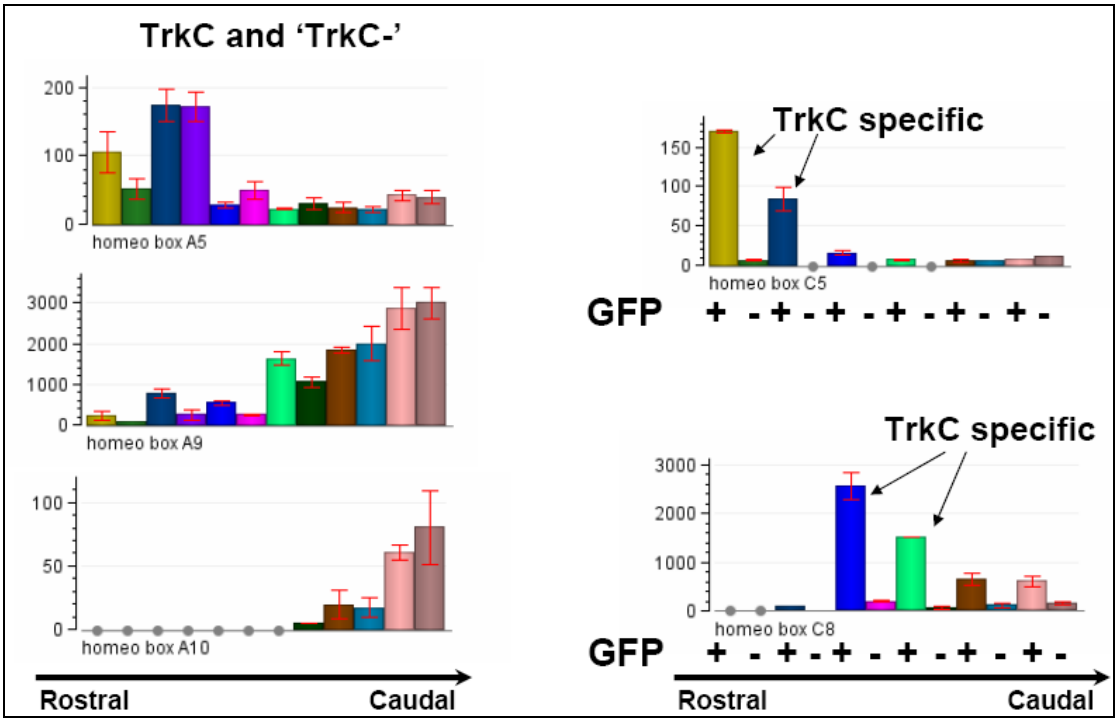

Figure 15: The left panel illustrates Hox gene clusters with increasing expression in cutaneous and proprioceptive afferents from anterior to posterior DRG, here depicted *HoxA5*, or vice versa as shown for *HoxA6* and *HoxA10* DRG. On the right side of the graph, we found *HoxC5* expression specifically by anterior proprioceptive afferents, whereas *HoxC8* expression declines in proprioceptive afferents from thoracic to lumbar levels. (Colors in bar graphs match with colors and segmental levels in Figure 15).

Brachial proprioceptive afferents express high levels of *HoxC5* diminishing posteriorally towards thoracic DRG. Proprioceptive afferents at the segmental level T4 express high levels of *HoxC8*, where *HoxC5* expression is lowest, and declines towards lumbar levels. The GFP- cutaneous afferent population

does not show any specific patterns of these genes. Transcripts for *Hox6* are not present on the gene array; therefore we cannot analyze its expression in DRG sensory neurons. However, just like in motor neurons, *Hox3* and *Hox7* paralogs do not show any particular expression either towards a certain DRG sensory neuron subpopulation nor expression restricted to DRG on certain segmental spinal levels.

In summary, we discovered very intriguing Hox gene expression patterns in DRG along various segmental levels and also within distinct DRG sensory neuron subpopulations. We found Hox genes with restricted expression patterns towards caudal or rostral DRG. More importantly, the two genes *Hoxc8* and *Hoxa5*, in our experimental setup show expression patterns with very similar characteristics as previously described to establish motor neuron pool identity. This raises the question of whether these genes play similar roles in the DRG to specify proprioceptive afferent subpopulations at different rostro-caudal levels.

Other Factors with Restricted Expression Patterns Along the Rostro–Caudal Axis

In our level-specific screen, we not only identified novel proprioceptive afferent markers. As shown in Figure 10, *Reg2* and *Igf1* were found already before to be expressed in subsets of proprioceptive afferents. Our level specific approach though revealed expression of *Reg2* mainly in C7 and L5 DRG (Figure 16 and 17). *Igf1* shows clear enriched expression in L5 and C7 DRG, but with no restriction to the proprioceptive afferent population as shown before already in Figure 10. A third gene we found to be expressed specifically by proprioceptive afferents in a level - specific manner is the *Gamma-aminobutyric acid receptor, gamma-1* (*Gabrg1*).

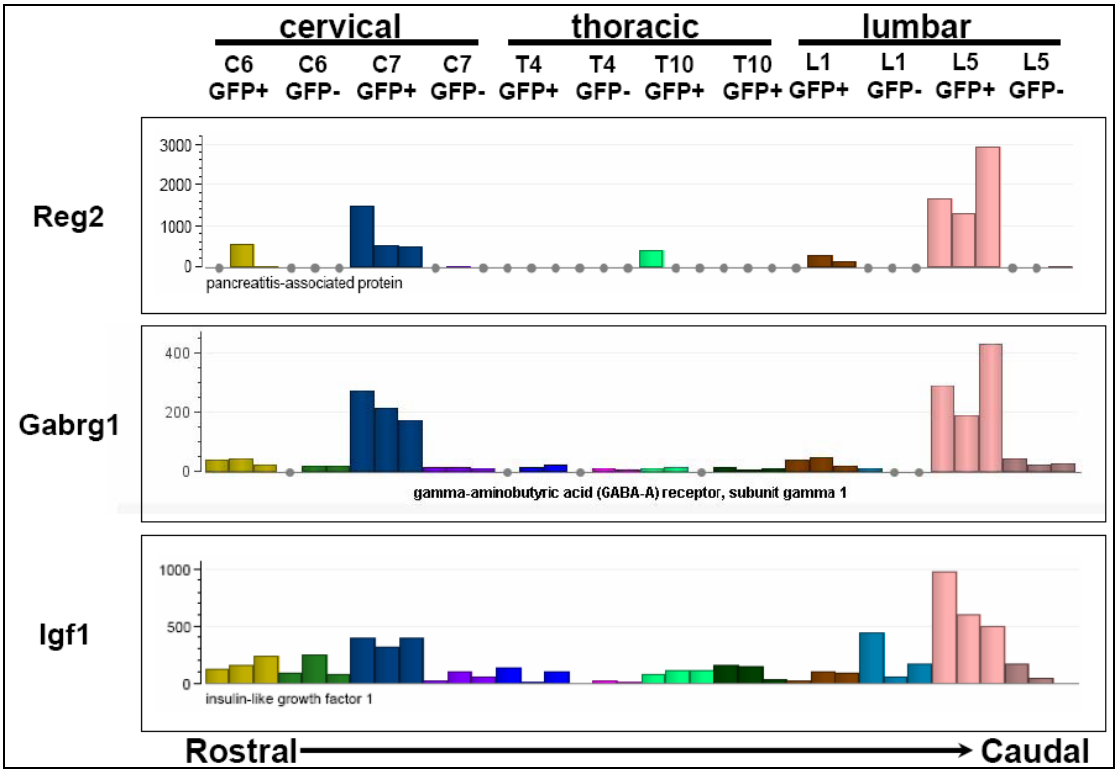

Figure 16: Analysis for three genes with a differentially regulated expression in rostro to caudal DRG. The GFP+ population represents the proprioceptive afferent population isolated by FACS. The GFP- population represents the remaining, mainly cutaneous afferent population.

ISH experiments for *Reg2* and *Gabrg1* focusing on lumbar DRG confirm the gene array data as shown in Figure 17. We reproduced the anterior to

posterior differences in gene expression as discovered by gene array analysis.

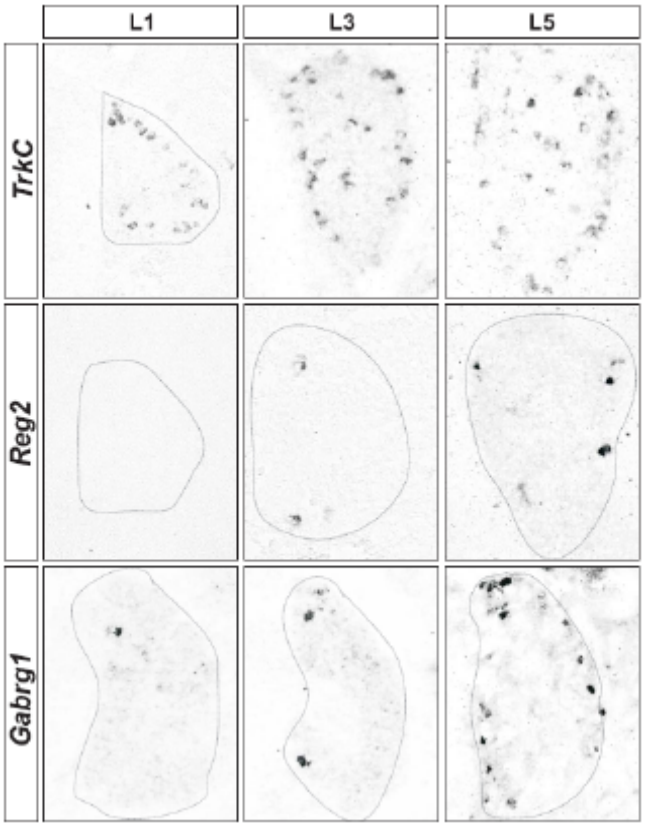

Figure 17: Increasing expression of *Gabrg1* and *Reg2* in lumbar anterior to lumbar posterior DRG. Note the increase in expression from L1 and L3 to L5 DRG. Note the expression in subsets of proprioceptive afferents by comparing the *TrkC* staining with *Reg2* and *Gabrg1* expression. *(ISH slides with Gabrg staining kindly provided by Jun Lee)*

Certainly, *Reg2* and *Gabrg1* expression does not reflect the total Ia proprioceptive afferent population that forms direct monosynaptic connections onto MNs. The Ia sensory afferent population is much bigger than the *Reg2* and *Gabrg1* positive cell population. Especially the absence of *Reg2* expressing cells in L1 DRG suggests that *Reg2* cannot label Ia proprioceptive afferents. Proprioceptive afferents are present throughout all anterior to posterior DRG. It is rather likely that these two genes represent a marker for sensory pools projecting to individual muscles or onto distinct motor pools.

We characterized the expression of *Igf1* in more detail. First, we validated the elevated expression of *Igf1* in L5 DRG compare to all other levels analyzed also in our gene expression arrays. Figure 18 represents a quantitative graph obtained by counting *Igf1*+ cells in *ISH* experiments.

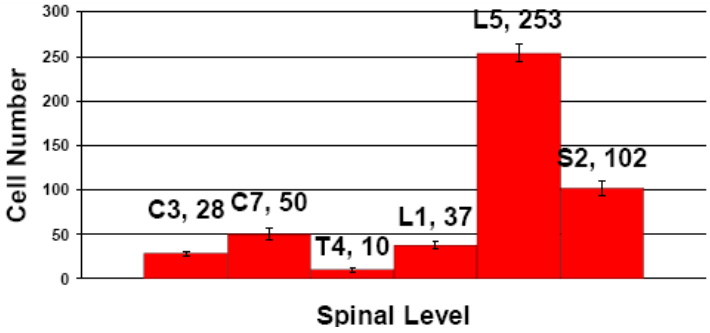

Figure 18: Igf1 expression in rostral to caudal DRGs. Counting was performed from three E18.5 embryos, sectioned in two series with which two independent *ISH* experiments were performed.

Igf1 expression is not restricted to the proprioceptive afferent population. As shown in Figure 10, *Igf1* expression is maintained in *TrkC*$^{-/-}$ mutant mice. Since no gene was described so far to be expressed in subsets of proprioceptive afferents, we validated our gene arrays by performing *ISH* experiments for *Igf1* in combination with antibody staining against DRG sensory neuron subpopulations. We co – stained the *Igf1 ISH* signal with antibodies against the three different neurotrophin tyrosine kinases, which label distinct DRG SN subpopulations, namely TrkA, TrkB and TrkC. Figure 19 shows the overlap in expression of the *Igf1 ISH* signal with TrkC and TrkA.

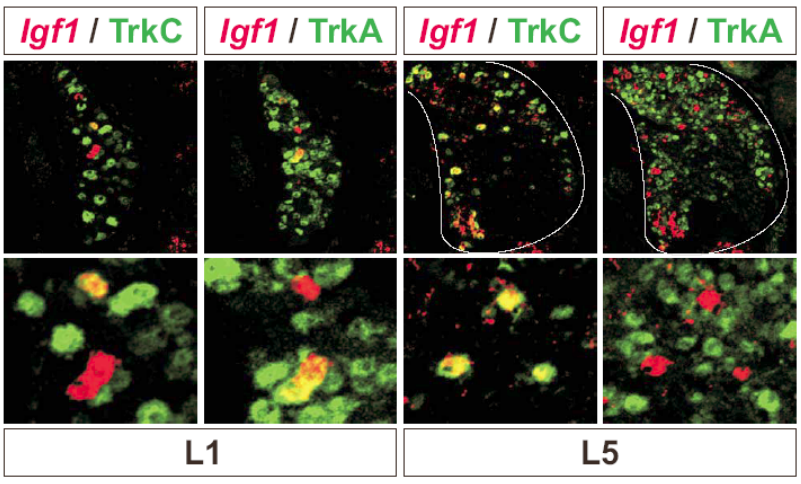

Figure 19: Igf1 *ISH* colabeling with TrkA and TrkC antibodies. On the section of an L1 DRG, we show one *Igf1*+ cell colabeled with TrkC and one cell with TrkA. In L5 most *Igf1*+ cells are also TrkC+.

Figure 20 shows colabeling of *Igf1* with the TrkB and TrkA. Similar to Figure 19, Igf1 expressing cells in L1 DRG preferentially coexpress TrkA. Only a few *Igf1*+ cells coexpress the neurotrophin receptor TrkB as illustrated in Figure 20.

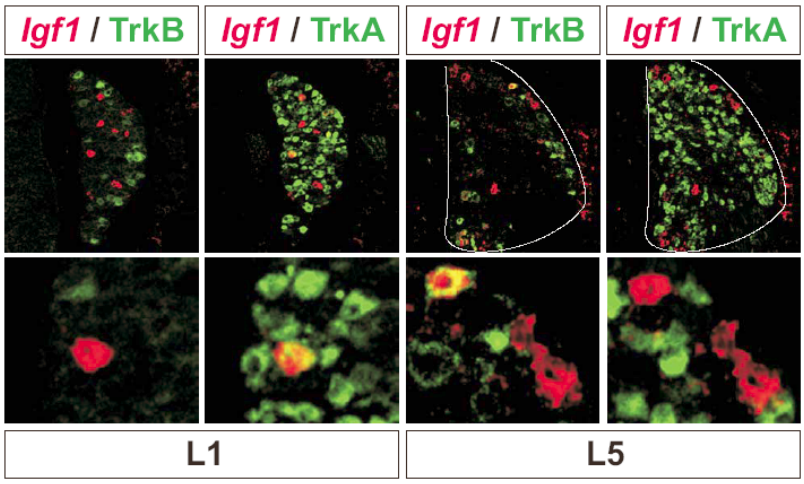

Figure 20: *Igf1 ISH* colabeling with TrkA and TrkB antibodies. In the L1 DRG, we show one *Igf1*+ cell colabeled with TrkA. On the section of an L1 DRG, most *Igf1*+ are negative for TrkA and TrkB, suggesting that these cells are TrkC+ as depicted already in Figure 19.

We also quantified the ratios of *Igf1*/TrkA, *Igf1*/TrkB and *Igf1*/TrkC expressing cells in L1 and L5 DRG. As already visible from Figure 19 and 20, we observe a very interesting distribution in that most *Igf1*+ cells in DRG L1 colabel with TrkA, whereas most *Igf1*+ cells in TrkC colabel with TrkC (data not shown).

In summary, the expression of *Igf1* represents a very interesting expression pattern. *Igf1* is expressed in subsets of proprioceptive afferents and numbers also increase in a rostro to caudal gradient. Its expression exhibits very selective changes in the association with different DRG subpopulations. *Igf1* expression in certain DRG sensory subpopulations at different segmental levels seems to be tightly regulated.

In additional experiments, we also assessed by real-time PCR, whether DRG neurons express a particular isoform of *Igf1*. There are two distinct Igf1 isoforms. One form is described as the circulating class of Igf1, which is predominantly expressed in the liver. The second isoform is described as a local form of Igf1 and referred as muscle-restricted Igf1 (m-Igf1) (Dobrowolny et al., 2005). m-Igf1 is expressed by many tissues, but remains confined to the tissue of expression. Our real-time PCR experiments revealed expression of both *Igf1* isoforms in the DRG, which increases the complexity of Igf1 and its role in DRG sensory neurons.

A role for Igf1 in DRG sensory neuron survival has been described already *in vitro* (Leinninger et al., 2004). In this study, apoptosis in DRG neurons was induced by application of high glucose levels. It was shown that Igf1 mediated signaling regulates the PI3K/Akt pathway to prevent apoptosis caused by high glucose levels. Igf1 also protects DRG sensory neurons from apoptosis upon NGF abolition and promotes axonal extension (Camarero et al., 2001; Jones et al., 2003; Ozdinler and Macklis, 2006; Rabinovsky et al., 2003). The *in-vivo* effect of Igf1 was further investigated using *Igf1* null mice. These mice exhibit a significant decline in neuron cell number in various brain regions analyzed (Beck et al., 1995; Camarero et al., 2001). In disease, a protective role for m-Igf1 was described in a mouse model for amyotrophic lateral sclerosis (ALS), which exhibits selective degeneration of motor neurons (Dobrowolny et al., 2005; Pun et al., 2006).

To date, most studies of Igf1 focused in neuronal survival and growth-promoting effects. A different role for Igf1 has been recently described for olfactory sensory map formation. In this study, Igf1 was described to function as chemoattractant and to be involved in axon guidance to innervate specifically the lateral olfactory bulb (Scolnick et al., 2008). In a further study, blockage of insulin receptor in retino - tectal neurons of *Xenopus*, resulted in defects in synapse number and maturation, dendritic arborizations and functional deficits such as light evoked responses (Chiu et al., 2008).

As described above, Igf1 signaling fulfills various functions in the developing CNS and in diseased stage. Therefore, future work in our laboratory focuses on the question whether tissue specific over-expression or deletion of Igf1 *in vivo* will alter the effect of natural occurring cell death and therefore cause changes in numbers of DRG sensory neurons. Using these genetic tools, various approaches of previous studies could be analyzed in more detail, for example whether Igf1 expression in DRG sensory neurons is required for the ingrowth of *Igf1 receptor* expressing cortico – spinal motor neurons into the spinal cord (Ozdinler and Macklis, 2006). Further experiments could focus on possible roles of Igf1 in the formation of sensory – motor connections in the spinal cord.

Dissecting the Er81 Downstream Cascade in Proprioceptive Afferents

Previous work has addressed the role of the transcription factor Er81 in proprioceptive afferents during monosynaptic stretch reflex circuit assembly (Arber et al., 2000). In the introduction, I described the induction of Er81 by peripheral NT3 expressed in muscles. It was also found that over-expression of NT3 leads to a disruption in specificity in the formation of sensory – motor connections in the spinal cord (Wang et al., 2007). These observations raise the interest to analyze the downstream signaling cascade of Er81 to further dissect its role in stretch reflex assembly. Our aim was to isolate genes downstream of Er81 to find molecules involved in synapse formation of Ia proprioceptive afferents and motor neurons. Moreover, we aimed to use pathway analysis software (Ingenuity) to better understand signaling cascades regulating axon growth to the ventral spinal cord and synapse formation. For this reason, we performed gene expression profiling experiments of wt and *Er81*$^{-/-}$ mutant proprioceptive afferents at developmental time point E14.5 and E16.5 (Arber et al., 2000). This time point represents developmental stages after *Er81* is fully expressed to fulfill its function.

As previously described, we validated our gene expression results by *ISH* and *IHC* experiments. Initially, we focused our analysis on genes down-regulated or not expressed in the absence of Er81. Except for parvalbumin (Arber et al., 2000), no further downstream gene of Er81 has been described so far. Table 2 represents genes with the biggest fold changes between wild-type and *Er81*$^{-/-}$ mutant proprioceptive afferents, which show enriched expression in proprioceptive afferents in *wild-type* conditions.

Table 2: Genes with enriched expression in proprioceptive afferents and down-regulated expression in *Er81*$^{-/-}$ proprioceptive afferents at E16.5

Name (Access. #)	**Description (Gene)**	**Fold Change wt vs Er81$^{-/-}$**
1417894_at	G protein- coupled receptor 97	32.6
1422607_at	Ets variant gene 1 (Er81)	27.1
1420402_at	ATPase, Ca++ transporting, plasma	12.3

	membrane 2	
1455361_at	diacylglycerol kinase, beta	11.5
1437434_a_at	RIKEN cDNA 5031439A09 gene	11.5
1435941_at	rhomboid, veinlet-like 4 (Drosophila)	10.2
1428664_at	vasoactive intestinal polypeptide	9.8
1417653_at	parvalbumin	9.2
1437268_at	LanC lantibiotic synthetase component C-like 3 (bacterial)	9.1
1444736_at	cadherin 7, type 2	6.4
1424767_at	cadherin 22	5.9
1450120_at	sodium channel, voltage-gated, type I, alpha polypeptide	5.6
1417051_at	protocadherin 8	4.8
1421027_a_at	myocyte enhancer factor 2C	4.2
1455267_at	estrogen-related receptor gamma	4.0
1423367_at	wingless-related MMTV integration site 7A	3.1

- genes with fold changes > 6.5 are appeared consecutively in initial list; genes with fold changes < 6.5 had been selectively picked to be illustrated in Table 2.

All genes listed in Table 2 also show decreased expression in *Er81*$^{-/-}$ mutant proprioceptive afferents at E14.5. One indication to trust the gene expression data received, is the fact that the gene deleted, *Er81*, appeared as one of the most down-regulated genes. Interestingly, many of the top hits have been discovered and validated in previous screens already to be specifically expressed by proprioceptive afferents. Figure 21 shows two such examples. As indicated by the gene chip results, antibody staining for Err3 and *Wnt7a ISH* show a complete down-regulation on *Er81*$^{-/-}$ mutant tissue.

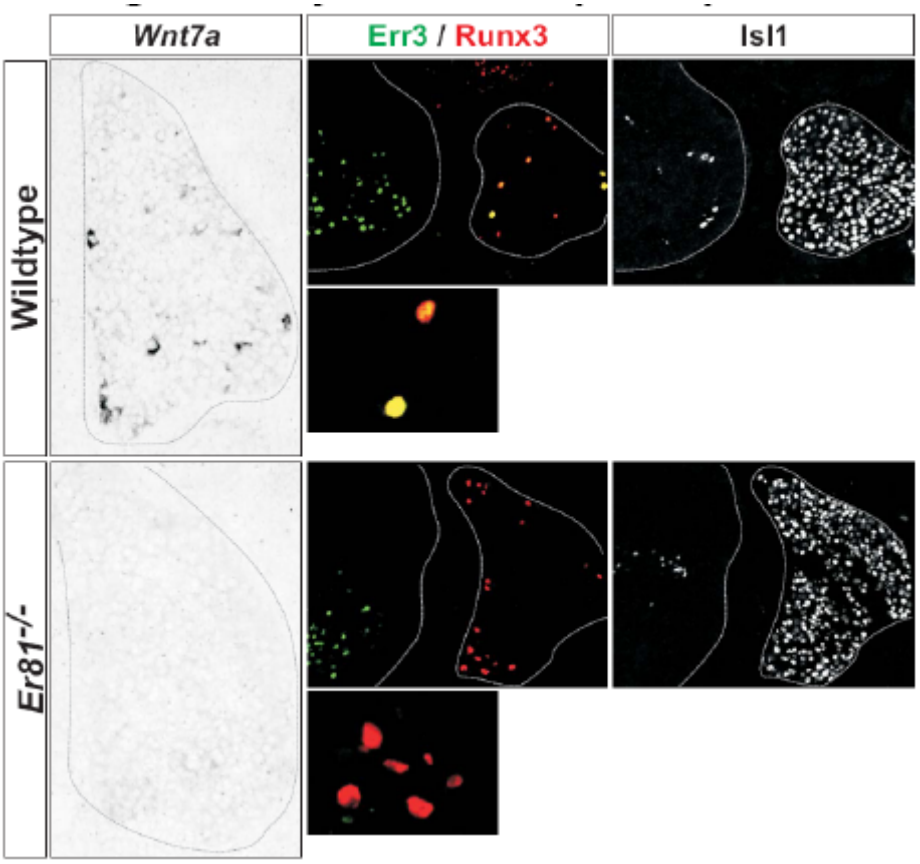

Figure 21: Down-regulation of *Wnt7a* and Err3 in *Er81*$^{-/-}$ mutant tissue. *Wnt7a* shows *ISH* signal and Err3 *IHC* signal, whereas Runx3 marks the entire proprioceptive afferent population. Note the remaining expression of Err3 in ventral motor neurons.

In contrast, many of other described proprioceptive marker genes, such as *TrkC*, *GPR64*, *Robo1, Runx3* are not significantly differentially regulated comparing *wild-type* and *Er81*$^{-/-}$ mutant animal expression profiles. A slight down-regulation in *Er81*$^{-/-}$ mutant proprioceptive afferents can be observed for *PTHR1* and *Slit2* with a fold change of 2.5 and 2.1, respectively.

The absence of *Wnt7a* in *Er81*$^{-/-}$ mutant tissue is in particular exciting, because Wnt signaling has previously been implicated in the process of synaptogenesis between proprioceptive afferents and motor neurons (Krylova et al., 2002). In vivo studies show that secreted Wnt3a by motor neurons elicits axon branching and growth cone maturation on NT3 responsive, hence Ia proprioceptive, DRG sensory neurons. A very similar retrograde acting mechanism has been found for the cerebellum. Here, Wnt7a is secreted by granule cells to regulate axon and growth cone remodeling in mossy fibers to

induce synaptic differentiation (Hall et al., 2000). In *Drosophila*, it has also been shown that Wnt signaling controls in an anterograde manner the assembly of the neuromuscular synapse (Packard et al., 2002). An anterograde or autocrine mode of action of Wnt7a in proprioceptive afferents has not been investigated yet and will hopefully be studied in the future.

The second gene we validated from our functional gene chip approach is Err3. At E14.5, there is clear *Err3 ISH* signal left on *Er81*$^{-/-}$ mutant tissue in the DRG. In contrast, we observe a severe down-regulation of Err3 at E16.5. Between E14.5 and E16.5, Ia proprioceptive afferents innervate the ventral spinal cord to form synapses with motor neurons, which represents the time window of Err3 down-regulation in proprioceptive afferents. *Err3*$^{-/-}$ mutants do not exhibit the same or a similar phenotype as observed in *Er81*$^{-/-}$ mutants and are also not ataxic. The proprioceptive afferent projections of these animals look like *wild-type* (data not shown). Therefore, *Err3* may not be a direct target gene of Er81, but it is directly or indirectly controlled by Er81. Not much is known about Err3 in neuronal development or synapse formation. Solely the cofactor Peroxisome proliferator-activated receptor-gamma, coactivator 1, alpha (PGC-1alpha) binding to Err3, but also to other nuclear receptors, has recently been studied in more detail. We also found *PGC-1alpha* to be enriched in proprioceptive afferents and 3 fold down-regulated in *Er81*$^{-/-}$ mutant proprioceptive afferents, although we were never able to validate these date by *ISH* or *IHC* due to a lack of a working AB and *in situ* probe. PGC-1alpha is known to regulate various levels of energy metabolism involving defects in mitochondrial biogenesis and respiration in muscle and heart tissue (Finck, 2006; Finck and Kelly, 2006; Leone et al., 2005; Wu et al., 1999). Therefore, there is an increasing interest to dissect the role of nuclear receptors and PGC-1 in various neurodegenerative diseases involving metabolic disorders. Since another member of the estrogen-related receptor family, namely estrogen-related receptor alpha (Err1), has been shown to interact with PGC-1alpha to regulate transcriptional control of energy metabolism, it is tempting to speculate that Err3 achieves similar functions in proprioceptive afferents (Huss et al., 2004).

Moreover, we have identified a number of other genes that might be downstream effectors of Er81 signaling. Cadherins for example as discussed previously, potentially play import roles in specific cell to cell interactions of proprioceptive afferents (Table 2). We also found genes to which we did not pay much attention so far. As seen in Table 2, one particular member of the sodium channel family, namely *SCN1A*, was specifically down-regulated in *Er81*$^{-/-}$ mutant proprioceptive DRG sensory neurons.

We observed in *wild-type* condition that certain members of gene families seem to have very interesting, but distinct, expression profiles, such as certain Hox genes, *GPR64*, *PTHR1*, *Gabrg1* and others. We became interested to study the expression patterns of all members of whole gene families that might play a role in neuronal circuit formation and function. This analysis was focused on ion channels, GABA receptors, semaphorins and plexins. Surprisingly, a high degree of specificity in expression towards DRG SN cell type and/or anterior to posterior DRG positioning can be observed, which we analyzed in more detail in the next paragraphs.

Channel Specificity in DRG Sensory Neurons

We detected the *sodium channel, voltage gated type I, alpha polypeptide* (*SCN1A*) in our *Er81*$^{-/-}$ mutant proprioceptive afferent screen to be 5.6 fold down-regulated and under *wild-type* conditions highly enriched in proprioceptive afferents. Specific expression of voltage-gated Na+ channels is essential to modulate an appropriate cell membrane potential and cell to cell action-potential (AP) propagation. There is a variety of Na+ channel subtypes expressed specifically by different tissues. SCN4A for example is expressed in heart, whereas SCN8A is broadly expressed in the CNS, PNS, heart glia and nodes of Ranvier (Chahine et al., 2005).

To increase complexity of channel modulation, these channels heterodimerize with β-subunits and associate with a variety of protein kinase C (PKC) and PKA isoforms as well as with G proteins, receptors, cytoskeletal elements an others (Chahine et al., 2005). Sensory neurons express several Na+ channel isoforms as it has been published and detected in our screens. So far, *SCN1A* expression has been described in the CNS, PNS and heart. In contrast to SCN1A, other voltage-gated Na+ channels show no specificity to any DRG sensory neuron subpopulation and seem not to be affected by the loss of Er81 in DRG as shown in Figure 22.

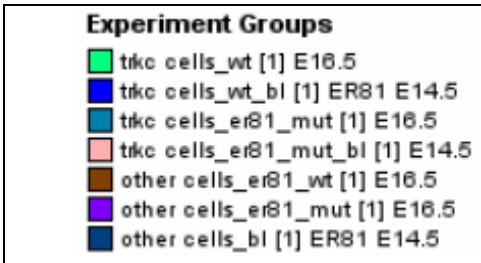

Figure 22: Na+ channel expression in wt and *Er81*$^{-/-}$ mutant DRG sensory neuron subpopulations at E14.5 and E16.5. 'other cells' represent the GFP-, mainly cutaneous, cell population.

SCN1A

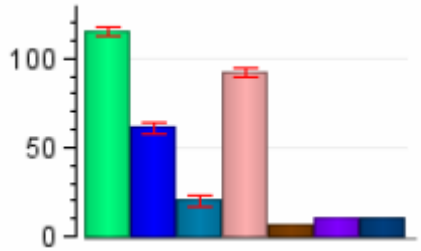

SCN1A is up-regulated at E14.5 and down-regulated at E16.5 in *Er81*$^{-/-}$ mutant proprioceptive afferents

SCN6A	
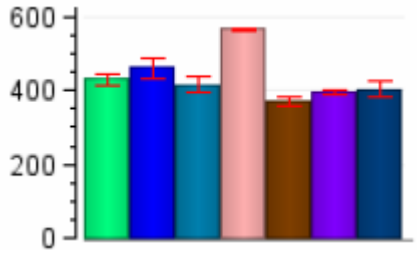	*SCN6A* expression is not restricted to a certain DRG sensory neuron subpopulation and is not affected by the loss of Er81.
SCN3A	
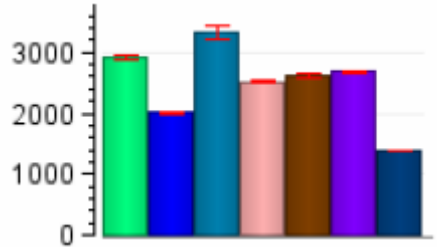	*SCN3A* expression is not restricted to a certain DRG sensory neuron subpopulation and is not affected by the loss of Er81.

As outlined in the Appendix, in contrast to SCN1A, the Na+ subunits SCN10A and SCN11A shows restricted expression to the GFP-, mainly cutaneous afferent DRG sensory neuron subpopulation.

We not only find defined sodium channel expression patterns, but also observe similar expression patterns for K+ channels and K+ channel interacting proteins as we summarize in the Appendix.

Correct channel expression is in particular important to modulate voltage thresholds of AP in individual fiber types. It was reported that multiple sodium channel isoforms and types contribute to electrical activity in DRG sensory neurons (Catterall et al., 2005; Yu et al., 2005). Proprioceptive afferents are present in all DRG sensory neurons along the entire anterior to posterior axis. Given the fact that proprioceptive afferents from various levels innervate a vast repertoire of different muscles throughout the body over various distances, exact channel expression and modulation is imperative for precise functionality and AP propagation over the axon. Therefore, it can be postulated that there must me a high degree of channel specificity not only between two distinct subsets of neurons, e.g. TrkA and TrkC cells as shown above, but also within one cell type, e.g. proprioceptive DRG neurons. Our level specific screen indeed exhibits anterior to posterior regulated expression of sodium and potassium channel subtypes. In Figure 23, we see a trend that

SCN1A expression is modulated among different DRG, whereas SCN1A expression in TrkC- cells remains unchanged. In comparison members of the type 4 family, namely SCN2B and SCN4B show elevated expression in C7 and L5 DRG. More specifically, SCN2B expression is restricted to spinal level C7, but is not restricted to any DRG sensory neuron subpopulation.

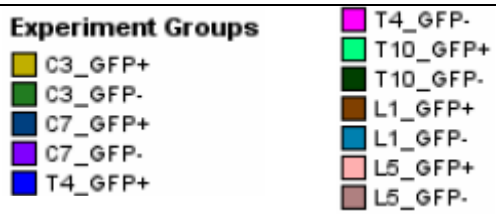

Figure 23: Gene expression analysis of GFP+ (TrkC+) and GFP- (TrkC-) cells of different anterior to posterior DRG.

SCN1A

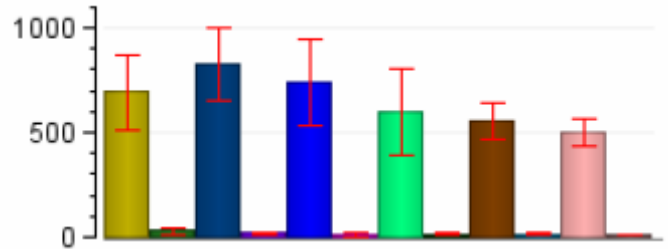

Specific expression of *SCN1A* in proprioceptive afferents along rostral to caudal DRG. It seems like *SCN1A* is higher expressed in anterior versus posterior DRG.

SCN4B

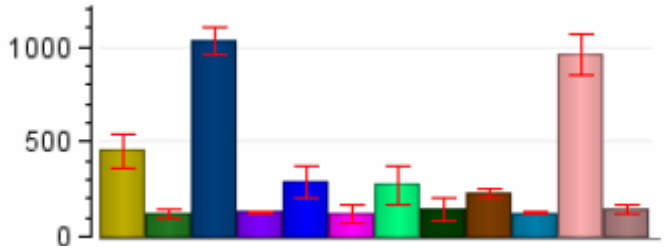

SCN4B expression is significantly enriched in C7 and L5 proprioceptive afferents, but at moderate levels also expressed in the GFP- subpopulation.

SCN2B

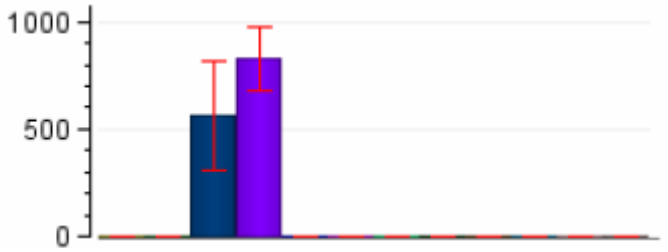

SCN2B expression is expressed specifically in C7 DRG, but not restricted to DRG sensory neuron subpopulations.

Together, we demonstrate a cell type and level specific expression of voltage-gated Na+ channels to modulate signal transduction properties from DRG sensory neurons. Similar specificity in expression can be detected for other

ion channel families and their binding proteins, for examples potassium channels, which are summarized in the Appendix.

Potential role of SCN1A in DRG proprioceptive afferents

Specific expression of voltage-gated Na+ channels is essential to modulate an appropriate cell membrane potential and cell to cell action potential (AP) propagation. There is a variety of Na+ channel isoforms expressed specifically by various tissues, but also in our experiments in specific patterns in the DRG.

Moreover, we show that SCN1A is responsive to Er81 and expressed by proprioceptive afferents in a level-specific manner. Yu *et al* described that correct expression of voltage-gated Na+ channels is required for the initiation of action potentials in GABAergic interneurons (Yu et al., 2006). A family of voltage-gated sodium channel binding proteins has recently been studied to control neuronal excitability through modulation of Na+ channels (Goldfarb et al., 2007).

Very similar to the *Er81*$^{-/-}$ mutant mouse, *SCN1A*$^{-/-}$ mutant mice display severe ataxia and die around postnatal day P15. Dependent on the background, 20 – 80% of the *SCN1A*$^{+/-}$ haplo-insufficient heterozygous mice died between the third and fifteenth postnatal week. A reduction in functional SCN1A in heterozygous animals leads to epileptic seizures in the fourth postnatal week that can be explained by a hyper-excitability in these animals phenocopying in humans the disease called severe myoclonic epilepsy in infancy (SMEI).

Ogiwara *et al* described that in the developing neocortex, SCN1A is clustered around the axon initial segments (AIS) of parvalbumin positive interneurons (Ogiwara et al., 2007). As described earlier, proprioceptive afferents also express parvalbumin. Ogiwara *et al* show also that homoyzgous knockout animals develop unstable tonic-clonic and polyspike-wave seizures in the second postnatal week, suggesting SCN1A to be an imperative factor for AP initiation at the AIS. Moreover, it was reported that increasing input currents to generate spike bursts in dissociated hippocampal neurons, results in a decline of the AP number and amplitude during the bursts in SCN1A heterozygous

and homozygous animals (Yu et al., 2006). Very similar to this phenomenon, Ia afferents in *Er81*$^{-/-}$ animals also fail to respond to high frequency stimulation via muscle tapping (Arber et al., 2000).

Supporting this hypothesis, the mechano-sensitivity of voltage gated sodium channels has been studied by expressing a human heart channel subunits in oocytes (Morris and Juranka, 2007). The phenotypic observations (ataxia and muscle tremors) in *SCN1A*$^{-/-}$ mutant animals might be explained by action potential decrement from muscles. Therefore, SCN1A might be a key molecule involved in the generation of stretch induced action potentials in proprioceptive afferents.

In summary, SCN1A is a very interesting molecule that might be crucial for AP initiation in proprioceptive afferents in response to stretch. If that was true, future functional analysis could prove the significance of SCN1A in the monosynaptic stretch reflex circuit functioning.

Chapter II – SUMMARY

Our screening strategy provided insights and evidence about molecular components expressed in specific components of the monosynaptic stretch reflex circuit. Identification and validation of many novel markers expressed by proprioceptive afferents slowly decode a gene expression based matrix to further specify and characterize proprioceptive afferents.

In addition, we were able to isolate genes downstream of Er81, a crucial transcription factor expressed in the DRG, imperative to form functional connections between proprioceptive sensory neurons and motor neurons in the spinal cord. By pushing our technical limitations even further, we were able to dissect genes expressed in very small neuronal subpopulations in DRG restricted by expression in rostro to caudal patterns. Interestingly, we have identified a number of genes the expression of which shows patterns in multiple DRG subpopulations, for example *Igf1*. Our screens detected also genes, which possibly play important functions in neuronal excitability, action potential initiation, propagation and transmission, such as various ion-, GABA channel- and G protein-coupled receptors.

Moreover, it can be speculated that a similar Hox based transcriptional code is involved in sensory neuron pool diversification, as it has been described already for motor neuron pools. Finally, we established tools and conditions to reliably perform RNA amplification techniques and presented convincing data arguing that when acquiring gene expression profiles from the nervous system, isolation of pure neuronal subpopulations is key to success.

Estrogen – Related Receptor Gamma Marks Gamma Motor Neurons

Andreas Friese*[1,2], Julia Kaltschmidt*[3], David Ladle*[1,2], Monika Mielich[1,2], Thomas M. Jessell[3] & Silvia Arber[1,2]

*equal contribution

[1]Biozentrum, Department of Cell Biology, University of Basel, Switzerland

[2]Friedrich - Miescher Institute for Biomedical Research, Basel, Switzerland

[3]Howard Hughes Medical Institute, Department of Biochemistry and Molecular Biophysics, Center for Neurobiology and Behavior, Columbia University, USA

Muscle spindles reside within muscles and provide information about changes in muscle length to the CNS. They are innervated by two main neuronal components. Proprioceptive sensory afferents forward information about axial and limb positioning to the CNS. Gamma motor neurons project to the peripheral domain of intrafusal muscle fibers and elicit small contractions of intrafusal muscle fibers to modify the sensitivity of the muscle spindle to stretch. Due to missing molecular markers, identification of gamma motor neurons in the central nervous system so far was only based on their smaller cell size. Previous studies focused on the formation and connectivity of muscle spindles in the periphery using various transgenic mouse lines. Here, we identify gamma motor neurons in the central nervous system on an anatomical and molecular basis.

We made use of three transgenic mouse lines (*PV-Cre;Isl2-DTX, Egr3*$^{-/-}$*, Er81*$^{-/-}$), mutants exhibiting muscle spindle defects of different severity. We identified motor neurons by using the backfilling technique with Rhodamine-Dextran and up-regulating the activating transcription factor 3 (ATF3) two days after nerve lesions. *PV-Cre;Isl2-DTX* mice, in which muscle spindles fail to differentiate due to the loss of proprioceptive innervation, showed loss of all gamma motor neurons in the spinal cord. Furthermore, we quantified the number of motor neurons projecting to quadriceps muscles and analyzed the loss of gamma motor neurons during muscle spindle degeneration in the *Egr3*$^{-/-}$ mutant mouse line. Our results demonstrate that muscle spindles are required for gamma motor neuron survival and identify a novel molecular fingerprint for gamma motor neurons.

Chapter III - INTRODUCTION

In recent years much progress has been made in understanding the development and maintenance of muscle spindles. Early studies showed that muscle spindles consist of intrafusal muscle fibers, which are innervated by two main neuronal components; proprioceptive sensory neurons and gamma motor neurons. Intrafusal muscle fibers can be categorized into two main classes; nuclear chain fibers (NCF) and nuclear bag fibers (NBF). It has been well established that gamma motor neurons innervate both NCFs and NBFs of muscle spindles to form the fusimotor command. In contrast, Ia proprioceptive afferents innervate the central domain of muscle spindles to measure stretch and change in muscle length (Rossi-Durand, 2006). As soon as proprioceptive afferent terminals reach their target region in the periphery, the neurotrophic factor neurotrophin 3 (NT3) becomes necessary for proprioceptive neuron survival by signaling through the tyrosine kinase receptor TrkC (Ernfors et al., 1994; Tessarollo et al., 1994). On the other hand, muscle spindle formation critically depends on proprioceptive neuron innervation and the release of Ig-Neuregulin, leading to induction of various transcription factors, such as expression of *Er81*, *Pea3*, *Egr3* (Hippenmeyer et al., 2002). In mice mutant for the zinc-finger transcription factor *Egr3,* spindles are initially generated, but degenerate progressively postnatally (Chen et al., 2002; Tourtellotte and Milbrandt, 1998). Mutant mice exhibiting severe failures in proprioceptive sensory neuron differentiation, such as mice expressing diphtheria toxin in proprioceptive afferents under the control of the parvalbumin promoter (PV-Cre;Isl2-DTX), fail to induce muscle spindles as already described in previous studies (Kucera et al., 1995). Together, these experiments provide evidence for the critical role of group Ia proprioceptive afferents in the induction of intrafusal muscle fiber differentiation.

Recently, it has been described that gamma motor neurons depend on GDNF signaling during a critical developmental time window (Gould et al., 2008). Although LacZ insertions into the genes of GDNF and its receptors Ret and GFRα1 clearly identify the loss of gamma motor neurons based on the type of projections into the muscle, up to date no molecular marker for these motor neurons has been identified. Therefore, analysis of gamma motor neuron cell bodies using molecular markers in transgenic mice with muscle spindle

defects was not possible. Experiments to differentiate between alpha and gamma motor neurons classically included ultrastructural analysis only on a cellular level (Ichiyama et al., 2006).

Here, we identified a specific marker to characterize in detail lumbar gamma motor neurons on an anatomical and molecular level. First, we show that gamma motor neurons express the orphan nuclear receptor, *estrogen-related receptor gamma* (*Err3*) and quantified the size and number of gamma motor neurons within a defined motor neuron pool in the spinal cord. We used a technique to specifically up-regulate the activating transcription factor 3 (ATF3) upon quadriceps nerve lesion. Using this method, we further monitored a significant loss of gamma motor neurons in mouse models revealing muscle spindle defects.

Chapter III – RESULTS

Expression of Err3 by motor neurons

By *IHC* we localized Err3 in the lumbar spinal cord. In the juvenile and adult mouse spinal cord, Err3 shows selective expression to subsets of motor neurons and interneurons. To determine the exact cell type in which Err3 is expressed, we stained mouse spinal cord with various motor neuron markers and neuronal nuclei (NeuN) at juvenile age (~P20). A strong expression of Err3 was observed in cells located in the ventral lumbar spinal cord in the area of motor neurons. To confirm the expression of Err3 to motor neurons, we performed co-staining with various motor neuron markers. Vesicular acetylcholine transporter (vAChT), choline actetyl transferase (ChAT) and the receptor tyrosine kinase Ret are known to be expressed by motor neurons (Dupuis et al., 2008; Gould et al., 2008; Salomon et al., 1998) and allowing us to use them for our co-localization experiments with Err3. Most Err3 expressing cells in the ventral horn of the spinal cord can be allocated to motor neurons using vAChT, ChAT and Ret as motor neuron markers (Figure 1 and S1). NeuN is known to label all neurons in the brain and spinal cord. Interestingly, the strongest Err3 stained cells express no or only very low levels of NeuN (Err3+;NeuN-); nevertheless can be clearly identified as motor neurons. L4 ventral root backfills with rhodamine-dextran confirmed that the Err3+;NeuN- cells projecting outside the spinal cord represent motor neurons. Again, clear identification of the Err3+;NeuN-;Rhd+ cells is possible, confirming again these cells to be motor neurons (Figure 1c).

Motor neuron size distribution of lumbar motor neurons

The patterns of Err3+;NeuN- expressing cells let us assume that these cells fall into a class of small sized motor neurons. Therefore, we performed a motor neuron size distribution analysis. Motor neuron size was determined by quantitative analysis of randomly sampled motor neurons at posterior lumbar levels. As described in previous studies (Ichiyama et al., 2006), the motor neurons mean diameter plotted in a histogram, results in a bimodal distribution. Since the mean diameter does not represent the motor neuron size, we determined the maximum crossectional frequency of motor neuron

areas, which also resulted in a bimodal distribution (Figure 2). The maximum crossectional area of motor neurons was determined using the imaging software *ImageJ*. Subsequent clustering of these cells into NeuN strong and NeuN weak expressing or negative cells, clearly shows that the ChAT+;NeuN- cells fall into a small sized motor neuron population, whereas ChAT+;NeuN+ cells are of bigger size in average. The small sized strong Err3 expressing motor neuron population represents 27% of the motor neurons quantified. Therefore, the small sized Err3+;NeuN- cells might represent the gamma motor neuron subpopulation. To investigate whether the Err3+;ChAT+;vAChT+;NeuN- cell population reflects the putative gamma motor neuron cell population, we next analyzed vGlut1 input onto these cells. Gamma motor neurons receive inhibitory input through the neurotransmitters gamma aminobutyric acid (GABA) and/or Glycine as well as excitatory input by glutamate. This glutamatergic input is not mediated by synapses from Ia proprioceptive afferents (Hatabu et al., 1996; Ornung et al., 1998). If the Err3+:NeuN- motor neuron population indeed reflect gamma motor neurons based in cell fraction and size, these motor neurons should also have less vesicular glutamate transporter signal (vGlut1) than the strong NeuN expressing motor neurons. As shown in Figure 2, the mean vGlut1 synaptic density on ChAT+;NeuN+ cells is 0.5±0.1 synapses per 100µm^2 (n=33). In contrast the terminal density on ChAT+;NeuN- cells is approximately 6.25 times lower (n=13), suggesting that these strong Err3 expressing cells might indeed represent the gamma motor neuron population.

Analysis of gamma motor neurons in mouse models with spindle defects

The molecular and anatomical characterization of these putative gamma motor neurons raises the question of the fate of these cells in mice exhibiting defects in muscle spindle differentiation (Kucera et al., 1995). PV-Cre;Isl2-DTX mice do not have proprioceptive afferents and therefore never induce muscle spindle differentiation. In our experiments, loss of muscle spindles results in a total loss of the ChAT+;NeuN- putative gamma motor neuron population (Figure 3A). Therefore, we can conclude that strong Err3 expressing, in this experiment ChAT+;NeuN-, cells are in fact gamma motor

neurons. *Er81*$^{-/-}$ mutant animals, exhibiting severe defects in the central projections of proprioceptive afferents, also display failures in muscle spindle differentiation (Arber et al., 2000). Similar to PV-Cre;Isl2-DTX animals, *Er81*$^{-/-}$ mutant mice also lack most gamma motor neurons (Figure 3B). In order to validate that the loss of the gamma motor neuron subpopulation is due to peripheral spindle defects and not caused by genetic alterations leading to defects of proprioceptive input, we analyzed gamma motor neurons in the area of the cutaneous maximus (CM) motor neuron pool, which in the *wild-type* does not receive proprioceptive afferent input (Vrieseling and Arber, 2006). Clearly, gamma motor neurons can be identified based on their molecular characteristics expressing high levels of Err3 and no or low levels of NeuN (Figure 3).

Analysis of gamma motor neurons projecting to the quadriceps muscle

The data suggest that gamma motor neurons do not die due to the loss of proprioceptive input, but rather due to peripheral spindle defects. To further investigate the loss of gamma motor neurons due to failures in muscle spindle differentiation, we analyzed *Egr3*$^{-/-}$ mutant mice in greater detail. These mice exhibit a muscle spindle degeneration defect, causing impairments of intrafusal muscle fiber development and subsequent Ia proprioceptive afferent denervation (Tourtellotte and Milbrandt, 1998). We focused our analysis on defined motor neuron pools projecting to the quadriceps muscles. We decided to label motor neurons projecting to the quadriceps muscle group by up-regulation of the activating transcription factor 3 (ATF3) after quadriceps nerve lesion (Huang et al., 2006; Tsujino et al., 2000). As shown in Figure 4, up-regulation of ATF3 in small sized and big NeuN+ motor neurons works equally well. This technique was further used to compare the number of ATF3 expressing cells in wt and *Egr3*$^{-/-}$ mutant mice (Figure 5). In average we quantified 254 motor neurons expressing ATF3 under *wild-type* conditions, of which 72 (28%) were identified as gamma motor neurons based on their molecular identity (ATF3+;ChaAT+;NeuN-). In *Egr3*$^{-/-}$ mutant animals, the total number of ATF3 expressing cells dropped to 195 cells, of which 15 cells (8%) were identified as gamma motor neurons. Consequently, the loss of ATF3+ motor neurons is likely to the gamma motor neuron population. As shown in

Figure S2, the small sized gamma motor neuron population, by determining the crossectional area and the NeuN status, cannot be detected anymore. Moreover, in P35 old *Egr3*$^{-/-}$ mutant animals, only 2% of gamma motor neurons could be detected; hence with increasing spindle degeneration, more gamma motor neurons die.

Chapter III – DISCUSSION

To date, only little is known about molecular differences of motor neuron types. Recent studies mainly focused on transcriptional differences between motor neuron pools and motor neuron columns within the spinal cord during development. Yet, basic principles between different motor neuron types, such as alpha and gamma motor neurons, are only poorly understood. Known studies are mainly based on their distinct innervation patterns into muscles or based on their synaptic inputs determined through ultrastructural classification.

In this study, we were able to specifically identify gamma motor neurons in *wild-type* and mutant conditions. We performed an anatomical and molecular characterization to prove that small sized strong Err3 and no or low NeuN expressing motor neurons are indeed gamma motor neurons.

In order to quantify distinct motor neurons projecting to a particular muscle, we used the methodology of ATF3 up-regulation upon quadriceps nerve lesion. This technique is in particular powerful, because ATF3 is not expressed in motor neurons of uninjured animals. The reproducibility of ATF3 expression after axotomy lies almost at 100% as shown by Tsujino *et al* and therefore provides an ideal technique to monitor neuronal cell numbers (Tsujino et al., 2000). Our results led to the conclusion that mouse mutants with severe defects in muscle spindle differentiation exhibit a significant loss of gamma motor neurons. These findings suggest that gamma motor neurons depend on the expression of intrafusal muscle fibers specific genes, which are lacking in *Egr3*$^{-/-}$ mutant mice (Chen et al., 2002). In contrast, upon gamma motor degeneration from spindles, their neuronal somata disappear as proven by a significant loss of motor neuron cell number. This means, there are certain aspects of proprioceptive afferents that will allow these cells to survive in the absence of NT3 in muscle spindles (Chen et al., 2002). Gamma motor

neurons apparently do not share these features, since these neurons denervate and die in *Egr3*$^{-/-}$ mutant animals. One possible mechanism could be the downregulation of GDNF in muscle spindles (Gould et al., 2008). To dissect the exact reasons for gamma motor neuron death compared to the maintenance of proprioceptive afferents, will require further studies. It will be interesting to understand whether there are factors expressed other than NT3 and GDNF by normal muscle spindles, required for postnatal proprioceptive afferent survival in *Egr3*$^{-/-}$ mutant animals. Identification of factors expressed by muscle spindles required for gamma motor neuron survival will provide insight into new molecular mechanisms involved in subtype specific motor neuron survival and hence, might shine light into the selective vulnerability of motor neurons in disease state.

Chapter III – RESULTS (Figures)

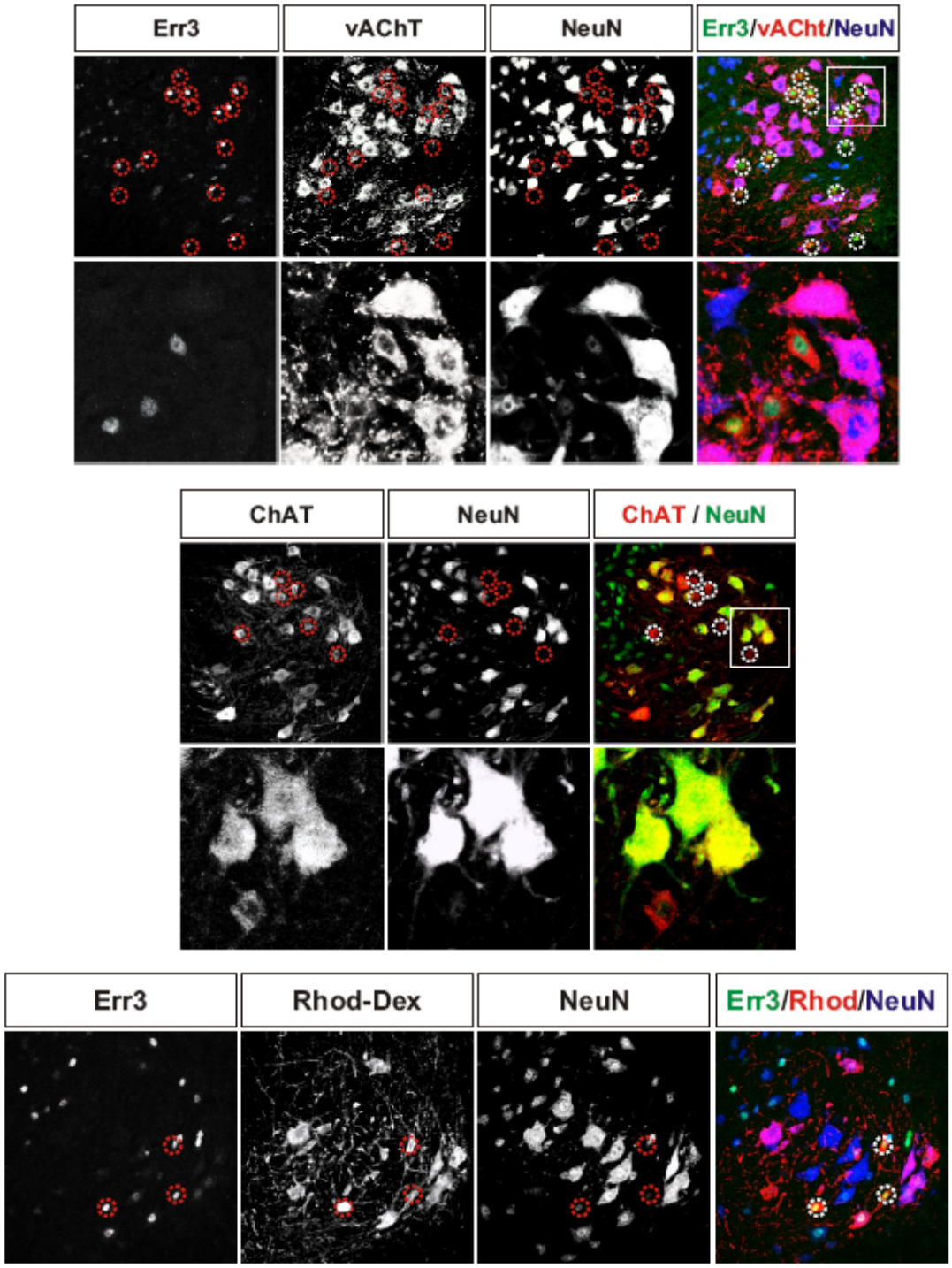

Figure 1: Err3 expression in a subset of motor neurons in the lumbar ventral spinal cord.
(A) Err3 is highly expressed in a subset of motor neurons in the spinal cord and co-expresses the motor neuron marker gene vAChT. These motor neurons express low level or no NeuN.
(B) Motor neurons are stained for ChAT, a different motor neuron marker gene. The same subpopulation of motor neurons can be identified to be negative for NeuN. Co-labeling with Err3 is not possible due to cross-reactivity of antibodies of the same species.
(C) L4 ventral root backfill with Rhodamine-Dextran also clearly reveals both NeuN negative and NeuN positive motor neurons.

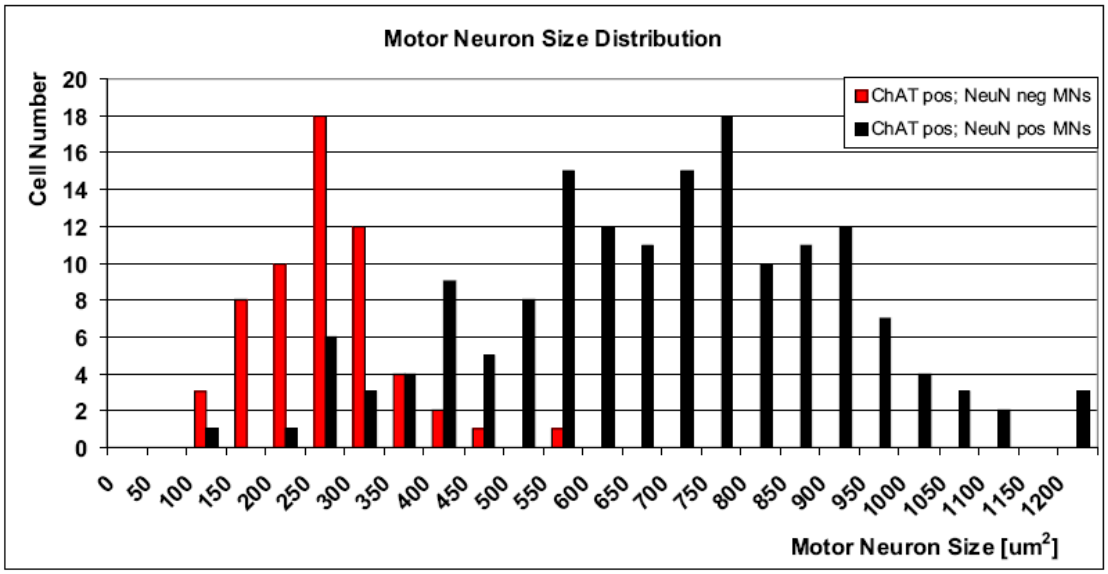

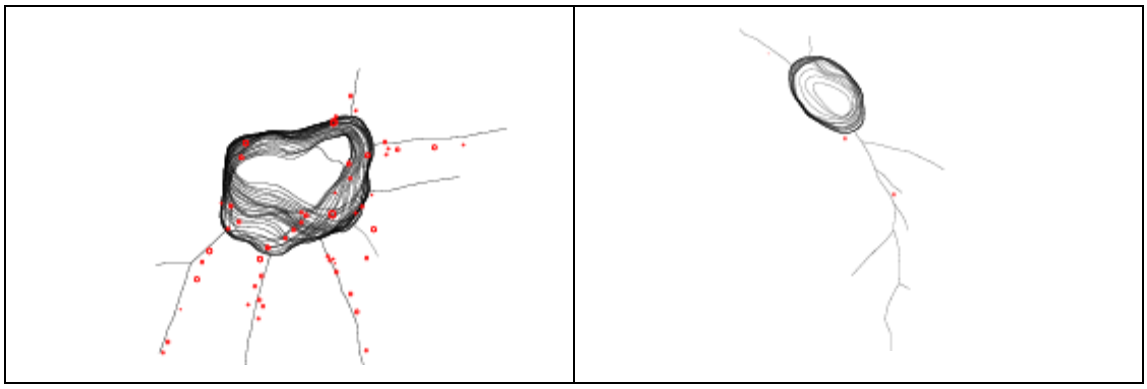

vGlut1 terminal density:
0.5±0.1synapses/100µm^2

vGlut1 terminal density:
0.08 synapses/100µm^2

Figure 2: Motor neuron size quantification based on ChAT and NeuN expression.
(A) We performed blind motor neuron size quantification of 219 ChAT+ motor neurons. Afterwards we checked expression of these motor neurons for NeuN in order to analyze the size of the ChAT+;NeuN- motor neuron subpopulation compared to rest of all motor neurons. ChAT+ motor neurons expressing no or low levels of NeuN clearly fall into a cluster of motor neurons small in size.
(B) Motor neurons which are NeuN- and small in size receive no or very little vGlut1 input.

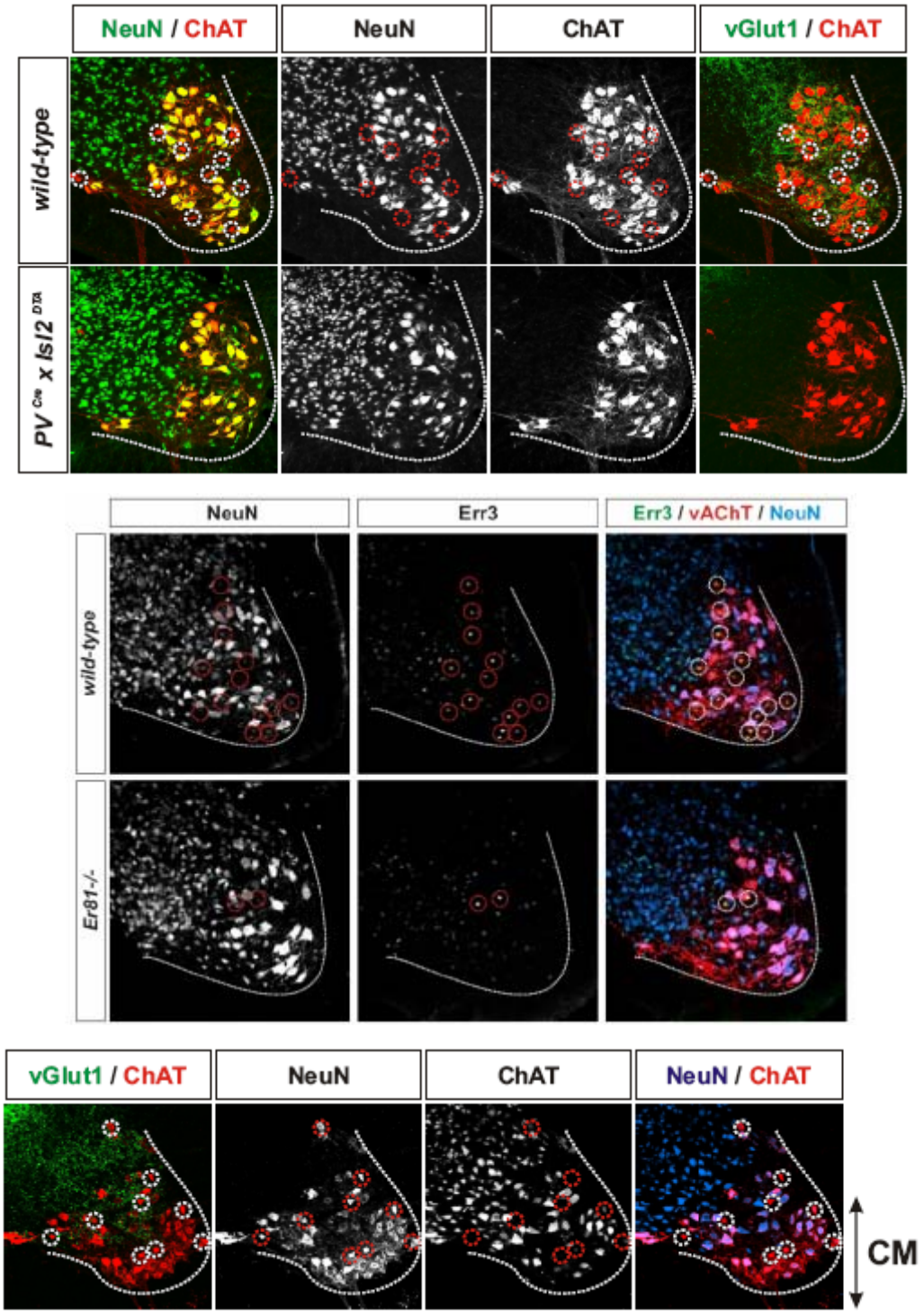

Figure 3: Analysis of small sized motor neurons in mice lacking Ia proprioceptive afferent input and muscle spindles. (A) Complete loss of small sized motor neuron subpopulation due to early loss of proprioceptive afferents and consequently muscle spindle differentiation in *PV-Cre;Isl2-DTX* mice. (B) Reduced number of small sized Err3+;NeuN- motor neurons in *Er81-/-* mutant mice exhibiting reduced muscle spindles and loss of Ia proprioceptive afferent input. (C) Identification of Err3+;NeuN- motor neurons in the cutaneous maximus (CM) motor neuron pool region, which does not receive monosynaptic input.

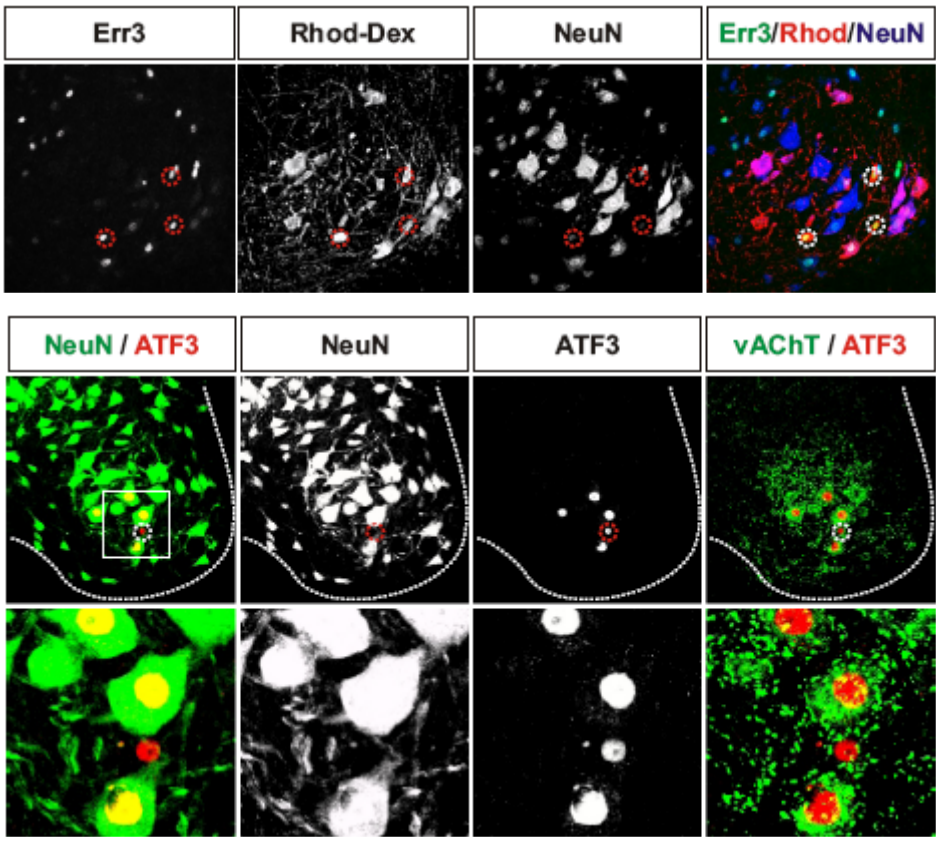

Figure 4: Labeling of motor neurons after nerve lesion.

(A) Retrograde labeling of motor neurons from L4 ventral roots include both large and small motor neurons; Err3-;Rhod+;NeuN+ and Err3+;Rhod+NeuN- motor neurons respectively. (B) 2 days after quadriceps nerve lesion, ATF3 is up-regulated in motor neurons projecting to the quadriceps muscle group. The same motor neuron subpopulation can be determined as described in (A).

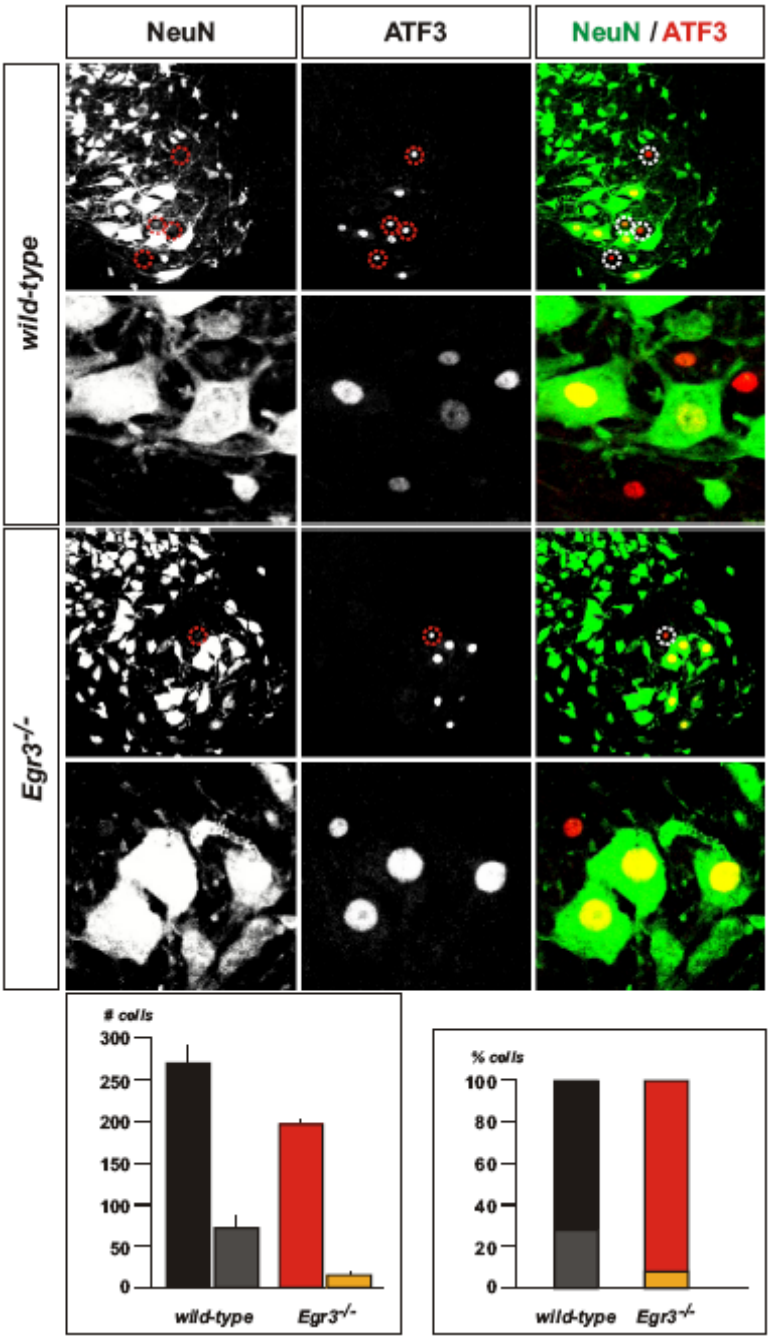

Figure 5: Analysis of putative gamma motor neuron fate in mice exhibiting muscle spindle degeneration defects. 2 days after quadriceps lesion, in *wild-type* conditions 70%, approximately 200 cells, of all motor neurons are ATF3+;NeuN+. Only a minor fraction of 25-30%, approximately 70 cells, falls into the class of putative gamma motor neurons. At ~P20 in *Egr3*$^{-/-}$ mice, almost the entire small sized putative gamma motor neuron subpopulation die; roughly 7% of the cells are maintained (n ≥ 3 animals for each bar graph). Data (here not shown) of a P35 *Egr3*$^{-/-}$ mutant mouse reveals that the loss of putative gamma motor neurons is progressing slowly. At P35, still 2% of this motor neuron subpopulation is present.

Chapter III – SUPPLEMENT

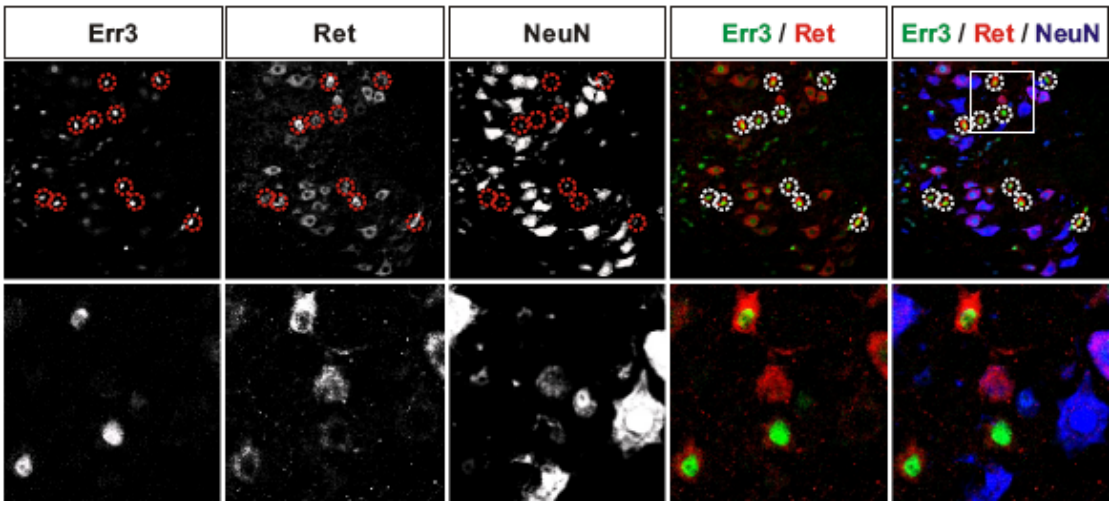

Figure S1: As described in Figure 1A, the high Err3 expressing motor neuron subpopulation can be co-labeled with a third motor neuron marker; Ret. The Err3+; Ret+: motor neuron subpopulation expresses low level or no NeuN.

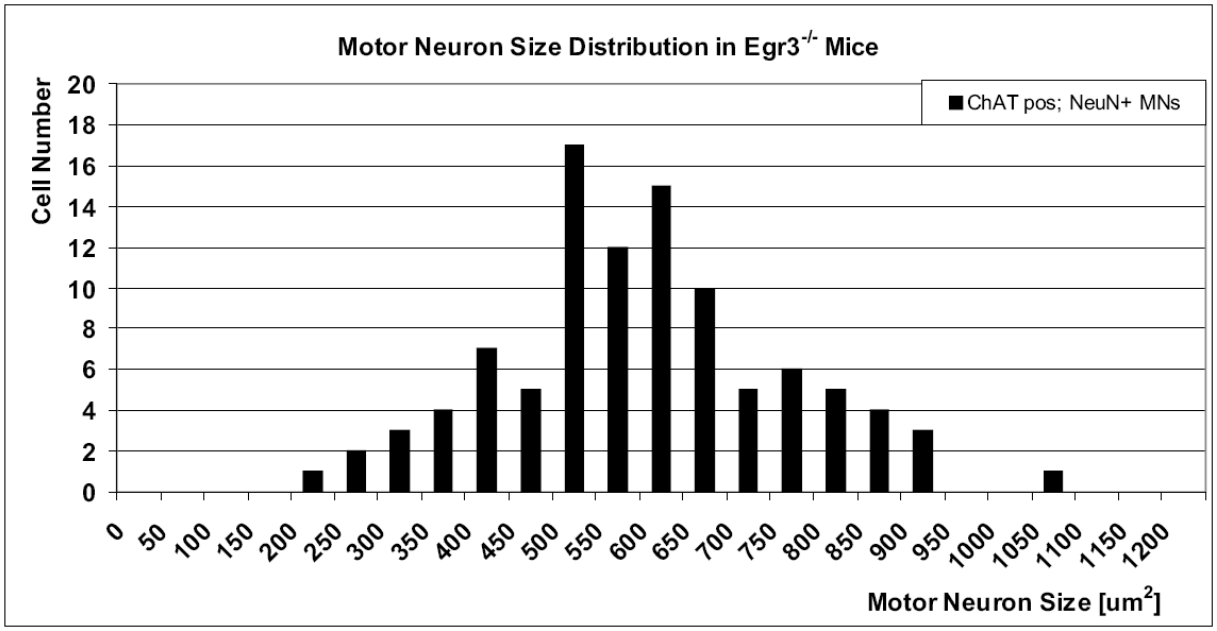

Figure S2: Motor neuron size quantification of motor neurons in *Egr3*$^{-/-}$ mutant mouse. The fraction of small sized gamma motor neurons is not present anymore.

Role of Estrogen – Related Receptor Gamma in a Mouse Model of Amyotrophic Lateral Sclerosis

in collaboration with

Smita Saxena & Pico Caroni

Amyotrophic lateral sclerosis (ALS) is a common, but only poorly understood form of a fatal neuromuscular disease, which causes progressive degeneration of motor neurons in the brain and spinal cord. This process of degeneration results in worsening of paralysis and terminates with the death of the patient.

The G93A *SOD1* mouse line is a well established model to study an inherited form of ALS. We used this mouse model in our analysis. Previous studies described that onset and progression of disease is tightly linked to different types of motor neuron populations, exhibiting selective temporal axonal vulnerability. Underlying mechanisms contributing to selective axonal vulnerability are however only poorly understood.

Here, we show that the transcription factor estrogen-related receptor gamma (Err3), a member of the nuclear receptor superfamily, may play a crucial role in motor neuron disease and more specifically in axonal vulnerability. We demonstrate that mainly small sized Err3+ gamma motor neurons resist disease progression until the mouse dies. Moreover, *SOD*/*Err3*$^{+/-}$ double transgenic mice exhibit a significant decrease in muscle strength compared to pure *SOD* or *Err3*$^{+/-}$ heterozygous mice. Nuclear receptor signaling pathways were shown to control various aspects of regulation on energy metabolism and mitochondrial biogenesis. We suggest that the disruption of these signaling cascades are possibly more affected in G93A/*Err3*$^{+/-}$ mice compared to pure G93A animals.

Chapter IV - INTRODUCTION

To date, onset and progression of many neurodegenerative diseases are only poorly understood. Two distinct forms of ALS have been described: First, a sporadic form possibly caused by neurotoxins, heavy metals or enzymatic dysfunctions. A second form of ALS is inherited and is therefore called familial amyotrophic lateral sclerosis (FALS), which accounts for approximately 5% - 10% of all ALS patients. 20% of these FALS cases were shown to have a mutation in the gene encoding *copper/zinc superoxide dismutase* (*SOD1*). Established mouse lines to study this neuromuscular disease, express a human mutated form of *SOD*, analogous with familial amyotrophic lateral sclerosis (ALS).

In this study, we used the G93A *SOD1* fast progressing disease model, which exhibit first clinical signs of paralysis around postnatal day P85 with a live expectancy of these animals of 136 ± 5 days (Bruijn et al., 2004; Gurney et al., 1994; Pun et al., 2006).

The temporal sequence of selective, reproducible synapse loss and axonal degeneration has been well established (Pun et al., 2006). However, the underlying molecular mechanisms leading to a selective vulnerability of motor neurons are not characterized well to date. Generally, motor neuron dysfunction has been linked to alterations of various cellular events such as mitochondrial dysfunctions (Wong et al., 1995), axonal transport defects (Collard et al., 1995) or endoplasmic reticulum stress (Nishitoh et al., 2008; Sekine et al., 2006).

Recent studies described the involvement of key transcriptional regulators in these metabolic abnormalities in neurodegenerative diseases. One such gene is the peroxisome proliferator-activated receptor gamma coactivator-1alpha (PGC-1α) (Cui et al., 2006; St-Pierre et al., 2006). Mitochondrial metabolism is the source of many reactive oxygen species (ROS), which can further react with oxygen to superoxide (Balaban et al., 2005). Superoxide interacts with DNA, proteins and lipids to fulfill important cellular functions. Therefore, the level of superoxide is crucial for regular cell functioning and must be tightly controlled. Activation of mitochondrial biogenesis results from transcriptional activation of PGC-1α with nuclear receptors, for example estrogen related receptor alpha (Err1) and gamma

(Err3) or the nuclear respiratory factor 2 (NRF-2) in high energy demanding tissues like heart, skeletal muscle or the nervous system (Dufour et al., 2007; Huss et al., 2007; Leone et al., 2005; Mootha et al., 2004; Rangwala et al., 2007; Wu et al., 1999). As we have shown in previous studies, Err3 is selectively expressed in subpopulations of sensory and motor neurons, hence we became interested in analyzing the role of Err3 in motor neurons subpopulations in a disease model for ALS. We speculated that the temporal sequence of synaptic loss in G93A *SOD* mice could possibly be achieved through molecular and/or anatomical properties regulated through nuclear receptor signaling in subsets of motor neurons.

In this study, we demonstrate the significance of Err3 expression in motor neurons of G93A *SOD* mice in various aspects. We show that G93A *SOD* mice carrying only a *Err3*$^{+/-}$ heterozygous allele exhibit more severe behavioral impairments during disease progression. Moreover, many of the neurons still present in the spinal cord at very late stage of disease in *SOD* mice, express high levels of Err3 and can be clearly identified as gamma motor neurons as described in chapter III. Our data suggest a selective role for Err3 in metabolic processes in a mouse model for familial amyotrophic lateral sclerosis and possibly other neurodegenerative diseases.

Chapter IV - RESULTS

Gamma motor neurons resist until endstage of disease in ALS mice

First, we aimed to identify and characterize the types of motor neurons, which are capable to resist motor neuron disease to late stages. We believed that it is important to know which motor neurons survive in order to understand the selective vulnerability of motor neurons in disease in more detail. Performing co-labeling experiments using vAChT as a motor neuron marker (Gould et al., 2008), we were able to show that motor neurons surviving disease to late endstage, express high levels of Err3 (Figure 1). Comparing *wild-type* and *SOD* animals at P130, it is obvious that most large sized motor neurons are absent in *SOD* mice.

We described in previous studies that gamma motor neurons can be identified based on their cell body size and their molecular profile by expressing high levels of Err3, but expressing only low or no levels of NeuN. Next, we asked the question, whether this is also the case for the remaining cells in the ventral spinal cord of the transgenic disease model. As shown in Figure 2, the majority of all motor neurons left in the LMC in a P130 diseased *SOD* mouse, are NeuN-;Err3+ small sized cells. Therefore, we can conclude that these cells belong indeed to the category of gamma motor neurons.

Behavioral Analysis of *SOD;Err3*$^{+/-}$ mice

To address the question whether a decreased expression of Err3 has an effect in SOD mice, we analyzed the *SOD;Err3*$^{+/-}$ double transgenic line in more detail. *Err3*$^{-/-}$ null mice are lethal a few hours after birth and therefore cannot be used in this approach. However, previous studies have shown that heart defects are even present in *Err3*$^{+/-}$ heterozygous mice (Dufour et al., 2007).

Figure 3 shows one SOD and one *SOD;Err3*$^{+/-}$ male mouse. Many of the double transgenic animals exhibit an earlier and more severe state of paralysis compared to pure *SOD* mice. Earlier paralysis was also monitored by analyzing footprint walking patterns of *wild-type*, *SOD* and *SOD;Err3*$^{+/-}$

animals as shown in Figure 4. Already at P91, *SOD;Err3*$^{+/-}$ mice show impaired walking behavior compared to *wild-type* and *SOD* mice. Walking patterns of *SOD/Err3*$^{+/-}$ mice analyzed at P111, show complete hindlimb paralysis, whereas *SOD* mice are not as severely affected. The early paralysis pointed us towards the direction to analyze *SOD/Err3*$^{+/-}$ mice at earlier stages.

We performed loaded grid tests of *wild-type*, *Err3*$^{+/-}$, *SOD*, and *SOD;Err3*$^{+/-}$ animals from the age of 5 weeks onwards as shown in Figure 5. We reasoned that a potential role of Err3 in *SOD* disease could be detected in loaded grid tests by one-allelic deletion of Err3 function in heterozygous animals. The loaded grid test is designed to detect muscle force changes between mice (Barneoud et al., 1997). We detected significant muscle force difference between male *SOD* and *SOD;Err3*$^{+/-}$ mice for week 5c, 6 and 10 ($p < 0.02$). Our results suggest that this difference is not due to impairments of *Err3*$^{+/-}$ mice, because these animals perform in this test at least as good as *wild-type* males. As illustrated by Figure 5, the muscle force difference between *SOD* and *SOD;Err3*$^{+/-}$ seems to peek at the age of week 6 and 11. Whether these time windows represent an earlier selective loss of synaptic vesicles or a pre-onset of nerve denervation can at this point only be speculated.

Survival analysis of *SOD* and *SOD;Err3*$^{+/-}$ animals

Based on the Kaplan-Meier plot, we can conclude that the elimination of one Err3 allele in *SOD* animals has no effect on the survival rate (Figure 6).

This can also be supported, because the most significant difference in muscle force behavior can only be detected within a distinct time window (week 5c, 6 and 10 Figure 5) .

Chapter IV - DISCUSSION

In recent years much progress has been made to better understand the motor neuron disease familial amyotrophic lateral sclerosis (FALS). On the one hand, studies focused on disease progression, in particular to dissect differences of vulnerable versus resistant motor neurons. On the other hand, much research was performed using various strategies to ameliorate disease in mice. Compounds such as ciliary neurotrophic factor (CNTF) or growth factors like the insulin-like growth factor 1 (Igf1) and vascular endothelial growth factor (VEGF) have been shown to have neuroprotective properties under pathological conditions in mouse models for ALS (Azzouz et al., 2004; Dobrowolny et al., 2005; Kaspar et al., 2003; Pun et al., 2006; Sagot et al., 1998). These substances, if not delivered retrograde using viral systems, exhibit many disadvantages, such as strong side effects or the limiting access to motor neurons (Mitchell et al., 2002). In contrast, we showed in our study that decreasing the action of the metabolic regulator Err3 in *SOD;Err3*$^{+/-}$ animals leads to a more severe phenotype. To our knowledge, this is the only study in which a worsening of the phenotype of the G93A *SOD* motor neuron disease model can be observed by interaction with a metabolic pathway. Molecular features for this observation could possibly be explained by the inability of *SOD;Err3*$^{+/-}$ motor neurons to cope with stress as efficiently as pure *SOD* animals. It is tempting to speculate that the metabolic regulator Err3 plays an important role in motor neurons metabolism.

The loaded grid test analysis of *Err3*$^{+/-}$ heterozygous mice did not reveal significant differences in muscle strength. Therefore, we can exclude that *Err3*$^{+/-}$ heterozygous mice are less strong than *wild-type* animals and therefore double transgenic *SOD;Err3*$^{+/-}$ animals mice are in fact weaker than pure SOD mice.

Interestingly, most motor neurons in the lateral motor column, which survive disease to the stage when the mouse dies, express high levels of Err3 and can therefore be identified as gamma motor neurons. We speculate that Err3 may be marking disease resistant motor neurons and possibly also exhibit a role in protecting them from disease.

Ligands for Err3 have not yet been identified. However, it is known that tamoxifen binds to Err3 and inhibits transcription (Coward et al., 2001).

Inhibition of Err3 by tamoxifen injections into SOD mice, could confirm its relevance in SOD mice as described previously using double transgenic *SOD;Err3*$^{+/-}$ animals. Moreover, viral retrograde delivery of Err3 to all motor neurons, might be key to success to ameliorate motor neuron disease by providing artificially an imperative metabolic regulator.

The question remains whether our molecular and behavior analysis reflect an earlier or more severe disease progression of *SOD;Err3*$^{+/-}$ animals. Future experiments will address these issues and hopefully point out the significance of metabolic regulators in neurodegenerative diseases.

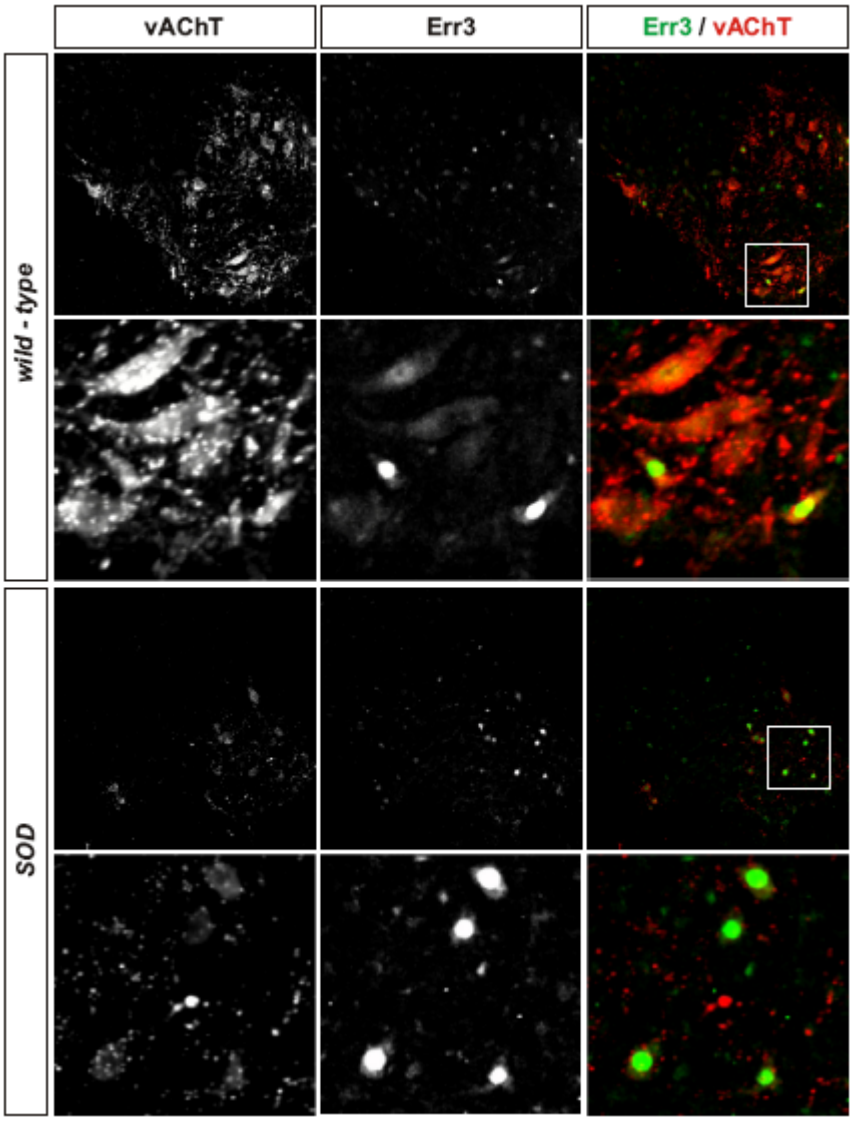

Figure 1: Analysis of motor neurons in wild-type and G93A *SOD* mice at P130. As shown in wild-type animals, strong Err3 expression is restricted to subsets of motor neurons in the posterior lumbar spinal cord. Note, other motor neurons express no or low levels of Err3. At late stages of disease, the majority of cells maintained in the spinal cord are small sized Err3+ putative gamma motor neurons.

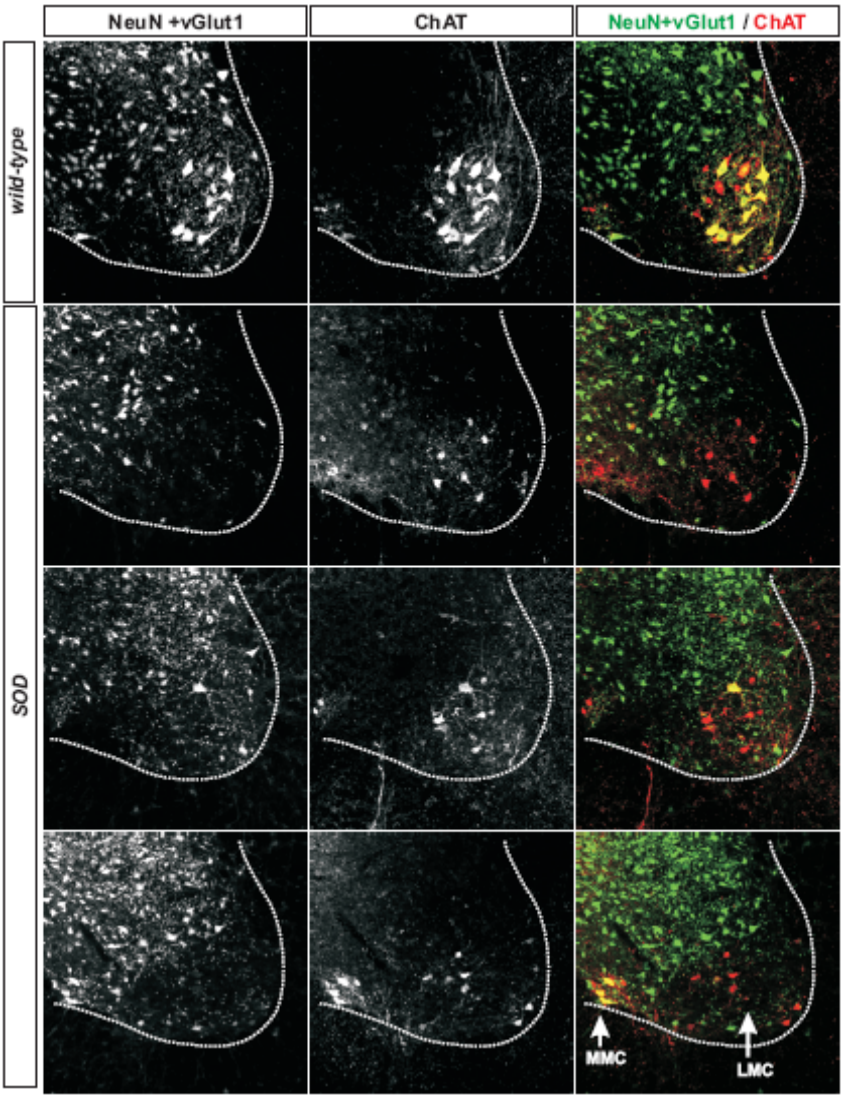

Figure 2: Gamma motor neuron cell bodies survive to endstage of SOD disease. At late stages of disease progression, most motor neurons denervated from the periphery and the cell bodies disappear in the spinal cord. The main fraction of motor neurons maintained in G93A *SOD* mice at P130, can be clearly identified as small sized NeuN negative gamma motor neurons in the region of the lateral motor column (LMC). Note, the presence of ChaT+;NeuN+ motor neurons belonging to the medial motor column (MMC).

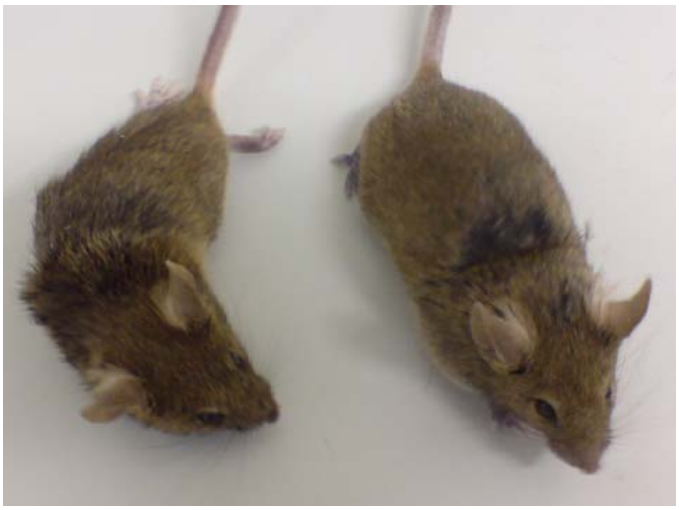

Figure 3: Degree of paralysis in *SOD;Err3*$^{+/-}$ (left) and pure *SOD* (right) mice at P125. Many *SOD; Err3*$^{+/-}$ mice exhibit an earlier, more severe degree of paralysis during disease progression and consequently a stronger weight loss likely due to atrophic muscles.

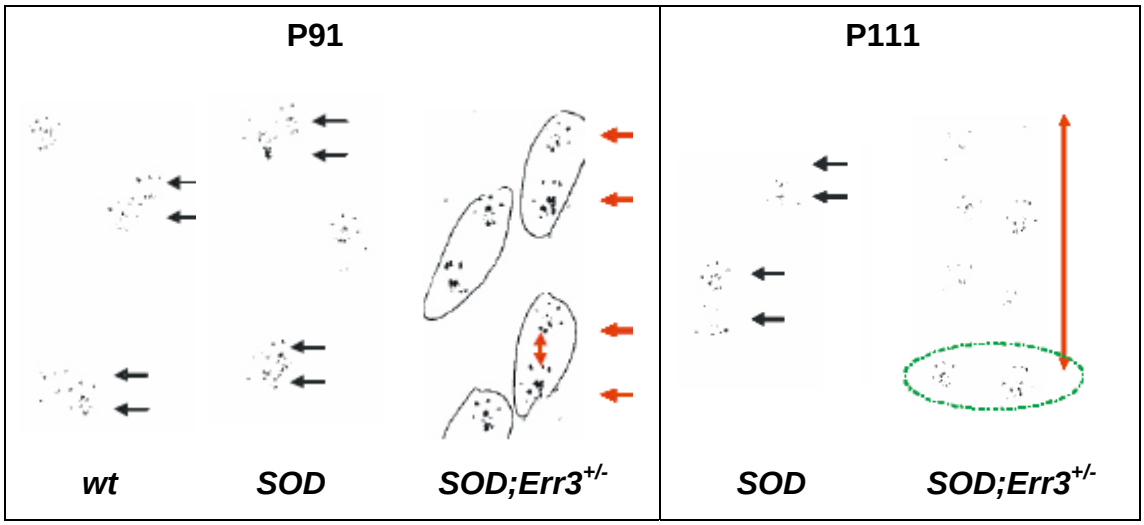

Figure 4: Footprints of *wild-type*, *SOD* and *SOD;Err3*$^{+/-}$ mice at intermediate and late stages of disease progression. At P91, footprint walking patterns of *wild-type* and SOD mice appear to be very similar. In comparison, *SOD;Err3*$^{+/-}$ mice show at this age already an increased stride length. At P111, the stride length of SOD mice is still very similar compared to P91, whereas many of the *SOD;Err3*$^{+/-}$ mice already suffer of severe paralysis.

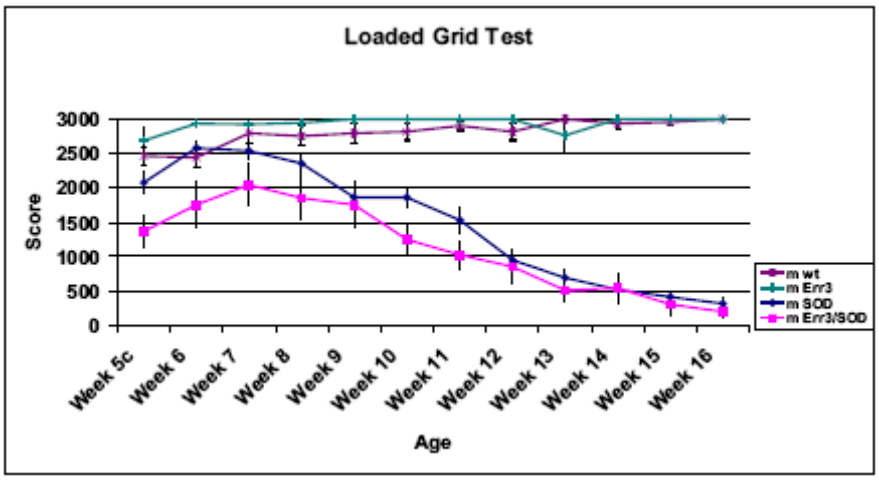

Figure 5: Muscle force measurement of SOD and *SOD;Err3*$^{+/-}$ mice during disease progression. Already at early age, *SOD;Err3*$^{+/-}$ animals suffer of lower muscle strength compared to pure *SOD* mice ($n < 0.02$ for week 5c, 6 and 10). Note, *Err3*$^{+/-}$ heterozygous mice tend to score in this test at least as good as *wild-type* animals at the age analyzed. (n = 8-15 animals for all genotypes, except for *Err3*$^{+/-}$ mice)

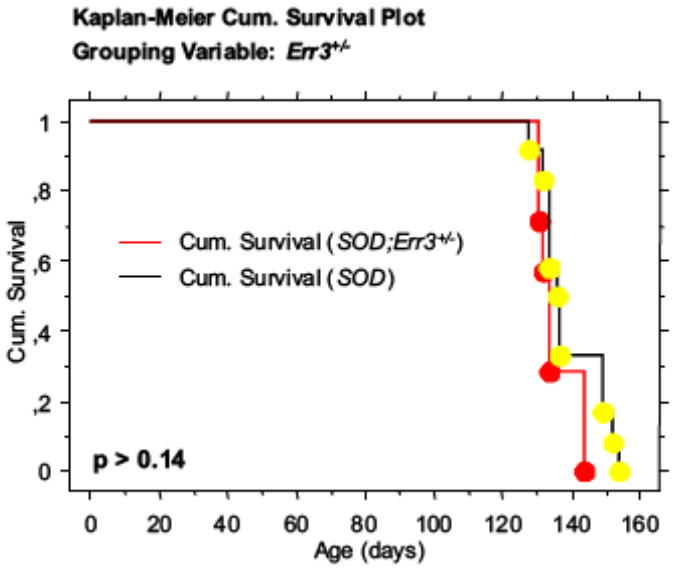

Figure 6: Cumulative survival plot of *SOD* and *SOD;Err3*$^{+/-}$ animals. There is no significant difference in the day of death between the two genotypes.
n[*SOD*] = 12
n[*SOD;Err3*$^{+/-}$] = 7

MATERIALS & METHODS

List of Antibodies

The neurotrophin receptor tyrosine kinase **(Trk–ABs)** antibodies and the islet1 antibody were used as described in (Kramer et al., 2006).

The estrogen - related receptor gamma Err3 **(Err3-AB)** antibody was purchased from Perseus Proteomics (cat. #: PP-H6812-00) and used with a dilution of 1:100 for three consecutive nights at 4dC. As secondary antibody the Alexa Fluorophore 488 was used from Invitrogen at 1:1000 (cat.#: A-21131)

Upregulation of activating transcription factor 3 **(ATF3)** was detected 2 days after quadriceps nerve lesion using a Santa Cruz antibody (cat. #: SC-188) at a dilution of 1:1000.

Further antibodies used:
Goat anti **ChAT**; Chemicon; cat. #: AB144P; dilution 1:100
Guinea pig anti **Isl1**: (Kramer et al., 2006)
Guinea pig anti **vGlut1**: Chemicon; cat. #: AB5905; dilution 1:20'000
Mouse anti **NeuN**; Chemicon; cat. #: MAB 377; dilution 1:1000
Rabbit anti **vAChT**; Sigma; cat. #: V5387; dilution 1:1000
Rabbit anti **Ret**: IBL; cat. #: 18121; dilution 1:100
Rabbit anti **Runx3**: (Kramer et al., 2006)

Any regular secondary antibodies can be used, for example from Invitrogen (Molecular Probes)

***ISH* pocedure:** (Arber et al., 2000; Hippenmeyer et al., 2007; Hippenmeyer et al., 2005).

Mouse lines used:

The initial proprioceptive specific screen was performed using the Cre - based binary genetic system (Hippenmeyer et al., 2005). Using this mouse

line, also most novel TrkC markers were identified. The level specific screen was performed using the **BAC TrkC-eGFP** mouse line from GENESAT. The expression of GFP was confirmed and mainly restricted to the TrkC+ population. FACS analysis and subsequent gene expression profiling confirmed the usefulness of this mouse line for further gene profiling experiments. This line was used to perform the level specific DRG screen.

The **G93A *SOD*** mouse line was purchased from the Jackson Laboratories.

Gene expression profiling of *Er81*$^{-/-}$ mutant DRG sensory neurons

Due to decreased parvalbumin levels in ***Er81***$^{-/-}$ mutant mice (Arber et al., 2000), we established a method to isolate *Er81*$^{-/-}$ mutant proprioceptive afferents by FACS using a biotinylated TrkC antibody.

Goat anti **mTrkC, biotinylated**; R&D, cat.#: BAF1404; dilution 1:100

Streptavidin – Allophycocyanin, eBioscience, cat. #: 17-4317-82; dilution 1:1000

Gene Expression Profiling Analysis

We used two gene expression profiling softwares:

Expressionist version 5

Gene Spring version 6

Expression Profiling of <10000 cells obtained by FACS

1.) The neurons are directly sorted into lysis buffer using the Absolutely RNA Nanoprep Kit from Stratagene (#400753)

2.) Elution is performed using elution buffer warmed up to 60°C

3.) After elution the total volume of 9.5µl is reduced using a cryo speedvac at medium temperature 4.0µl. This process takes ideally ~5min to prevent RNA degradation.

Expression Profiling of a Single DRG

1.) Isolation of dextral L5 DRG in PBS

2.) Transfer of the single DRG using fine forceps to a 1.5ml reaction tube containing 100 µl lysis buffer

3.) Continue with Absolutely RNA Nanoprep Kit from Stratagene (#400753)

4.) After elution the total volume of 9.5µl is reduced using a cryo speedvac at medium temperature 4.0µl. This process takes ideally ~5min to prevent RNA degradation.

Expression Profiling of 12 DRG (single embryo lumbar level)

1.) Isolation of DRG in PBS
2.) Transfer of DRG into a 1.5ml reaction tube containing PBS
3.) Removal of PBS
4.) Addition of 100 µl RLT/MeETOH
5.) Continue RNeasy Mini Kit from Qiagen (Cat. # 74104)

After isolation of RNA, the standard **Affymetrix "Two Cycle Target Labeling"** Method was followed (P/N 900494).

Fluorescent Acivated Cell Sorting

MoFlo (DAKO) high-speed 4-way cell sorter

The machine used has a 3-laser set-up: two water-cooled Coherent EnterpriseII lasers (one Model610 emitting at 488nm and one Model653 allowing UV excitation) and one air-cooled Spectra Physics Helium-Neon laser emitting at 633nm.

Prior the cell sorting process, the cell suspension was filtered through a self-made 40um filter. To sort DRG sensory neurons, a 100µm nozzle was used at 20psi.

Dorsal Root Ganglia Dissection and Dissociation

If a certain subpopulation of DRG will be isolated based on antibody staining using a Trk receptor antibody, then follow also blue instructions.

1.) Isolation of DRG

- Ideally, the laminectomy should be performed in ice cold HBSS medium w/o Ca^{2+}/Mg^{2+}.

- The FACS tube was first coated with sterile filtered FCS.

- After isolating DRG, they are transferred into a FACS tube with some ice cold HBSS medium w/o Ca^{2+}/Mg^{2+}. Easiest, the DRG can be transferred by sucking them into a 1000 µl siliconized pipette tip, from which the tip was cut off. During collection of the DRG, the FACS tube should be kept on ice.

- For expression profiling experiments, first all vertebral columns should be dissected, before continuing collection of the DRG. In the

meanwhile, the vertebral columns should be covered with HBSS medium w/o Ca^{2+}/Mg^{2+} medium in a Petri dish, which also should be kept on ice.

2.) Trypsin / Collagenase H Treatment

- The HBSS solution must be removed. Use a fine pipette in order to remove most of the supernatant, carefully. Avoid loosing DRG or tissue.

- Add 1 ml 0.25% trypsin solution and 100 µl Collagenase H enzyme solution (final concentration 0.1%). Thaw the enzyme right before use.

- Mix gently by flipping with fingers the bottom of the tube.

- Incubate the mix for 10 minutes at 37°C. Occasionally, flip the tube carefully.

- Stop digestion by adding 2.5 ml HBSS.

- Mix gently and centrifuge the mix for 7 minutes at 800 rpm.

- Discard the supernatant using a fine pipette.

- Resuspend the pellet in 1 ml ice cold HBSS medium w/o Ca^{2+}/Mg^{2+}. Do not wonder if cell clumps are formed.

3.) Trituration

- Dissociate cells by drawing them through a fire – polished Pasteur pipette tip and expelling them along the Falcon tube. Repeat this step approximately 20 times until the tissue is dissociated.

- Check under the binocular dissecting microscope if a single cell suspension is obtained. Otherwise, the dissociation step might be repeated.

- Centrifuge cells for 7 minutes at 800 rpm and take off as much supernatant as possible.

- *1st Antibody:* Add up to 1 ml PBS and incubate for 1 h on ice with 40 ul biotinylated anti mTrkC AB (1:25)

- Gently turn the suspension once in a while.

- Centrifuge cells for 7 minutes at 800 rpm and take off as much supernatant as possible.

- Add 750 ul PBS shake and centrifuge cells for 7 minutes at 800 rpm. Take off as much supernatant as possible.

- *2ary Antibody:* Add up to 400 ul PBS and incubate for 15 minutes on ice with 1 ul streptavidin-Allophycocyanin (1:400).

- Centrifuge cells for 7 minutes at 800 rpm and take off as much supernatant as possible.

- Add 1 ml PBS to the suspension, centrifuge cells for 7 minutes at 800 rpm and take off as much supernatant as possible.

- Add 2 ml PBS to the suspension and turn the suspension for approximately 15 min in the cold room using a turning wheel.

- Centrifuge the cells for 7 minutes at 800 rpm, discard the supernatant and resuspend the pellet in an appropriate medium for further use (eg HBSS or PBS). After dissociation of the pellet check under the binocular again, whether a single cell suspension is maintained.

Material

- Binocular dissecting microscope
- Dissection tools
- Incubator 37°C
- 1000 µl pipette with regular and siliconized tips
- Centrifuge for 15 mlreaction tubes, 800 rpm
- Fire – polished Pasteur pipette
- Turning Wheel

Media / Solutions

- Hank's modified solution, Hank's balanced salt solution (HBSS) medium w/o Ca^{2+}/Mg^{2+}, Gibco Nr. 14170-138, store at 4°C
- Fetal Calf Serum, Amimed, Bioconcepts, 500 ml, heat inactivate for 30 minutes in 56°C, store at -20°C in appropriate aliquots
- Trypsin 0.25%, Amimed, Bioconcepts Nr. 5-50 F00-H07, 100 ml, or Sigma Nr. T-8253, store at -20°C in appropriate aliquots
- 1 g Collagenase H, Boehringer Mannheim Nr. 1074032, dilute to 1% in HBSS medium w/o Ca^{2+}/Mg^{2+}, sterilization of the medium through 0.45 µm filter under a laminar flow hood, store 100 µl aliquots at -20°C

Appendix – FURTHER INTERESTING GENE EXPRESSION PROFILES

Our gene expression studies led to the identification of various genes and gene expression patterns mainly discussed throughout this thesis. In the following paragraph, further genes and gene families with enriched expression in the proprioceptive afferent population will be listed and briefly discussed.

Right bar TrkC+ population,- blue bar TrkC- DRG sensory neurons, mainly cutaneous afferents:

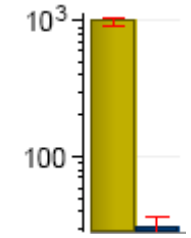

Cadherin 13

Expression not restricted to TrkC population – remaining signal on *TrkC*$^{-/-}$ mutant tissue.

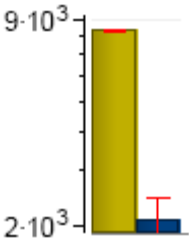

Chromogranin B

Expression not restricted to TrkC population – remaining signal on *TrkC*$^{-/-}$ mutant tissue.

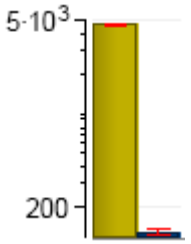

Protocadherin 8

Clear expression in subpopulations of proprioceptive afferents.

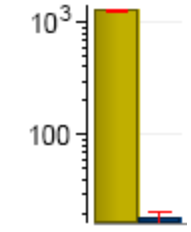

One cut domain, family member 1

Some signal left on *TrkC*$^{-/-}$ mutant tissue.

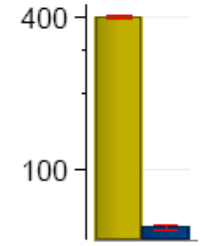

Thyroid hormone receptor interactor 10

Expression not restricted to TrkC+ population – remaining signal on *TrkC*$^{-/-}$ mutant tissue.

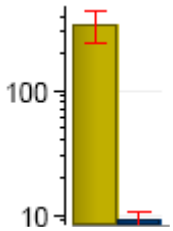

G-protein coupled receptor 97

Expression restricted to the proprioceptive afferent population.

Down-regulated on *Er81*$^{-/-}$ mutant tissue.

Figure 24: Genes with enriched expression in proprioceptive afferents.

In-Situ Hybridization Experiments of *Protocadherin 8*

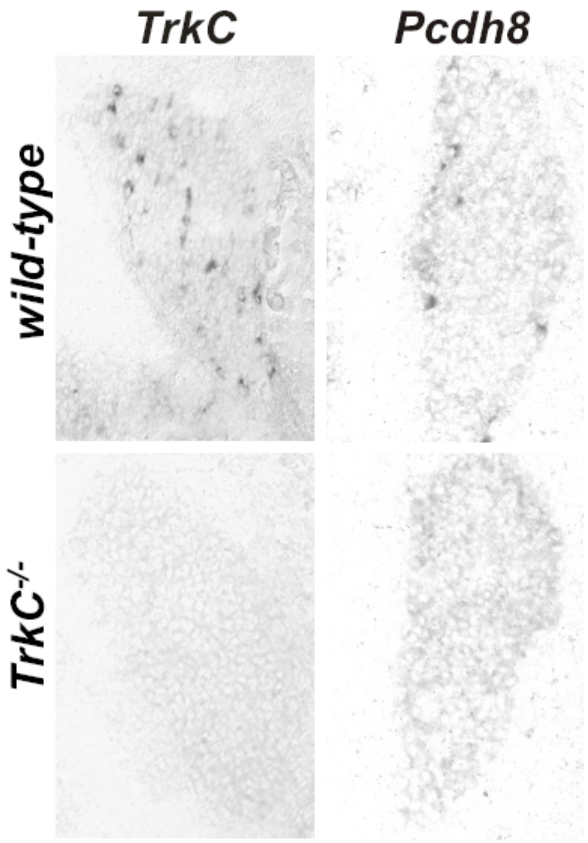

Figure 25: Expression of *Protocadherin 8* in subpopulation of lumbar proprioceptive afferents.

Semaphorin and Plexin Expression

Sema – Plexin interactions are mainly known as repulsive guidance events. As described throughout this thesis, functional specificity in the sensory - motor system is highly selective and until to date only poorly understood. Recent work also focuses on interactions within the sensory - motor system mediated by Sema – Plexin signaling (Chauvet et al., 2007; Gu et al., 2005).

In our screen we were able to identify a number of such genes potentially involved in the generation of specific connections between proprioceptive afferents and motor neurons in the spinal cord. Afterwards, PlexinA1 has been described to be expressed by proprioceptive DRG neurons and to be involved in the segregation of proprioceptive afferents in the spinal cord (Yoshida et al., 2006). Recent work from our lab suggests that PlexinD1–Sema3E signaling plays a role in gating specific sensory to motor connections (Pecho-Vrieseling *et al*, unpublished observation).

Interestingly, there are still a number of similar molecules expressed by DRG neurons, with enriched expression in proprioceptive, but also cutaneous subpopulations.

Surprisingly, Plexins are not exclusively expressed by proprioceptive afferents and the corresponding Sema molecules within the target area. Our screen also reveals expression of certain semaphorins with enriched expression in proprioceptive afferents: Sema5a (46fold), Sema3d (11fold), Sema3a (14fold) enrichment. Future studies will be necessary to dissect the diverse mechanisms of other Sema – Plexin signaling cascades involved in the formation of sensory – motor connectivity in the spinal cord.

GABA Receptor Subunit Expression

We identified *GABA A receptor, subunit gamma 1 (Gabrg1)* to be expressed in subpopulations of proprioceptive afferents with enriched expression in L5 and C7 DRG as previously discussed and also validated by *ISH* experiments. Further, our gene expression analysis reveals *Gabra5* to be expressed by proprioceptive afferents in all rostro to caudal DRG. In contrast, the *GABA BR 1*, *GABA BR* binding proteins and *GABA AR* associated protein are expressed on high levels by all DRG sensory neurons, without particular expression patterns.

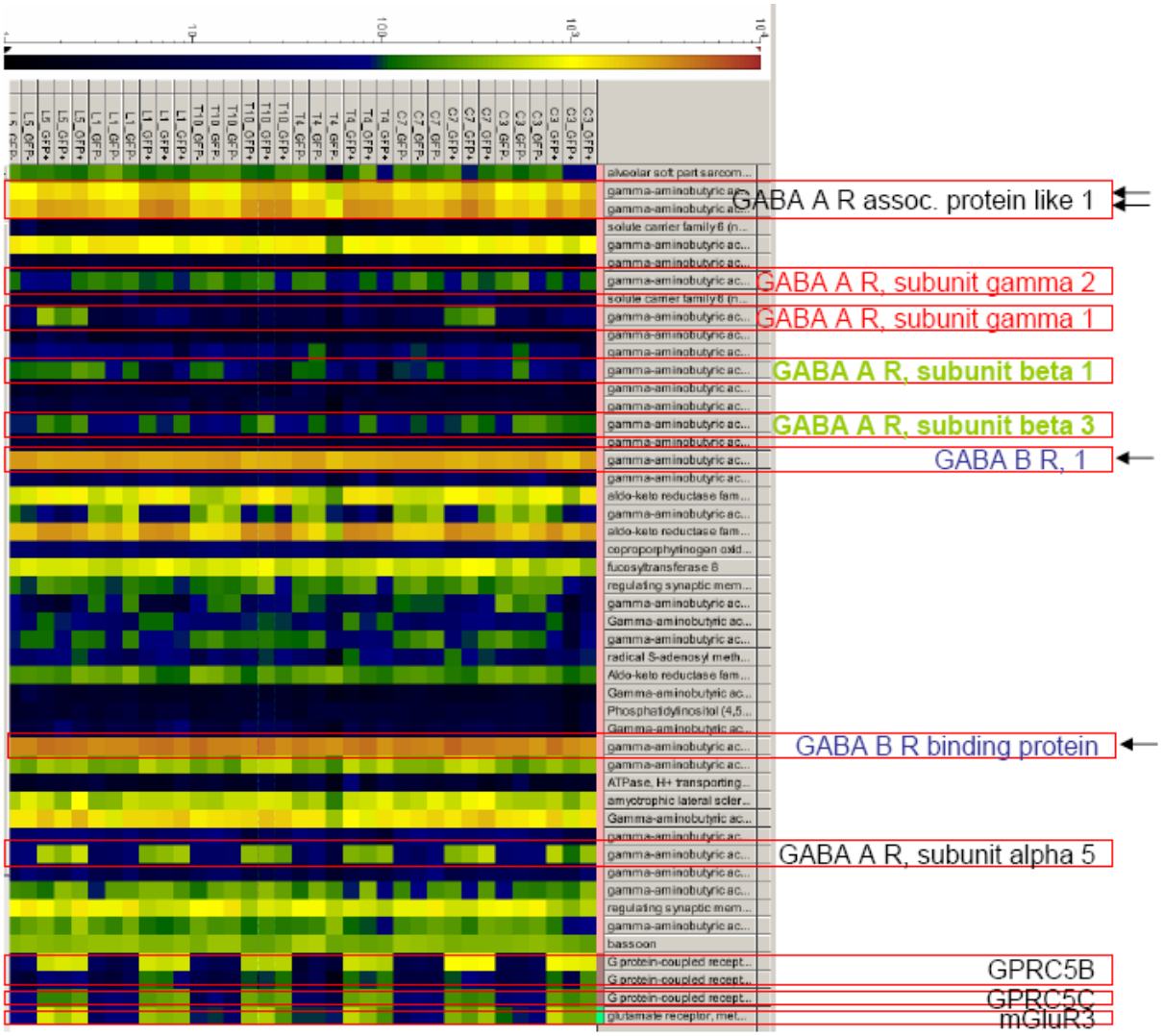

Figure 26: Heat map of GABA receptor gene expression profiles in anterior to posterior DRG sensory neuron subpopulations. Red squares indicate high expression; blue squares indicate low expression. Left squares represent the profile of expression of posterior DRG, right squares represent the expression of anterior DRG, separated in triplicates of the GFP+;TrkC+ and GFP- cell population.

Hox Gene Expression in DRG Sensory Neurons

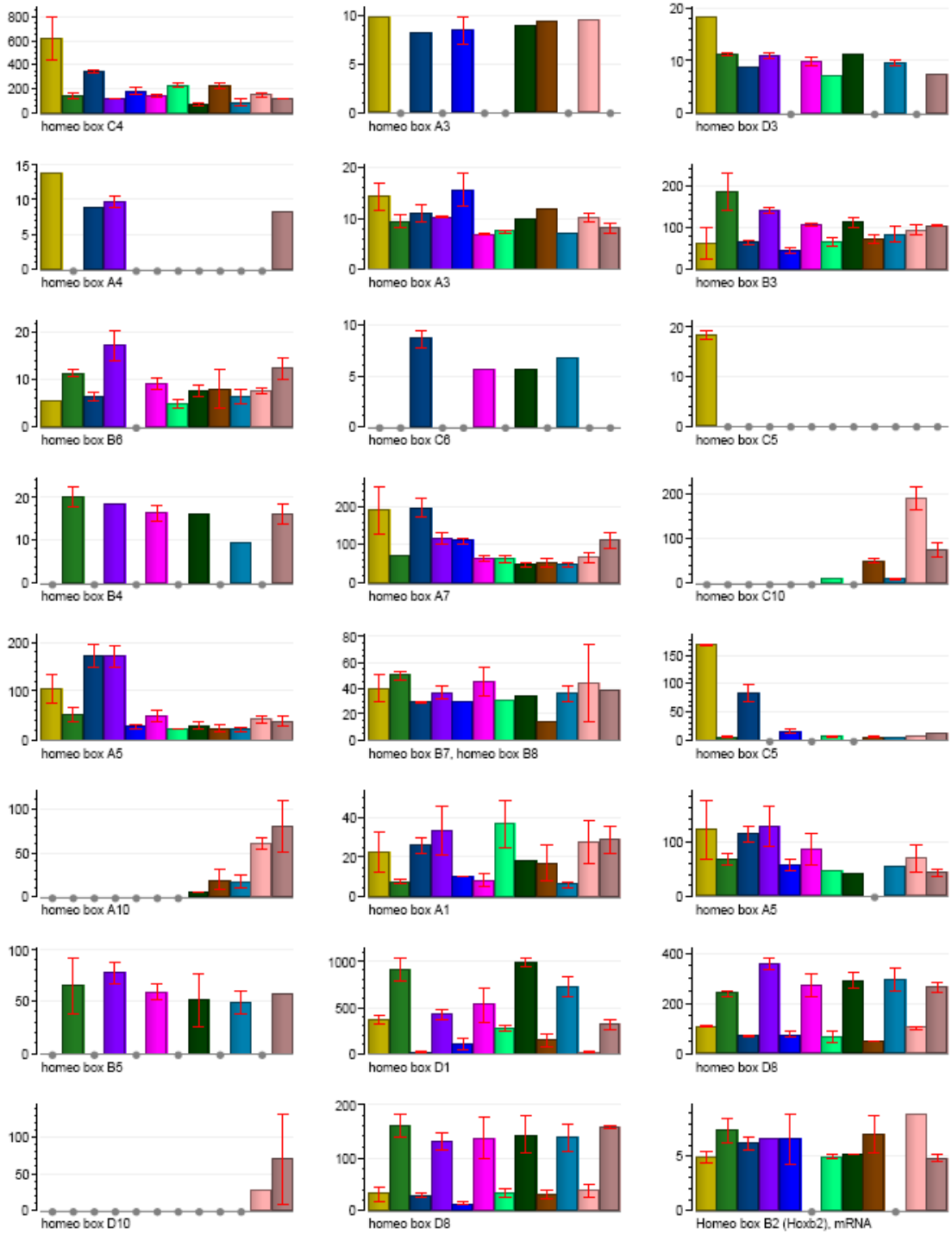

Figure 27: Expression of Hox genes in DRG sensory neuron subpopulations. Note, the expression of some Hox genes in specific subpopulations of DRG or in anterior to posterior restricted patterns (Colors in bar graphs match with colors and segmental levels in Figure 15).

Sodium and Potassium Channel Specificity in DRG Sensory Neurons

The following section summarizes the expression patterns of voltage-gated sodium and potassium channels in DRG sensory neurons (for detailed information read ‘Channel Specificity in DRG Sensory Neurons’; page 54).

Sodium Channel Expression

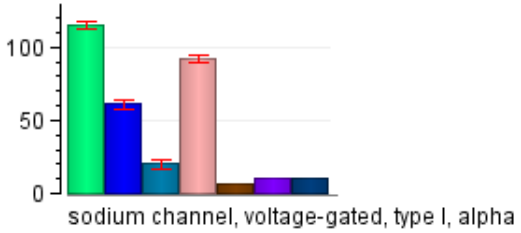

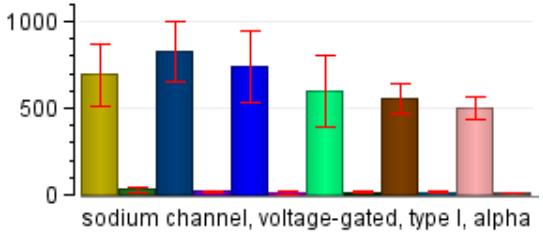

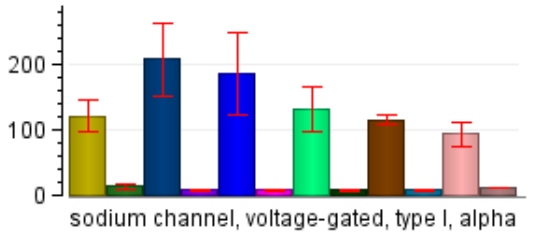

E16.5: 20 fold TrkC specific
E16.5: 6 fold down-regulated in *Er81*$^{-/-}$ mutant mice
E14.5: 7 fold TrkC specific
E14.5: ~40% up regulated *Er81*$^{-/-}$ mutant mice
P0: 27 fold TrkC specific

P0: highly TrkC specific on all rostro - caudal levels

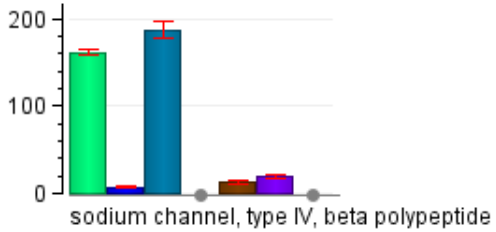

E16.5: highly TrkC specific
P0: only 3 fold TrkC specific considering L1 – L5 TrkC+ cells

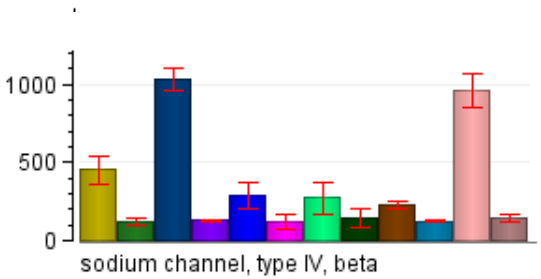

P0: enriched expression in TrkC cells at levels C7 and L5

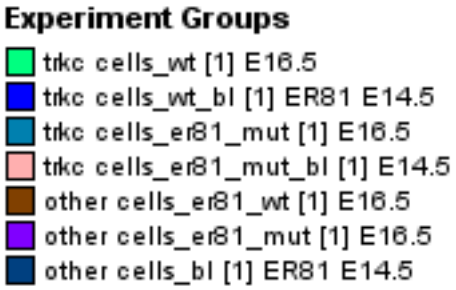

Sodium Channel Expression

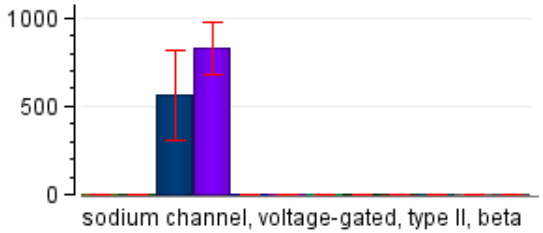

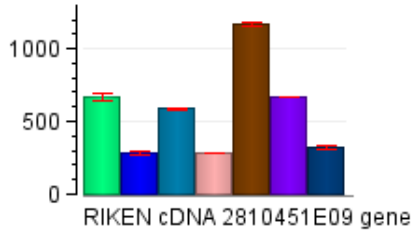

P0: highly enriched in all DRG SNs at spinal level C7
E16.5: expression 50% reduced in TrkC- cells (also sodium-gated, type II, beta)

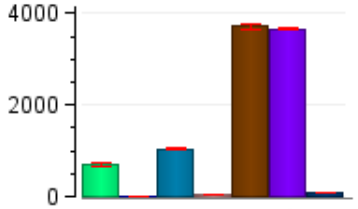

Not TrkC cell specific at **E16.5**
At **P0** still 14 fold specific to TrkC- cells

Experiment Groups
- trkc cells_wt [1] E16.5
- trkc cells_wt_bl [1] ER81 E14.5
- trkc cells_er81_mut [1] E16.5
- trkc cells_er81_mut_bl [1] E14.5
- other cells_er81_wt [1] E16.5
- other cells_er81_mut [1] E16.5
- other cells_bl [1] ER81 E14.5

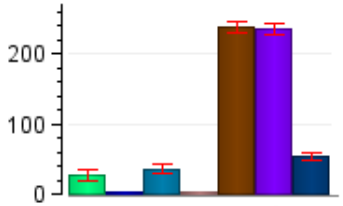

Not TrkC cell specific at **E16.5**
At **P0** still 14 fold specific to TrkC- cells

Experiment Groups
- C6_GFP+
- C6_GFP-
- C7_GFP+
- C7_GFP-
- T4_GFP+
- T4_GFP-
- T10_GFP+
- T10_GFP-
- L1_GFP+
- L1_GFP-
- L5_GFP+
- L5_GFP-

Sodium Channel Expression

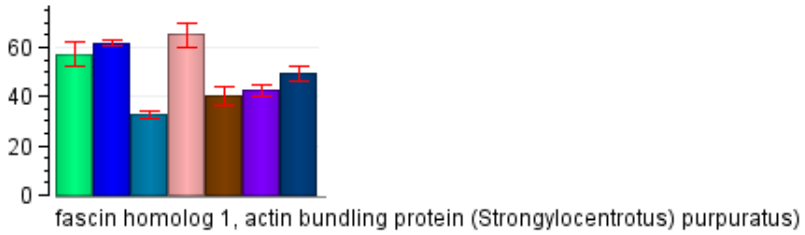

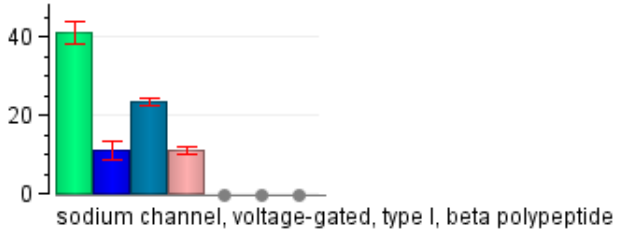

Experiment Groups

- trkc cells_wt [1] E16.5
- trkc cells_wt_bl [1] ER81 E14.5
- trkc cells_er81_mut [1] E16.5
- trkc cells_er81_mut_bl [1] E14.5
- other cells_er81_wt [1] E16.5
- other cells_er81_mut [1] E16.5
- other cells_bl [1] ER81 E14.5

Down regulated at **E16.5** in *Er81*$^{-/-}$ mutant proprioceptive afferents,
but not yet at **E14.5**.

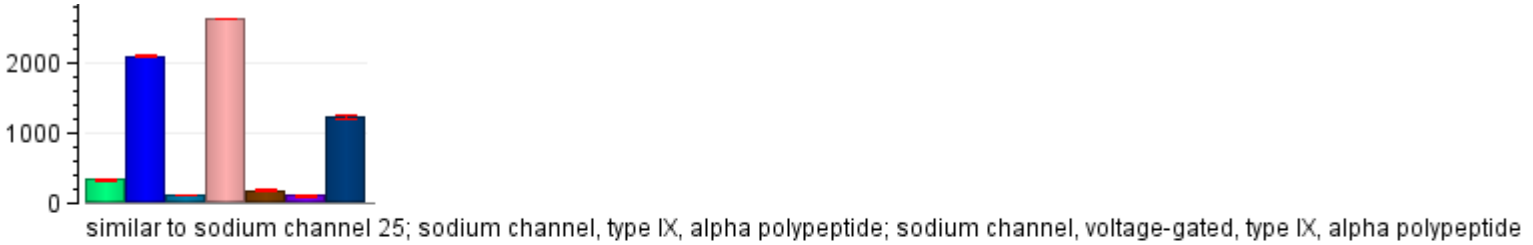

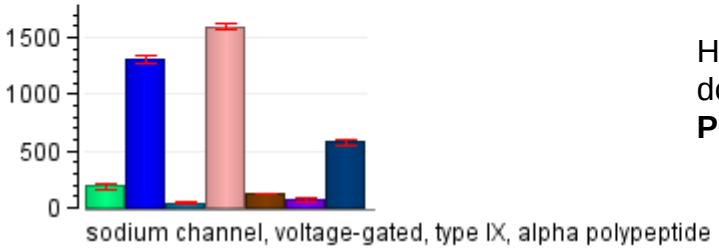

Highly expressed at **E14.5** in TrkC+ cells and low in TrkC- cells,
down regulated at **E16.5** in TrkC+ cells,-
P0: still 9 fold TrkC specific

Sodium Channel Expression

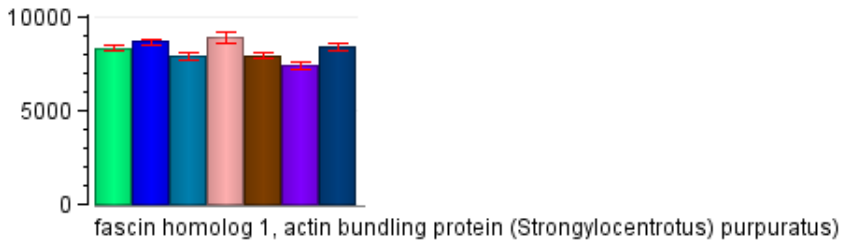

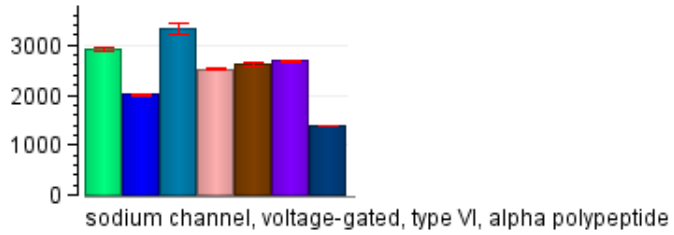

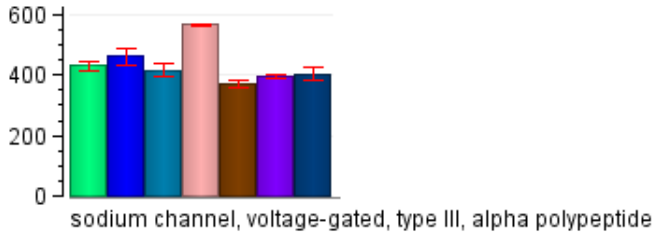

Experiment Groups

- trkc cells_wt [1] E16.5
- trkc cells_wt_bl [1] ER81 E14.5
- trkc cells_er81_mut [1] E16.5
- trkc cells_er81_mut_bl [1] E14.5
- other cells_er81_wt [1] E16.5
- other cells_er81_mut [1] E16.5
- other cells_bl [1] ER81 E14.5

Highly expressed in all DRG SNs at **E16.5** & **E14.5** in wt and *Er81*$^{-/-}$ mutants

Potassium Channel Expression

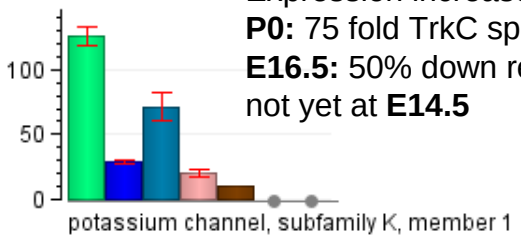

Expression increases from **E14.5** until **P0**, TrkC specific
P0: 75 fold TrkC specific, high raw values
E16.5: 50% down regulated in *Er81*$^{-/-}$ mutant TrkC cells, not yet at **E14.5**

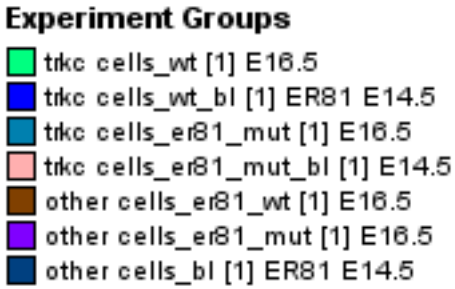

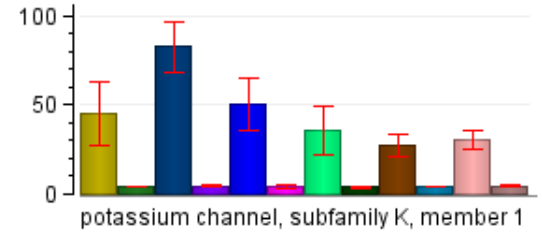

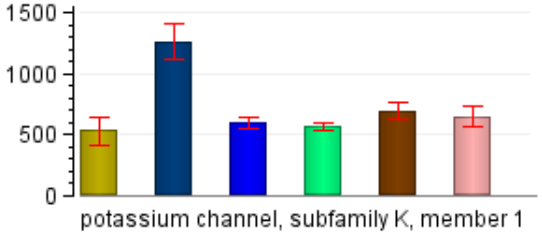

Specific expression to proprioceptive afferents, with decreased expression to caudal levels.

Potassium Channel Expression

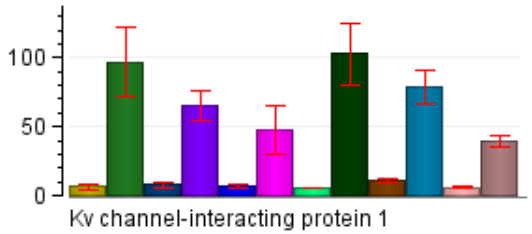

P0: Enriched expression to cutaneous afferent subpopulation.

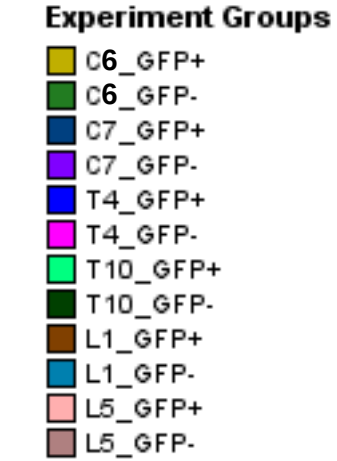

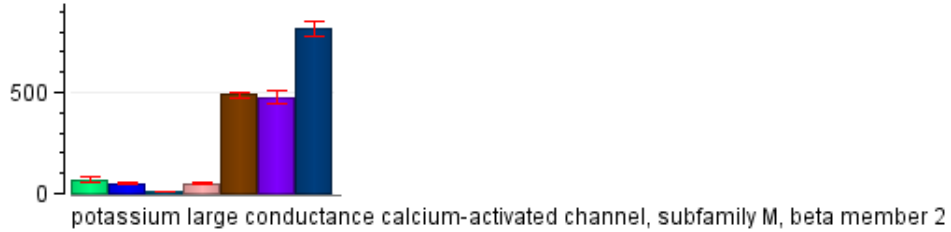

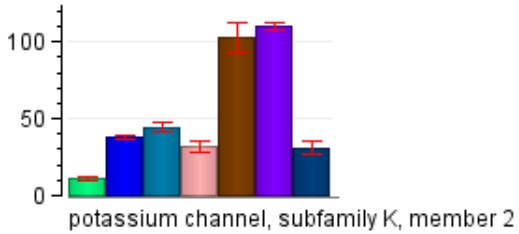

Not TrkC specific, but 3 fold up regulated in *Er81*$^{-/-}$ mutant TrkC cells at **E16.5**

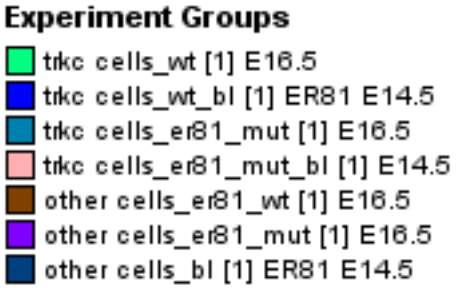

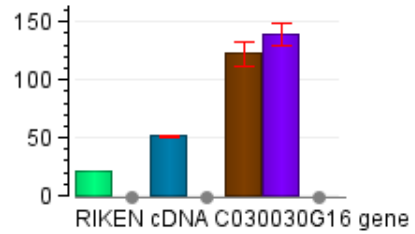

potassium channel, subfamily T, member 1
Highly enriched to the TrkC- cell populations at **E14.5** and **E16.5**
2 fold up in *Er81*$^{-/-}$ mutant TrkC cells at **E16.5**

Potassium Channel Expression

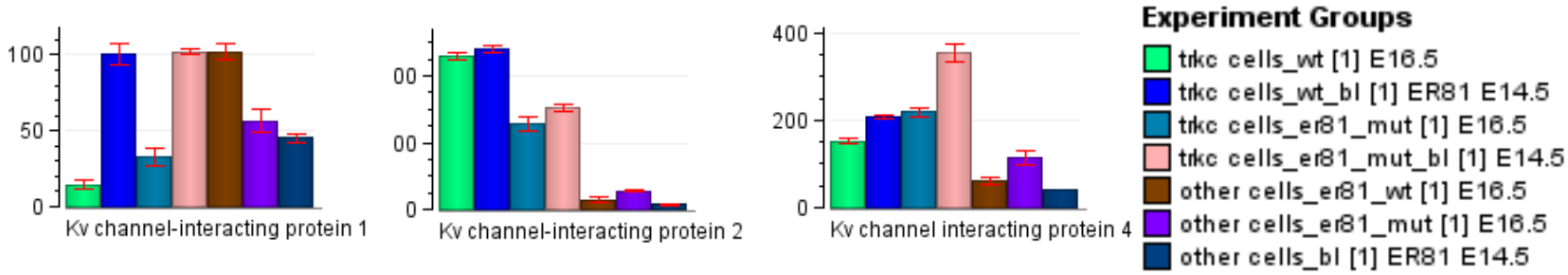

In *wild-type Kvcnip1* is higher expressed at **E14.5** compared to **E16.5**, whereas it is not TrkC specifically regulated Interestingly, it is up regulated at **E16.5** in TrkC cells and in non-TrkC cells

In contrast *Kvcnip2* is TrkC specifically regulated. It is also ~50% down regulated in *Er81*$^{-/-}$ mutant TrkC cells. (other Kv channel interacting proteins are not present on the chips)

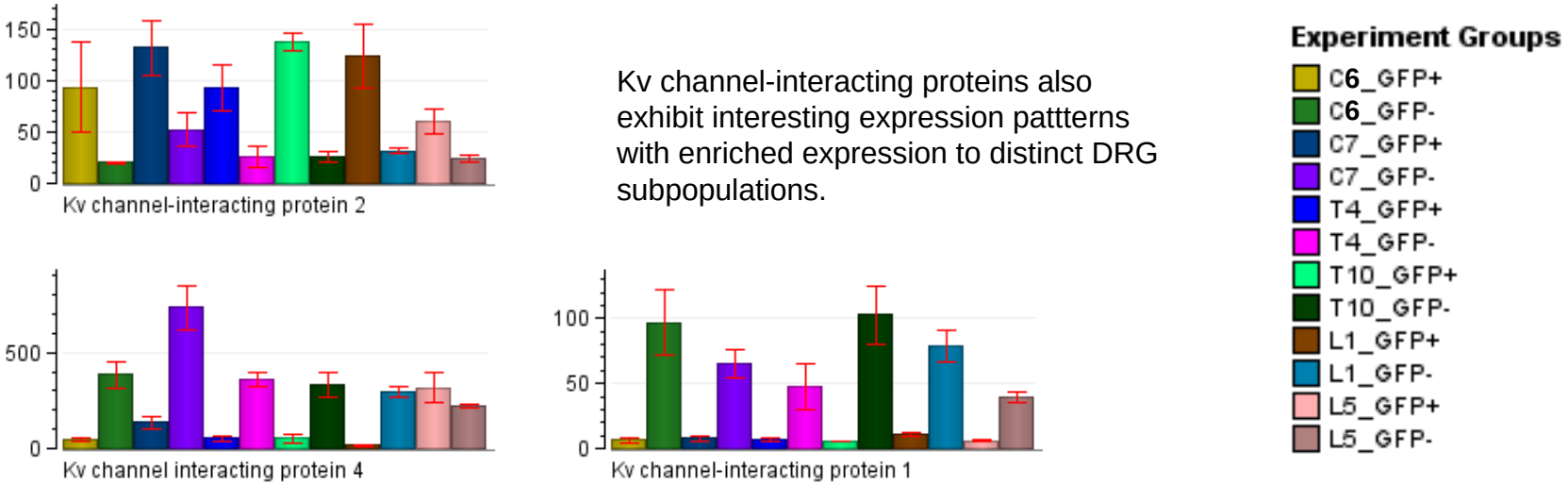

Kv channel-interacting proteins also exhibit interesting expression pattterns with enriched expression to distinct DRG subpopulations.

Appendix – REFERENCES

Allan, E.H., K.D. Hausler, T. Wei, J.H. Gooi, J.M. Quinn, B. Crimeen-Irwin, S. Pompolo, N.A. Sims, M.T. Gillespie, J.E. Onyia, and T.J. Martin. 2008. EphrinB2 regulation by PTH and PTHrP revealed by molecular profiling in differentiating osteoblasts. *J Bone Miner Res*. 23:1170-81.

Altman, J., and S.A. Bayer. 1984. The development of the rat spinal cord. *Adv Anat Embryol Cell Biol*. 85:1-164.

Anderson, D.J. 1999. Lineages and transcription factors in the specification of vertebrate primary sensory neurons. *Curr Opin Neurobiol*. 9:517-24.

Arber, S., D.R. Ladle, J.H. Lin, E. Frank, and T.M. Jessell. 2000. ETS gene Er81 controls the formation of functional connections between group Ia sensory afferents and motor neurons. *Cell*. 101:485-98.

Arlotta, P., B.J. Molyneaux, J. Chen, J. Inoue, R. Kominami, and J.D. Macklis. 2005. Neuronal subtype-specific genes that control corticospinal motor neuron development in vivo. *Neuron*. 45:207-21.

Arndt, K., S. Nakagawa, M. Takeichi, and C. Redies. 1998. Cadherin-defined segments and parasagittal cell ribbons in the developing chicken cerebellum. *Mol Cell Neurosci*. 10:211-28.

Averill, S., D.R. Davis, P.J. Shortland, J.V. Priestley, and S.P. Hunt. 2002. Dynamic pattern of reg-2 expression in rat sensory neurons after peripheral nerve injury. *J Neurosci*. 22:7493-501.

Bagri, A., O. Marin, A.S. Plump, J. Mak, S.J. Pleasure, J.L. Rubenstein, and M. Tessier-Lavigne. 2002. Slit proteins prevent midline crossing and determine the dorsoventral position of major axonal pathways in the mammalian forebrain. *Neuron*. 33:233-48.

Balaban, R.S., S. Nemoto, and T. Finkel. 2005. Mitochondria, oxidants, and aging. *Cell*. 120:483-95.

Barneoud, P., J. Lolivier, D.J. Sanger, B. Scatton, and P. Moser. 1997. Quantitative motor assessment in FALS mice: a longitudinal study. *Neuroreport*. 8:2861-5.

Baudet, C., A. Mikaels, H. Westphal, J. Johansen, T.E. Johansen, and P. Ernfors. 2000. Positive and negative interactions of GDNF, NTN and ART in developing sensory neuron subpopulations, and their collaboration with neurotrophins. *Development*. 127:4335-44.

Beck, K.D., L. Powell-Braxton, H.R. Widmer, J. Valverde, and F. Hefti. 1995. Igf1 gene disruption results in reduced brain size, CNS

hypomyelination, and loss of hippocampal granule and striatal parvalbumin-containing neurons. *Neuron*. 14:717-30.

Bjarnadottir, T.K., R. Fredriksson, P.J. Hoglund, D.E. Gloriam, M.C. Lagerstrom, and H.B. Schioth. 2004. The human and mouse repertoire of the adhesion family of G-protein-coupled receptors. *Genomics*. 84:23-33.

Boggon, T.J., J. Murray, S. Chappuis-Flament, E. Wong, B.M. Gumbiner, and L. Shapiro. 2002. C-cadherin ectodomain structure and implications for cell adhesion mechanisms. *Science*. 296:1308-13.

Bononi, J., A. Cole, P. Tewson, A. Schumacher, and R. Bradley. 2008. Chicken protocadherin-1 functions to localize neural crest cells to the dorsal root ganglia during PNS formation. *Mech Dev*.

Brose, K., K.S. Bland, K.H. Wang, D. Arnott, W. Henzel, C.S. Goodman, M. Tessier-Lavigne, and T. Kidd. 1999. Slit proteins bind Robo receptors and have an evolutionarily conserved role in repulsive axon guidance. *Cell*. 96:795-806.

Bruijn, L.I., T.M. Miller, and D.W. Cleveland. 2004. Unraveling the mechanisms involved in motor neuron degeneration in ALS. *Annu Rev Neurosci*. 27:723-49.

Camarero, G., C. Avendano, C. Fernandez-Moreno, A. Villar, J. Contreras, F. de Pablo, J.G. Pichel, and I. Varela-Nieto. 2001. Delayed inner ear maturation and neuronal loss in postnatal Igf-1-deficient mice. *J Neurosci*. 21:7630-41.

Carroll, P., O. Gayet, C. Feuillet, S. Kallenbach, B. de Bovis, K. Dudley, and S. Alonso. 2001. Juxtaposition of CNR protocadherins and reelin expression in the developing spinal cord. *Mol Cell Neurosci*. 17:611-23.

Carroll, S.L., I. Silos-Santiago, S.E. Frese, K.G. Ruit, J. Milbrandt, and W.D. Snider. 1992. Dorsal root ganglion neurons expressing trk are selectively sensitive to NGF deprivation in utero. *Neuron*. 9:779-88.

Catterall, W.A., A.L. Goldin, and S.G. Waxman. 2005. International Union of Pharmacology. XLVII. Nomenclature and structure-function relationships of voltage-gated sodium channels. *Pharmacol Rev*. 57:397-409.

Chahine, M., R. Ziane, K. Vijayaragavan, and Y. Okamura. 2005. Regulation of Na v channels in sensory neurons. *Trends Pharmacol Sci*. 26:496-502.

Chang, Q., M. Gonzalez, M.J. Pinter, and R.J. Balice-Gordon. 1999. Gap junctional coupling and patterns of connexin expression among neonatal rat lumbar spinal motor neurons. *J Neurosci*. 19:10813-28.

Chauvet, S., S. Cohen, Y. Yoshida, L. Fekrane, J. Livet, O. Gayet, L. Segu, M.C. Buhot, T.M. Jessell, C.E. Henderson, and F. Mann. 2007. Gating of Sema3E/PlexinD1 signaling by neuropilin-1 switches axonal repulsion to attraction during brain development. *Neuron*. 56:807-22.

Chen, C.L., D.C. Broom, Y. Liu, J.C. de Nooij, Z. Li, C. Cen, O.A. Samad, T.M. Jessell, C.J. Woolf, and Q. Ma. 2006. Runx1 determines nociceptive sensory neuron phenotype and is required for thermal and neuropathic pain. *Neuron*. 49:365-77.

Chen, H.H., S. Hippenmeyer, S. Arber, and E. Frank. 2003. Development of the monosynaptic stretch reflex circuit. *Curr Opin Neurobiol*. 13:96-102.

Chen, H.H., W.G. Tourtellotte, and E. Frank. 2002. Muscle spindle-derived neurotrophin 3 regulates synaptic connectivity between muscle sensory and motor neurons. *J Neurosci*. 22:3512-9.

Chen, Z., B.B. Gore, H. Long, L. Ma, and M. Tessier-Lavigne. 2008. Alternative splicing of the Robo3 axon guidance receptor governs the midline switch from attraction to repulsion. *Neuron*. 58:325-32.

Chiu, S.L., C.M. Chen, and H.T. Cline. 2008. Insulin receptor signaling regulates synapse number, dendritic plasticity, and circuit function in vivo. *Neuron*. 58:708-19.

Collard, J.F., F. Cote, and J.P. Julien. 1995. Defective axonal transport in a transgenic mouse model of amyotrophic lateral sclerosis. *Nature*. 375:61-4.

Cox, P.J., T. Pitcher, S.A. Trim, C.H. Bell, W. Qin, and R.A. Kinloch. 2008. The effect of deletion of the orphan G - protein coupled receptor (GPCR) gene MrgE on pain-like behaviours in mice. *Mol Pain*. 4:2.

Cui, L., H. Jeong, F. Borovecki, C.N. Parkhurst, N. Tanese, and D. Krainc. 2006. Transcriptional repression of PGC-1alpha by mutant huntingtin leads to mitochondrial dysfunction and neurodegeneration. *Cell*. 127:59-69.

Dasen, J.S., A. De Camilli, B. Wang, P.W. Tucker, and T.M. Jessell. 2008. Hox repertoires for motor neuron diversity and connectivity gated by a single accessory factor, FoxP1. *Cell*. 134:304-16.

Dasen, J.S., B.C. Tice, S. Brenner-Morton, and T.M. Jessell. 2005. A Hox regulatory network establishes motor neuron pool identity and target-muscle connectivity. *Cell*. 123:477-91.

De Calisto, J., C. Araya, L. Marchant, C.F. Riaz, and R. Mayor. 2005. Essential role of non-canonical Wnt signalling in neural crest migration. *Development*. 132:2587-97.

Dobrowolny, G., C. Giacinti, L. Pelosi, C. Nicoletti, N. Winn, L. Barberi, M. Molinaro, N. Rosenthal, and A. Musaro. 2005. Muscle expression of a local Igf-1 isoform protects motor neurons in an ALS mouse model. *J Cell Biol*. 168:193-9.

Dong, X., S. Han, M.J. Zylka, M.I. Simon, and D.J. Anderson. 2001. A diverse family of GPCRs expressed in specific subsets of nociceptive sensory neurons. *Cell*. 106:619-32.

Dufour, C.R., B.J. Wilson, J.M. Huss, D.P. Kelly, W.A. Alaynick, M. Downes, R.M. Evans, M. Blanchette, and V. Giguere. 2007. Genome-wide orchestration of cardiac functions by the orphan nuclear receptors ERRalpha and gamma. *Cell Metab*. 5:345-56.

Dupuis, L., M. Pehar, P. Cassina, F. Rene, R. Castellanos, C. Rouaux, M. Gandelman, L. Dimou, M.E. Schwab, J.P. Loeffler, L. Barbeito, and J.L. Gonzalez de Aguilar. 2008. Nogo receptor antagonizes p75NTR-dependent motor neuron death. *Proc Natl Acad Sci U S A*. 105:740-5.

Eccles, J.C., R.M. Eccles, and A. Lundberg. 1957. The convergence of monosynaptic excitatory afferents on to many different species of alpha motoneurones. *J Physiol*. 137:22-50.

Ehrhard, P.B., and U. Otten. 1994. Postnatal ontogeny of the neurotrophin receptors trk and trkB mRNA in rat sensory and sympathetic ganglia. *Neurosci Lett*. 166:207-10.

Ernfors, P., K.F. Lee, J. Kucera, and R. Jaenisch. 1994. Lack of neurotrophin-3 leads to deficiencies in the peripheral nervous system and loss of limb proprioceptive afferents. *Cell*. 77:503-12.

Finck, B.N. 2006. Effects of PPARalpha on cardiac glucose metabolism: a transcriptional equivalent of the glucose-fatty acid cycle? *Expert Rev Cardiovasc Ther*. 4:161-71.

Finck, B.N., and D.P. Kelly. 2006. PGC-1 coactivators: inducible regulators of energy metabolism in health and disease. *J Clin Invest*. 116:615-22.

Gehring, W.J. 1993. Exploring the homeobox. *Gene*. 135:215-21.

Gilman, A.G. 1987. G proteins: transducers of receptor-generated signals. *Annu Rev Biochem*. 56:615-49.

Goldfarb, M., J. Schoorlemmer, A. Williams, S. Diwakar, Q. Wang, X. Huang, J. Giza, D. Tchetchik, K. Kelley, A. Vega, G. Matthews, P. Rossi, D.M. Ornitz, and E. D'Angelo. 2007. Fibroblast growth factor homologous factors control neuronal excitability through modulation of voltage-gated sodium channels. *Neuron*. 55:449-63.

Gould, T.W., S. Yonemura, R.W. Oppenheim, S. Ohmori, and H. Enomoto. 2008. The neurotrophic effects of glial cell line-derived neurotrophic factor on spinal motoneurons are restricted to fusimotor subtypes. *J Neurosci*. 28:2131-46.

Gu, C., Y. Yoshida, J. Livet, D.V. Reimert, F. Mann, J. Merte, C.E. Henderson, T.M. Jessell, A.L. Kolodkin, and D.D. Ginty. 2005. Semaphorin 3E and plexin-D1 control vascular pattern independently of neuropilins. *Science*. 307:265-8.

Guo, J., U.I. Chung, H. Kondo, F.R. Bringhurst, and H.M. Kronenberg. 2002. The PTH/PTHrP receptor can delay chondrocyte hypertrophy in vivo without activating phospholipase C. *Dev Cell*. 3:183-94.

Gurney, M.E., H. Pu, A.Y. Chiu, M.C. Dal Canto, C.Y. Polchow, D.D. Alexander, J. Caliendo, A. Hentati, Y.W. Kwon, H.X. Deng, and et al. 1994. Motor neuron degeneration in mice that express a human Cu,Zn superoxide dismutase mutation. *Science*. 264:1772-5.

Haase, G., E. Dessaud, A. Garces, B. de Bovis, M. Birling, P. Filippi, H. Schmalbruch, S. Arber, and O. deLapeyriere. 2002. GDNF acts through PEA3 to regulate cell body positioning and muscle innervation of specific motor neuron pools. *Neuron*. 35:893-905.

Hall, A.C., F.R. Lucas, and P.C. Salinas. 2000. Axonal remodeling and synaptic differentiation in the cerebellum is regulated by WNT-7a signaling. *Cell*. 100:525-35.

Harada, Y., C. Yokota, R. Habas, D.C. Slusarski, and X. He. 2007. Retinoic acid-inducible G protein-coupled receptors bind to frizzled receptors and may activate non-canonical Wnt signaling. *Biochem Biophys Res Commun*. 358:968-75.

Hatabu, H., J. Gaa, D. Kim, W. Li, P.V. Prasad, and R.R. Edelman. 1996. Pulmonary perfusion: qualitative assessment with dynamic contrast-enhanced MRI using ultra-short TE and inversion recovery turbo FLASH. *Magn Reson Med*. 36:503-8.

Hippenmeyer, S., R.M. Huber, D.R. Ladle, K. Murphy, and S. Arber. 2007. ETS transcription factor Erm controls subsynaptic gene expression in skeletal muscles. *Neuron*. 55:726-40.

Hippenmeyer, S., N.A. Shneider, C. Birchmeier, S.J. Burden, T.M. Jessell, and S. Arber. 2002. A role for neuregulin1 signaling in muscle spindle differentiation. *Neuron*. 36:1035-49.

Hippenmeyer, S., E. Vrieseling, M. Sigrist, T. Portmann, C. Laengle, D.R. Ladle, and S. Arber. 2005. A developmental switch in the response of DRG neurons to ETS transcription factor signaling. *PLoS Biol*. 3:e159.

Huang, E.J., and L.F. Reichardt. 2003. Trk receptors: roles in neuronal signal transduction. *Annu Rev Biochem*. 72:609-42.

Huang, W.L., D. Robson, M.C. Liu, V.R. King, S. Averill, P.J. Shortland, and J.V. Priestley. 2006. Spinal cord compression and dorsal root injury cause up-regulation of activating transcription factor-3 in large-diameter dorsal root ganglion neurons. *Eur J Neurosci*. 23:273-8.

Huss, J.M., K. Imahashi, C.R. Dufour, C.J. Weinheimer, M. Courtois, A. Kovacs, V. Giguere, E. Murphy, and D.P. Kelly. 2007. The nuclear receptor ERRalpha is required for the bioenergetic and functional adaptation to cardiac pressure overload. *Cell Metab*. 6:25-37.

Huss, J.M., I.P. Torra, B. Staels, V. Giguere, and D.P. Kelly. 2004. Estrogen-related receptor alpha directs peroxisome proliferator-activated receptor alpha signaling in the transcriptional control of energy metabolism in cardiac and skeletal muscle. *Mol Cell Biol*. 24:9079-91.

Ichiyama, R.M., J. Broman, V.R. Edgerton, and L.A. Havton. 2006. Ultrastructural synaptic features differ between alpha- and gamma-motoneurons innervating the tibialis anterior muscle in the rat. *J Comp Neurol*. 499:306-15.

Inoue, T., T. Tanaka, S.C. Suzuki, and M. Takeichi. 1998. Cadherin-6 in the developing mouse brain: expression along restricted connection systems and synaptic localization suggest a potential role in neuronal circuitry. *Dev Dyn*. 211:338-51.

Ito, Y. 2004. Oncogenic potential of the RUNX gene family: 'overview'. *Oncogene*. 23:4198-208.

Jessell, T.M. 2000. Neuronal specification in the spinal cord: inductive signals and transcriptional codes. *Nat Rev Genet*. 1:20-9.

Jones, D.M., B.A. Tucker, M. Rahimtula, and K.M. Mearow. 2003. The synergistic effects of NGF and IGF-1 on neurite growth in adult sensory neurons: convergence on the PI 3-kinase signaling pathway. *J Neurochem*. 86:1116-28.

Kidd, T., K.S. Bland, and C.S. Goodman. 1999. Slit is the midline repellent for the robo receptor in Drosophila. *Cell*. 96:785-94.

Kiehn, O. 2006. Locomotor circuits in the mammalian spinal cord. *Annu Rev Neurosci*. 29:279-306.

Klein, R., I. Silos-Santiago, R.J. Smeyne, S.A. Lira, R. Brambilla, S. Bryant, L. Zhang, W.D. Snider, and M. Barbacid. 1994. Disruption of the neurotrophin-3 receptor gene trkC eliminates la muscle afferents and results in abnormal movements. *Nature*. 368:249-51.

Klur, S., K. Toy, M.P. Williams, and U. Certa. 2004. Evaluation of procedures for amplification of small-size samples for hybridization on microarrays. *Genomics*. 83:508-17.

Kobayashi, T., U.I. Chung, E. Schipani, M. Starbuck, G. Karsenty, T. Katagiri, D.L. Goad, B. Lanske, and H.M. Kronenberg. 2002. PTHrP and Indian hedgehog control differentiation of growth plate chondrocytes at multiple steps. *Development*. 129:2977-86.

Kohmura, N., K. Senzaki, S. Hamada, N. Kai, R. Yasuda, M. Watanabe, H. Ishii, M. Yasuda, M. Mishina, and T. Yagi. 1998. Diversity revealed by a novel family of cadherins expressed in neurons at a synaptic complex. *Neuron*. 20:1137-51.

Kramer, I., M. Sigrist, J.C. de Nooij, I. Taniuchi, T.M. Jessell, and S. Arber. 2006. A role for Runx transcription factor signaling in dorsal root ganglion sensory neuron diversification. *Neuron*. 49:379-93.

Krylova, O., J. Herreros, K.E. Cleverley, E. Ehler, J.P. Henriquez, S.M. Hughes, and P.C. Salinas. 2002. WNT-3, expressed by motoneurons, regulates terminal arborization of neurotrophin-3-responsive spinal sensory neurons. *Neuron*. 35:1043-56.

Kucera, J., G. Fan, R. Jaenisch, S. Linnarsson, and P. Ernfors. 1995. Dependence of developing group Ia afferents on neurotrophin-3. *J Comp Neurol*. 363:307-20.

Landmesser, L.T. 2001. The acquisition of motoneuron subtype identity and motor circuit formation. *Int J Dev Neurosci*. 19:175-82.

Leinninger, G.M., C. Backus, M.D. Uhler, S.I. Lentz, and E.L. Feldman. 2004. Phosphatidylinositol 3-kinase and Akt effectors mediate insulin-like growth factor-I neuroprotection in dorsal root ganglia neurons. *FASEB J*. 18:1544-6.

Leone, T.C., J.J. Lehman, B.N. Finck, P.J. Schaeffer, A.R. Wende, S. Boudina, M. Courtois, D.F. Wozniak, N. Sambandam, C. Bernal-Mizrachi, Z. Chen, J.O. Holloszy, D.M. Medeiros, R.E. Schmidt, J.E. Saffitz, E.D. Abel, C.F. Semenkovich, and D.P. Kelly. 2005. PGC-1alpha deficiency causes multi-system energy metabolic derangements: muscle dysfunction, abnormal weight control and hepatic steatosis. *PLoS Biol*. 3:e101.

Levanon, D., D. Bettoun, C. Harris-Cerruti, E. Woolf, V. Negreanu, R. Eilam, Y. Bernstein, D. Goldenberg, C. Xiao, M. Fliegauf, E. Kremer, F. Otto, O. Brenner, A. Lev-Tov, and Y. Groner. 2002. The Runx3 transcription factor regulates development and survival of TrkC dorsal root ganglia neurons. *EMBO J*. 21:3454-63.

Lin, J.H., T. Saito, D.J. Anderson, C. Lance-Jones, T.M. Jessell, and S. Arber. 1998. Functionally related motor neuron pool and muscle sensory afferent subtypes defined by coordinate ETS gene expression. *Cell*. 95:393-407.

Livet, J., M. Sigrist, S. Stroebel, V. De Paola, S.R. Price, C.E. Henderson, T.M. Jessell, and S. Arber. 2002. ETS gene Pea3 controls the central position and terminal arborization of specific motor neuron pools. *Neuron*. 35:877-92.

Loconto, J., F. Papes, E. Chang, L. Stowers, E.P. Jones, T. Takada, A. Kumanovics, K. Fischer Lindahl, and C. Dulac. 2003. Functional expression of murine V2R pheromone receptors involves selective association with the M10 and M1 families of MHC class Ib molecules. *Cell*. 112:607-18.

Luo, W., S.R. Wickramasinghe, J.M. Savitt, J.W. Griffin, T.M. Dawson, and D.D. Ginty. 2007. A hierarchical NGF signaling cascade controls Ret-dependent and Ret-independent events during development of nonpeptidergic DRG neurons. *Neuron*. 54:739-54.

Luscher, H.R., J. Mathis, and E. Henneman. 1984. Wiring diagrams of functional connectivity in monosynaptic reflex arcs of the spinal cord. *Neurosci Lett*. 45:217-22.

Ma, L., and M. Tessier-Lavigne. 2007. Dual branch-promoting and branch-repelling actions of Slit/Robo signaling on peripheral and central branches of developing sensory axons. *J Neurosci*. 27:6843-51.

Ma, Q., C. Fode, F. Guillemot, and D.J. Anderson. 1999. Neurogenin1 and neurogenin2 control two distinct waves of neurogenesis in developing dorsal root ganglia. *Genes Dev*. 13:1717-28.

MacLean, H.E., and H.M. Kronenberg. 2005. Localization of Indian hedgehog and PTH/PTHrP receptor expression in relation to chondrocyte proliferation during mouse bone development. *Dev Growth Differ*. 47:59-63.

Makarenkova, H., H. Sugiura, K. Yamagata, and G. Owens. 2005. Alternatively spliced variants of protocadherin 8 exhibit distinct patterns of expression during mouse development. *Biochim Biophys Acta*. 1681:150-6.

McConnell, S.K. 1995. Strategies for the generation of neuronal diversity in the developing central nervous system. *J Neurosci*. 15:6987-98.

Mears, S.C., and E. Frank. 1997. Formation of specific monosynaptic connections between muscle spindle afferents and motoneurons in the mouse. *J Neurosci*. 17:3128-35.

Mentis, G.Z., F.J. Alvarez, A. Bonnot, D.S. Richards, D. Gonzalez-Forero, R. Zerda, and M.J. O'Donovan. 2005. Noncholinergic excitatory actions of motoneurons in the neonatal mammalian spinal cord. *Proc Natl Acad Sci U S A*. 102:7344-9.

Milner, L.D., and L.T. Landmesser. 1999. Cholinergic and GABAergic inputs drive patterned spontaneous motoneuron activity before target contact. *J Neurosci*. 19:3007-22.

Molliver, D.C., D.E. Wright, M.L. Leitner, A.S. Parsadanian, K. Doster, D. Wen, Q. Yan, and W.D. Snider. 1997. IB4-binding DRG neurons switch from NGF to GDNF dependence in early postnatal life. *Neuron*. 19:849-61.

Mootha, V.K., C. Handschin, D. Arlow, X. Xie, J. St Pierre, S. Sihag, W. Yang, D. Altshuler, P. Puigserver, N. Patterson, P.J. Willy, I.G. Schulman, R.A. Heyman, E.S. Lander, and B.M. Spiegelman. 2004. Erralpha and Gabpa/b specify PGC-1alpha-dependent oxidative phosphorylation gene expression that is altered in diabetic muscle. *Proc Natl Acad Sci U S A*. 101:6570-5.

Morris, C.E., and P.F. Juranka. 2007. Nav channel mechanosensitivity: activation and inactivation accelerate reversibly with stretch. *Biophys J*. 93:822-33.

Myers, C.P., J.W. Lewcock, M.G. Hanson, S. Gosgnach, J.B. Aimone, F.H. Gage, K.F. Lee, L.T. Landmesser, and S.L. Pfaff. 2005. Cholinergic input is required during embryonic development to mediate proper assembly of spinal locomotor circuits. *Neuron*. 46:37-49.

Nelson, S.B., K. Sugino, and C.M. Hempel. 2006. The problem of neuronal cell types: a physiological genomics approach. *Trends Neurosci*. 29:339-45.

Nguyen-Ba-Charvet, K.T., N. Picard-Riera, M. Tessier-Lavigne, A. Baron-Van Evercooren, C. Sotelo, and A. Chedotal. 2004. Multiple roles for slits in the control of cell migration in the rostral migratory stream. *J Neurosci*. 24:1497-506.

Nishimaru, H., C.E. Restrepo, J. Ryge, Y. Yanagawa, and O. Kiehn. 2005. Mammalian motor neurons corelease glutamate and acetylcholine at central synapses. *Proc Natl Acad Sci U S A*. 102:5245-9.

Nishimune, H., S. Vasseur, S. Wiese, M.C. Birling, B. Holtmann, M. Sendtner, J.L. Iovanna, and C.E. Henderson. 2000. Reg-2 is a motoneuron neurotrophic factor and a signalling intermediate in the CNTF survival pathway. *Nat Cell Biol*. 2:906-14.

Nishitoh, H., H. Kadowaki, A. Nagai, T. Maruyama, T. Yokota, H. Fukutomi, T. Noguchi, A. Matsuzawa, K. Takeda, and H. Ichijo. 2008. ALS-linked

mutant SOD1 induces ER stress- and ASK1-dependent motor neuron death by targeting Derlin-1. *Genes Dev*. 22:1451-64.

Oakley, R.A., F.B. Lefcort, D.O. Clary, L.F. Reichardt, D. Prevette, R.W. Oppenheim, and E. Frank. 1997. Neurotrophin-3 promotes the differentiation of muscle spindle afferents in the absence of peripheral targets. *J Neurosci*. 17:4262-74.

Ogiwara, I., H. Miyamoto, N. Morita, N. Atapour, E. Mazaki, I. Inoue, T. Takeuchi, S. Itohara, Y. Yanagawa, K. Obata, T. Furuichi, T.K. Hensch, and K. Yamakawa. 2007. Na(v)1.1 localizes to axons of parvalbumin-positive inhibitory interneurons: a circuit basis for epileptic seizures in mice carrying an Scn1a gene mutation. *J Neurosci*. 27:5903-14.

Ornung, G., O.P. Ottersen, S. Cullheim, and B. Ulfhake. 1998. Distribution of glutamate-, glycine- and GABA-immunoreactive nerve terminals on dendrites in the cat spinal motor nucleus. *Exp Brain Res*. 118:517-32.

Overduin, M., T.S. Harvey, S. Bagby, K.I. Tong, P. Yau, M. Takeichi, and M. Ikura. 1995. Solution structure of the epithelial cadherin domain responsible for selective cell adhesion. *Science*. 267:386-9.

Ozdinler, P.H., and J.D. Macklis. 2006. IGF-I specifically enhances axon outgrowth of corticospinal motor neurons. *Nat Neurosci*. 9:1371-81.

Packard, M., E.S. Koo, M. Gorczyca, J. Sharpe, S. Cumberledge, and V. Budnik. 2002. The Drosophila Wnt, wingless, provides an essential signal for pre- and postsynaptic differentiation. *Cell*. 111:319-30.

Patel, S.D., C. Ciatto, C.P. Chen, F. Bahna, M. Rajebhosale, N. Arkus, I. Schieren, T.M. Jessell, B. Honig, S.R. Price, and L. Shapiro. 2006. Type II cadherin ectodomain structures: implications for classical cadherin specificity. *Cell*. 124:1255-68.

Patel, T.D., A. Jackman, F.L. Rice, J. Kucera, and W.D. Snider. 2000. Development of sensory neurons in the absence of NGF/TrkA signaling in vivo. *Neuron*. 25:345-57.

Patel, T.D., I. Kramer, J. Kucera, V. Niederkofler, T.M. Jessell, S. Arber, and W.D. Snider. 2003. Peripheral NT3 signaling is required for ETS protein expression and central patterning of proprioceptive sensory afferents. *Neuron*. 38:403-16.

Price, S.R., N.V. De Marco Garcia, B. Ranscht, and T.M. Jessell. 2002. Regulation of motor neuron pool sorting by differential expression of type II cadherins. *Cell*. 109:205-16.

Pun, S., A.F. Santos, S. Saxena, L. Xu, and P. Caroni. 2006. Selective vulnerability and pruning of phasic motoneuron axons in motoneuron disease alleviated by CNTF. *Nat Neurosci*. 9:408-19.

Rabinovsky, E.D., E. Gelir, S. Gelir, H. Lui, M. Kattash, F.J. DeMayo, S.M. Shenaq, and R.J. Schwartz. 2003. Targeted expression of IGF-1 transgene to skeletal muscle accelerates muscle and motor neuron regeneration. *FASEB J*. 17:53-5.

Rangwala, S.M., X. Li, L. Lindsley, X. Wang, S. Shaughnessy, T.G. Daniels, J. Szustakowski, N.R. Nirmala, Z. Wu, and S.C. Stevenson. 2007. Estrogen-related receptor alpha is essential for the expression of antioxidant protection genes and mitochondrial function. *Biochem Biophys Res Commun*. 357:231-6.

Redies, C. 2000. Cadherins in the central nervous system. *Prog Neurobiol*. 61:611-48.

Rexed, B. 1952. The cytoarchitectonic organization of the spinal cord in the cat. *J Comp Neurol*. 96:414-95.

Rexed, B. 1954. A cytoarchitectonic atlas of the spinal cord in the cat. *J Comp Neurol*. 100:297-379.

Robbins, M.J., K.J. Charles, D.C. Harrison, and M.N. Pangalos. 2002. Localisation of the GPRC5B receptor in the rat brain and spinal cord. *Brain Res Mol Brain Res*. 106:136-44.

Robbins, M.J., D. Michalovich, J. Hill, A.R. Calver, A.D. Medhurst, I. Gloger, M. Sims, D.N. Middlemiss, and M.N. Pangalos. 2000. Molecular cloning and characterization of two novel retinoic acid-inducible orphan G-protein-coupled receptors (GPRC5B and GPRC5C). *Genomics*. 67:8-18.

Rodbell, M., L. Birnbaumer, S.L. Pohl, and F. Sundby. 1971. The reaction of glucagon with its receptor: evidence for discrete regions of activity and binding in the glucagon molecule. *Proc Natl Acad Sci U S A*. 68:909-13.

Rossi-Durand, C. 2006. Proprioception and myoclonus. *Neurophysiol Clin*. 36:299-308.

Rousso, D.L., Z.B. Gaber, D. Wellik, E.E. Morrisey, and B.G. Novitch. 2008. Coordinated actions of the forkhead protein Foxp1 and Hox proteins in the columnar organization of spinal motor neurons. *Neuron*. 59:226-40.

Salomon, R., T. Attie, J. Amiel, A. Pelet, P. Niaudet, and S. Lyonnet. 1998. RET proto-oncogene: role in kidney development and molecular pathology. *Adv Nephrol Necker Hosp*. 28:401-17.

Sanes, J.R., and J.W. Lichtman. 2001. Induction, assembly, maturation and maintenance of a postsynaptic apparatus. *Nat Rev Neurosci*. 2:791-805.

Schier, A.F., and W.J. Gehring. 1992. Direct homeodomain-DNA interaction in the autoregulation of the fushi tarazu gene. *Nature*. 356:804-7.

Scolnick, J.A., K. Cui, C.D. Duggan, S. Xuan, X.B. Yuan, A. Efstratiadis, and J. Ngai. 2008. Role of IGF signaling in olfactory sensory map formation and axon guidance. *Neuron*. 57:847-57.

Sekine, Y., K. Takeda, and H. Ichijo. 2006. The ASK1-MAP kinase signaling in ER stress and neurodegenerative diseases. *Curr Mol Med*. 6:87-97.

Shapiro, L., A.M. Fannon, P.D. Kwong, A. Thompson, M.S. Lehmann, G. Grubel, J.F. Legrand, J. Als-Nielsen, D.R. Colman, and W.A. Hendrickson. 1995. Structural basis of cell-cell adhesion by cadherins. *Nature*. 374:327-37.

Sherrington, C.S. 1910. Flexion-reflex of the limb, crossed extension-reflex, and reflex stepping and standing. *J Physiol*. 40:28-121.

Sommer, L., Q. Ma, and D.J. Anderson. 1996. neurogenins, a novel family of atonal-related bHLH transcription factors, are putative mammalian neuronal determination genes that reveal progenitor cell heterogeneity in the developing CNS and PNS. *Mol Cell Neurosci*. 8:221-41.

St-Pierre, J., S. Drori, M. Uldry, J.M. Silvaggi, J. Rhee, S. Jager, C. Handschin, K. Zheng, J. Lin, W. Yang, D.K. Simon, R. Bachoo, and B.M. Spiegelman. 2006. Suppression of reactive oxygen species and neurodegeneration by the PGC-1 transcriptional coactivators. *Cell*. 127:397-408.

Sugino, K., C.M. Hempel, M.N. Miller, A.M. Hattox, P. Shapiro, C. Wu, Z.J. Huang, and S.B. Nelson. 2006. Molecular taxonomy of major neuronal classes in the adult mouse forebrain. *Nat Neurosci*. 9:99-107.

Suzuki, S.C., T. Inoue, Y. Kimura, T. Tanaka, and M. Takeichi. 1997. Neuronal circuits are subdivided by differential expression of type-II classic cadherins in postnatal mouse brains. *Mol Cell Neurosci*. 9:433-47.

Tessarollo, L., K.S. Vogel, M.E. Palko, S.W. Reid, and L.F. Parada. 1994. Targeted mutation in the neurotrophin-3 gene results in loss of muscle sensory neurons. *Proc Natl Acad Sci U S A*. 91:11844-8.

Tietjen, I., J. Rihel, and C.G. Dulac. 2005. Single-cell transcriptional profiles and spatial patterning of the mammalian olfactory epithelium. *Int J Dev Biol*. 49:201-7.

Tietjen, I., J.M. Rihel, Y. Cao, G. Koentges, L. Zakhary, and C. Dulac. 2003. Single-cell transcriptional analysis of neuronal progenitors. *Neuron*. 38:161-75.

Tourtellotte, W.G., and J. Milbrandt. 1998. Sensory ataxia and muscle spindle agenesis in mice lacking the transcription factor Egr3. *Nat Genet*. 20:87-91.

Tsujino, H., E. Kondo, T. Fukuoka, Y. Dai, A. Tokunaga, K. Miki, K. Yonenobu, T. Ochi, and K. Noguchi. 2000. Activating transcription factor 3 (ATF3) induction by axotomy in sensory and motoneurons: A novel neuronal marker of nerve injury. *Mol Cell Neurosci*. 15:170-82.

Vassilatis, D.K., J.G. Hohmann, H. Zeng, F. Li, J.E. Ranchalis, M.T. Mortrud, A. Brown, S.S. Rodriguez, J.R. Weller, A.C. Wright, J.E. Bergmann, and G.A. Gaitanaris. 2003. The G protein-coupled receptor repertoires of human and mouse. *Proc Natl Acad Sci U S A*. 100:4903-8.

Vrieseling, E., and S. Arber. 2006. Target-induced transcriptional control of dendritic patterning and connectivity in motor neurons by the ETS gene Pea3. *Cell*. 127:1439-52.

Wang, K.H., K. Brose, D. Arnott, T. Kidd, C.S. Goodman, W. Henzel, and M. Tessier-Lavigne. 1999. Biochemical purification of a mammalian slit protein as a positive regulator of sensory axon elongation and branching. *Cell*. 96:771-84.

Wang, Z., L.Y. Li, M.D. Taylor, D.E. Wright, and E. Frank. 2007. Prenatal exposure to elevated NT3 disrupts synaptic selectivity in the spinal cord. *J Neurosci*. 27:3686-94.

Wohrn, J.C., L. Puelles, S. Nakagawa, M. Takeichi, and C. Redies. 1998. Cadherin expression in the retina and retinofugal pathways of the chicken embryo. *J Comp Neurol*. 396:20-38.

Wojtowicz, W.M., W. Wu, I. Andre, B. Qian, D. Baker, and S.L. Zipursky. 2007. A vast repertoire of Dscam binding specificities arises from modular interactions of variable Ig domains. *Cell*. 130:1134-45.

Wong, P.C., C.A. Pardo, D.R. Borchelt, M.K. Lee, N.G. Copeland, N.A. Jenkins, S.S. Sisodia, D.W. Cleveland, and D.L. Price. 1995. An adverse property of a familial ALS-linked SOD1 mutation causes motor neuron disease characterized by vacuolar degeneration of mitochondria. *Neuron*. 14:1105-16.

Wu, Q., and T. Maniatis. 1999. A striking organization of a large family of human neural cadherin-like cell adhesion genes. *Cell*. 97:779-90.

Wu, Y., G. Wang, S.A. Scott, and M.R. Capecchi. 2008. Hoxc10 and Hoxd10 regulate mouse columnar, divisional and motor pool identity of lumbar motoneurons. *Development*. 135:171-82.

Wu, Z., P. Puigserver, U. Andersson, C. Zhang, G. Adelmant, V. Mootha, A. Troy, S. Cinti, B. Lowell, R.C. Scarpulla, and B.M. Spiegelman. 1999.

Mechanisms controlling mitochondrial biogenesis and respiration through the thermogenic coactivator PGC-1. *Cell*. 98:115-24.

Yamagata, K., K.I. Andreasson, H. Sugiura, E. Maru, M. Dominique, Y. Irie, N. Miki, Y. Hayashi, M. Yoshioka, K. Kaneko, H. Kato, and P.F. Worley. 1999. Arcadlin is a neural activity-regulated cadherin involved in long term potentiation. *J Biol Chem*. 274:19473-1979.

Yamamoto, M., G. Sobue, K. Yamamoto, S. Terao, and T. Mitsuma. 1996. Expression of mRNAs for neurotrophic factors (NGF, BDNF, NT-3, and GDNF) and their receptors (p75NGFR, trkA, trkB, and trkC) in the adult human peripheral nervous system and nonneural tissues. *Neurochem Res*. 21:929-38.

Yoon, M.S., L. Puelles, and C. Redies. 2000. Formation of cadherin-expressing brain nuclei in diencephalic alar plate divisions. *J Comp Neurol*. 427:461-80.

Yoshida, Y., B. Han, M. Mendelsohn, and T.M. Jessell. 2006. PlexinA1 signaling directs the segregation of proprioceptive sensory axons in the developing spinal cord. *Neuron*. 52:775-88.

Yu, F.H., M. Mantegazza, R.E. Westenbroek, C.A. Robbins, F. Kalume, K.A. Burton, W.J. Spain, G.S. McKnight, T. Scheuer, and W.A. Catterall. 2006. Reduced sodium current in GABAergic interneurons in a mouse model of severe myoclonic epilepsy in infancy. *Nat Neurosci*. 9:1142-9.

Yu, F.H., V. Yarov-Yarovoy, G.A. Gutman, and W.A. Catterall. 2005. Overview of molecular relationships in the voltage-gated ion channel superfamily. *Pharmacol Rev*. 57:387-95.

Zelena, J., and T. Soukup. 1977a. The development of Golgi tendon organs. *J Neurocytol*. 6:171-94.

Zelena, J., and T. Soukup. 1977b. The ultrastructural development of Golgi tendon organs. *Folia Morphol (Praha)*. 25:76-8.

Zirlinger, M., L. Lo, J. McMahon, A.P. McMahon, and D.J. Anderson. 2002. Transient expression of the bHLH factor neurogenin-2 marks a subpopulation of neural crest cells biased for a sensory but not a neuronal fate. *Proc Natl Acad Sci U S A*. 99:8084-9.